Characterization of type III secretion system-dependent protein secretion in *Y. enterocolitica*

DISSERTATION

Zur

Erlangung des Doktorgrades

Der Naturwissenschaften

(Dr. rer. nat.)

dem Fachbereich Biologie

der Philipps-Universität Marburg

vorgelegt

von

BAILEY ABIGAIL MILNE-DAVIES

Aus Orange Park, Florida/Vereinigte Staaten von Amerika

Marburg/Lahn im Januar 2021

Die Untersuchungen zur vorliegenden Arbeit wurden von Oktober 2017 bis Januar 2021 am Max-Planck-Institut für Terrestrische Mikrobiologie unter der Leitung von Dr. Andreas Diepold durchgeführt.

Vom Fachbereich Biologie der Philipps-Universität Marburg als Dissertation angenommen am:

____.____._____

Erstgutachter: Prof. Dr. Lotte Søgaard-Andersen

Zweitgutachter: Prof. Dr. Anke Becker

Weitere Mitglieder der Prüfungskommission:

Prof. Dr. Lennart Randau

Dr. Andreas Diepold

Tag der mündlichen Prüfung am: ____.____._____

Die während der Promotion erzielten Ergebnisse wurden zum Teil in folgenden Originalpublikationen veröffentlicht:

Milne-Davies B, Helbig C, Wimmi S, Cheng DWC, Paczia N, Diepold A. Life After Secretion – *Yersinia enterocolitica* Rapidly Toggles Effector Secretion and Can Resume Cell Division in Response to Changing External Conditions. Front Microbiol. 2019 Sep 13;10:2128. doi: 10.3389/fmicb.2019.02128. PMID: 31572334; PMCID: PMC6753693.

Lindner F, Milne-Davies B, Langenfeld K, Stiewe T, Diepold A. LITESEC-T3SS – Light-controlled protein delivery into eukaryotic cells with high spatial and temporal resolution. Nat Commun. 2020 May 13;11(1):2381. doi: 10.1038/s41467-020-16169-w. PMID: 32404906; PMCID: PMC7221075.

To my family, friends, educators and mentors who believed in me

Table of Contents

Table of Figures

Table of Supplementary Figures

Table of Tables

Abstract

The type III secretion system (T3SS) is utilized by many Gram-negative bacteria to promote survival in a variety of symbiotic or pathogenic relationships. Many pathogenic bacteria use their T3SS, commonly called the injectisome, to translocate bacterial effector proteins to manipulate host cells and promote infection. The injectisome consists of a membrane-spanning nanosyringe that translocates effector proteins from the bacterial cytosol into the host cytoplasm. Using *Yersinia enterocolitica* as a model organism, we characterized the post-secretion events (deactivation, reactivation, and re-initiation of division following secretion) and explored secretion regulation prior to and during activation. Our results show that *Y. enterocolitica* can quickly adapt to different environmental conditions, allowing rapid deactivation of secretion and when re-introduced into a secreting environment, the bacteria immediately reactivate the T3SS. Notably, *Y. enterocolitica* survives secretion and can reestablish growth and division. We also established cell culture-based infection assays to test controlled protein translocation by the T3SS and demonstrated that the cognate chaperone is vital for exporting complex non-native proteins into host cells. The effector chaperones don't appear to directly interact with the injectisome, but are essential in establishing efficient effector export. Furthermore, we show that *Yersinia* appears to prepare a small pool of pre-synthesized effectors that is ready to be exported once secretion is activated. Lastly, we found that the gatekeepers, which controls the activation or inhibition of effector secretion, are localized throughout the cytosol, suggesting *Y. enterocolitica* utilizes a different mechanism to govern secretion than *E. coli*. The data shows that events during and after secretion are highly regulated, utilizing a variety of mechanisms to sense and adapt to the environment and promote swift and decisive secretion to bolster survival during infection.

Zusammenfassung

Das Typ-III-Sekretionssystem (T3SS) wird von vielen gramnegativen Bakterien genutzt, um das Überleben in einer Vielzahl von symbiotischen Beziehungen zu fördern. Viele pathogene Bakterien nutzen ihr T3SS, allgemein als Injektisom bezeichnet, zur Translokation bakterieller Effektorproteine, um Wirtszellen zu manipulieren und die Infektion zu fördern. Das Injektisom besteht aus einer membranüberspannenden Nanospritze, die Effektorproteine aus dem bakteriellen Cytosol in das Zytoplasma des Wirts transloziert. Unter Verwendung von *Yersinia enterocolitica* als Modellorganismus haben wir die Ereignisse nach der Sekretion (Deaktivierung, Reaktivierung und erneute Teilungsinitiation nach der Sekretion) charakterisiert und die Sekretionsregulation vor und während der Aktivierung untersucht. Unsere Ergebnisse zeigen, dass sich *Y. enterocolitica* schnell an unterschiedliche Umweltbedingungen anpassen kann, was eine schnelle Deaktivierung der Sekretion ermöglicht. Wenn das Bakterium wieder in eine sekretierende Umgebung gebracht wird, reaktiviert es das T3SS sofort. Bemerkenswert ist, dass *Y. enterocolitica* die Sekretion überlebt und Wachstum und Teilung wiederherstellen kann. Darüberhinaus etablichte etablierte ich zellkulturbasierte Infektionsassays, um die kontrollierte Proteintranslokation durch das T3SS zu testen Diese Experimente zeigten, dass das kognate Chaperon für den Export komplexer nicht-nativer Proteine in die Wirtszellen entscheidend ist. Die Effektor-Chaperone scheinen nicht direkt mit dem Injektisom zu interagieren, sind aber essentiell, um einen effizienten Effektor-Export zu ermöglichen. Darüber hinaus zeigen wir, dass *Yersinia* einen kleinen Pool von vorsynthetisierten Effektoren vorbereit, der exportiert werden kann, sobald die Sekretion aktiviert wird. Schließlich haben wir festgestellt, dass Gatekeeper Proteine, der die Aktivierung oder Hemmung der Effektorsekretion steuert, im gesamten Zytosol lokalisiert sind, was darauf hindeutet, dass *Y. enterocolitica* einen anderen Mechanismus zur Steuerung der Sekretion verwendet als *E. coli*. Unsere Daten zeigen, dass die Vorgänge während und nach der Sekretion hochgradig reguliert sind und eine Vielzahl von Mechanismen benutzt wird, um die Umgebung zu erkennen und sich an sie anzupassen Dies erlaubt eine schnelle und effiziente Sekretion, um das Überleben der Bakterien während der Infektion zu sichern.

1. Introduction

Bacteria have evolved a variety of mechanisms to survive in different environments and interactions with eukaryotic organisms. Through evolution bacteria have developed complex machinery like the bacterial flagellum, which facilitates chemotaxis, and the injectisome, which translocates proteins from the bacteria into host cells. These apparatuses play a vital role in bacterial survival and although the flagella and injectisome differ in structure, they share the common protein export machinery called the type III secretion system (T3SS). The T3SS is highly conserved and essential for the function of both the flagellum and injectisome. The flagellum allows for bacterial motility in a variety of environments (McCarter *et al*, 1988; Kearns, 2010; Altegoer *et al*, 2014) and aids in attachment to surfaces (McCarter *et al*, 1988; La Ragione *et al*, 2003; Robertson *et al*, 2003; Friedlander *et al*, 2013, 2015); whereas the injectisome is used to translocate effector proteins into the host cytoplasm. The T3SS allows the export of extracellular components of the flagellar filament and injectisome (Cornelis, 2006; Galán & Wolf-Watz, 2006; Diepold & Armitage, 2015; Shaulov *et al*, 2017). Although the T3SS is an essential component in both the flagellum and injectisome systems, from this point forward we will use T3SS in reference to the injectisome and not the flagellum.

1.1 Structure of the T3SS injectisome

The injectisome consists of a membrane-spanning nanosyringe that translocates effector proteins from the bacteria into eukaryotic host cells. The injectisome is utilized by Gram-negative pathogens to manipulate host cells, ultimately allowing the bacteria to successfully disseminate throughout the host. Pathogens like *Salmonella*, *Shigella*, *Escherichia coli*, *Yersinia* and *Pseudomonas* utilize the T3SS for successful infection (Coburn *et al*, 2007). As shown in Figure 1, the injectisome can be divided into four distinct sections: the needle, the membrane rings, the export apparatus and the cytosolic components.

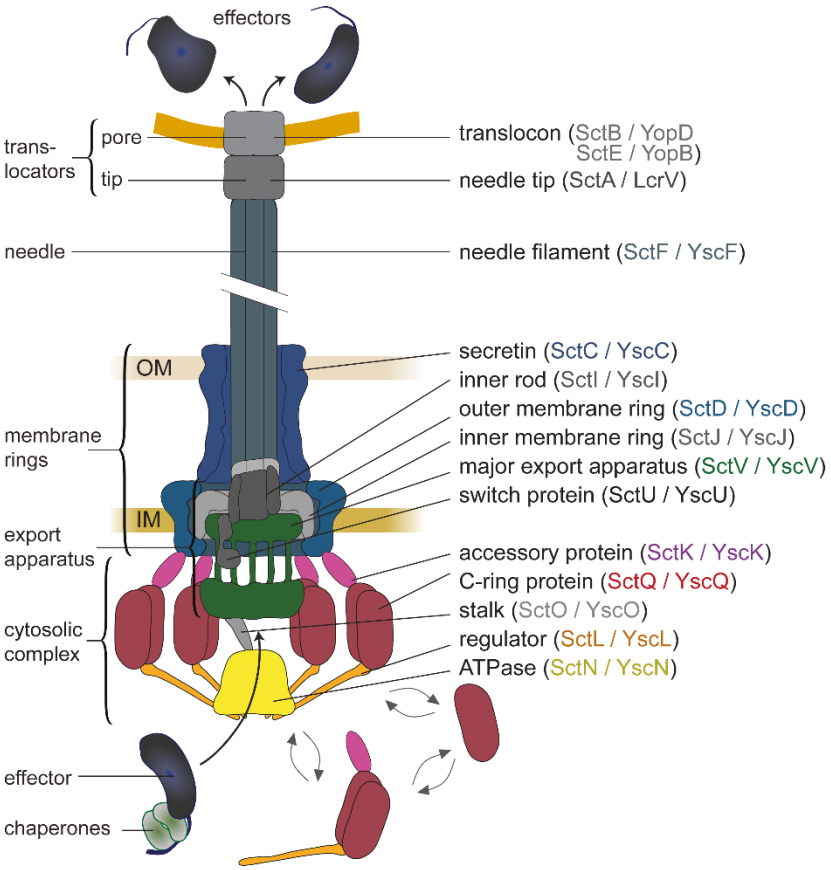

Figure 1: Overview of the type III secretion system.
The left side of injectisome is divided into four major components: the needle, the membrane rings, export apparatus and cytosolic complex. On the right, component names are given in common Sct and *Yersinia* specific (Ysc) nomenclature (Hueck, 1998; Wagner & Diepold, 2020). OM, outer bacterial membrane; IM, inner bacterial membrane. (Wimmi *et al*, 2019)

The needle bridges the bacterial cytosol and host cytoplasm by creating a pore in the host plasma membrane, which allows the translocation of bacterial effector proteins into the host (Håkansson *et al*, 1996; Nauth *et al*, 2018; Park *et al*, 2018). The needle is composed of SctF subunits that form an extracellular tube (Hoiczyk & Blobel, 2001) and SctI acts as an adapter between the export apparatus and the needle (Torres-Vargas *et al*, 2019). Needle length is determined by the "ruler protein", SctP (Journet *et al*, 2003). SctP measures the length of the needle by interaction with the base and the growing end of the needle (Agrain *et al*, 2005; Botteaux *et al*, 2008). Once at desired length, it is thought that SctP interacts with SctU to cease needle extension (Botteaux *et al*, 2008; Feria *et al*, 2012). At the distal end of the needle is the needle tip, that consists of SctA, which senses host cell contact (Deane *et al*, 2006). The membrane rings anchor the injectisome into the peptidoglycan and inner and outer membranes of the bacteria. The rings are composed of SctC, the outer membrane ring, as well as SctD and SctJ, which make up the inner membrane ring (Marlovits *et al*, 2004). The export apparatus (SctV), which is located within the inner membrane rings, facilitates the transition of effectors from the cytosol into the injectisome and without the export apparatus substrate export is inhibited or significantly reduced (Sukhan *et al*, 2001; Wagner *et al*, 2010). The components that make

up the export apparatus consist of the auto-protease SctU, and the inner membrane channel proteins SctR, SctS, SctT (Deng *et al*, 2017). The cytosolic components, commonly called the "sorting platform" (Lara-Tejero *et al*, 2011), are a dynamic set of proteins that interchange between the cytosol and the injectisome (Diepold *et al*, 2015, 2017), which may facilitate the attachment of chaperone-effector complexes prior to export (Spaeth *et al*, 2009; Lara-Tejero *et al*, 2011). It has been found that the cytosolic components in *Salmonella* actually aid in establishing a secretion hierarchy (Lara-Tejero *et al*, 2011), however, this has not been established in all organisms. The cytosolic components consist of SctN, SctQ, SctL, SctK and SctO. SctN is an ATPase, which is used to disengage the chaperone from the effector and unfold the effector prior to export (Akeda & Galán, 2005). SctQ, SctL and SctK form a pod-like complex and act as the sorting platform (Lara-Tejero *et al*, 2011), whereas SctO links SctN to SctV (Hu *et al*, 2015, 2017).

1.2 Function of the injectisome in T3SS-utilizing organisms

Many bacteria utilize the T3SS to promote survival in a variety of symbiotic and pathogenic relationships and the system is strongly conserved among Gram-negative bacteria (Hueck, 1998). For example, *Rhizobia* bacteria establish a mutualistic relationship with plants via the T3SS to promote survival in soil environments. On the other hand, pathogens like *Salmonella*, *Shigella* and *Pseudomonas* utilize their T3SS to manipulate the host immune system and promote infection. The T3SS is ultimately used to manipulate host cell behavior, which promotes bacterial survival.

Rhizobia are soil bacteria that belong to the *Azorhizobium*, *Bradyrhizobium* and *Rhizobium* genera (Viprey *et al*, 1998). These bacteria are able to create a symbiosis with legumes. This relationship allows for the legumes to utilize fixed nitrogen from the bacteria and the bacteria to receive nutrients from the legumes (Nelson & Sadowsky, 2015). The host plant initiates symbiosis by releasing flavonoids in the soil. The rhizobia sense the flavonoids and this allows the activation of nod factor production (Spaink *et al*, 1989). The bacteria can enter the legume through cracks in the lateral root (D'haeze *et al*, 2003), stem, or enter through curling of the root hair, which results from nod factor recognition (Esseling *et al*, 2003). The effectors are potentially used to promote nodule formation, suppress the plant immune response during invasion and manipulate the autoregulation of nodulation controlled by the plant (Macho & Zipfel, 2015).

Salmonella enterica is a gastro-intestinal pathogen that uses the T3SS to invade and colonize the host. Individuals become infected through the consumption of contaminated food and the bacteria travel to the small intestine (Giannella, 1996). *Salmonella* utilizes two T3SSs encoded on the *Salmonella* Pathogenicity Island (SPI) 1 and 2 (Van Der Heijden & Finlay, 2012). First the SPI-1 system is used to

invade host cells and elicit an inflammatory response. This enables the bacteria to invade immune and epithelial cells (Lou *et al*, 2019). Then the SPI-2 system is utilized to escape the *Salmonella* containing vacuole to allow for intracellular replication (Figueira & Holden, 2012). Both injectisomes are expressed heterogeneously among the population, resulting in two subpopulations (Sturm *et al*, 2011; Rundell *et al*, 2016). The SPI-1 active cells are used to invade epithelial and immune cells, thus inducing an inflammatory response, which removes competition in the intestinal lumen (Stecher *et al*, 2007; Müller *et al*, 2009; Knodler *et al*, 2010; Behnsen *et al*, 2014). Once competition is removed from the intestine, SPI-1 inactive bacteria are able to colonize the intestine (Diard *et al*, 2013). Together these subpopulations work together by using division of labor and bet-hedging strategies to promote successful infection (Weigel & Dersch, 2018; Davis & Isberg, 2019).

Shigella flexneri is an intracellular gastro-intestinal pathogen that utilizes a multistep infection process with the help of their T3SS. When *Shigella* is ingested, the bacteria travel to the large intestine where they cross the epithelial barrier via the M (microfold) cells and into the Peyer's patches (Wassef *et al*, 1989; Perdomo *et al*, 1994b). The bacteria will then encounter macrophages, where they are able to escape the vacuolar membrane and enter the macrophage cytoplasm. Within the macrophage cytoplasm, *Shigella* exports effector proteins that induce apoptosis (Zychlinsky *et al*, 1994; Schroeder *et al*, 2007). The bacteria that are able to escape the macrophage can then invade the basolateral side of the epithelial cell with the aid of the injectisome (Perdomo *et al*, 1994b). *Shigella* is ultimately able to invade neighboring epithelial cells by inducing actin polymerization (Bernardini *et al*, 1989) and stress fibers (Vasselon *et al*, 1991) within the host cell, allowing further dissemination throughout the host. Additionally, the recruitment of immune cells and subsequent permeability of the epithelial layer results in further invasion of bacteria (Perdomo *et al*, 1994a, 1994b). The T3SS enables *Shigella* to invade host cells (High *et al*, 1992; Du *et al*, 2016), replicate within epithelial cells (Sansonetti *et al*, 1986) and control immune responses during invasion (Ashida *et al*, 2015).

Pseudomonas aeruginosa is an opportunistic pathogen that is capable of colonizing a variety of locations within the host (wounds, respiratory tract, bloodstream and urinary tract) (Bodey *et al*, 1983). *P. aeruginosa* utilizes the T3SS to manipulate the host and promote infection by killing host cells and compromising epithelial integrity (Hauser, 2009). Specifically, the T3SS effectors modify the actin cytoskeleton (Cowell *et al*, 2005), inhibit phagocytosis (Frithz-Lindsten *et al*, 1997; Rocha *et al*, 2003) and induce cell death (Finck-Barbanç *et al*, 1997; Pederson & Barbieri, 1998). Although the T3SS promotes virulence within the host, the T3SS is not homogenously expressed and the T3SS-inactive subpopulation can benefit from the T3SS-active population during infection (Czechowska *et al*, 2014).

1.3 *Yersinia enterocolitica* as a pathogen and model organism

Yersinia enterocolitica is a Gram-negative, gastrointestinal pathogen closely related to *Y. pseudotuberculosis* and *Y. pestis. Y. enterocolitica* has a coccobacillus morphology and at temperatures below 28°C, is motile and peritrichous. However, at 37°C the bacterium has very few or no flagella resulting in poor motility (Bottone & Mollaret, 1977). *Y. enterocolitica* is commonly found in both wild and domesticated animals and is transmitted to humans through undercooked or raw food, as well as contaminated water (Bottone, 1997; Rosner *et al*, 2010; Råsbäck *et al*, 2018). Symptoms of a *Y. enterocolitica* infection (yersiniosis) consist of diarrhea, vomiting, fever and abdominal pain. Although most infections are self-limiting (Bottone, 1997) and do not require antibiotic intervention, severe infections can be treated with beta-lactam, third-generation cephalosporin and fluoroquinolone antibiotics (Gayraud *et al*, 1993; Jiménez-Valera *et al*, 1998; Fàbrega & Vila, 2012).

Y. enterocolitica is a gastrointestinal pathogen that invades the small intestine by using the T3SS to manipulate host epithelial and immune cells. Once *Yersinia* is ingested by the host, the temperature shift from the environment to the host (temperature of 37°C) results in assembly of the injectisome and expression of effectors, which are, however, not exported yet (Kupferberg & Higuchi, 1958). *Yersinia* pass through the gastrointestinal tract until reaching the small intestine, where the bacteria are able to enter the lymphatic system through M cells. Once the bacteria breach the intestinal epithelium, they begin replication in the Peyer's patches (Grutzkau *et al*, 1990) and will disseminate into the mesenteric lymph nodes (Fredriksson-Ahomaa *et al*, 2006) and in severe cases, result in systemic infections (Bottone, 1999).

When *Yersinia* comes into contact with immune cells, the bacteria significantly upregulate the expression and export of effectors (Cornelis *et al*, 1987; Pettersson *et al*, 1996; Wiley *et al*, 2007), as well as a 2-fold increase in injectisome components (Kudryashev *et al*, 2015). Attachment to host cells is facilitated by the binding of invasins (inv) and adhesions (ail) (Fredriksson-Ahomaa *et al*, 2006; Bottone, 1999) and this close contact is essential for the T3SS to create a pore. The pore is formed by the SctE and SctB (YopB and YopD) translocators, which establish a bridge between the bacterial cytosol and host cytoplasm (Håkansson *et al*, 1993, 1996; Neyt & Cornelis, 1999). The role of the effectors is to dampen the initial immune responses, which allows *Yersinia* to combat phagocytic cells long enough for infection to occur. Specifically, the effectors modify the host actin cytoskeleton preventing phagocytosis, controlling immune cell death, inhibiting inflammatory responses and pyroptosis (Grosdent *et al*, 2002; Philip *et al*, 2016).

In the lab, two strain backgrounds of *Yersinia enterocolitica* are used, ΔHOPEMTasd and MRS40. MRS40 is derived from the wild-type (WT) strain that secretes all effectors and is classified as biosafety level 2. ΔHOPEMTasd lacks the main virulence effectors (YopH, O, P, E, M, and T) and is auxotrophic for diaminopimelic acid (amino acid required for cell wall production) for survival and is classified as biosafety level 1.

1.4 Function of the effectors during infection in *Y. enterocolitica*

Effector proteins are used to modify host cell behavior, as shown in Figure 2, dampening the immune response and promoting dissemination throughout the host (Cornelis, 2006; Galán, 2009). *Yersinia* translocates YopH, O, P, E, M, T and Q (*Yersinia* outer protein) into the host cytoplasm. These effectors can be categorized by their function and target proteins: modify actin cytoskeleton – YopH, YopO, YopE and YopT (Grosdent *et al*, 2002); inhibition of cytokine and inflammatory responses – YopO, YopE, YopM, YopT and YopQ; induction of apoptosis – YopP (Philip *et al*, 2016); translocation regulation – SctW (YopN) and YopQ (Bamyaci *et al*, 2018).

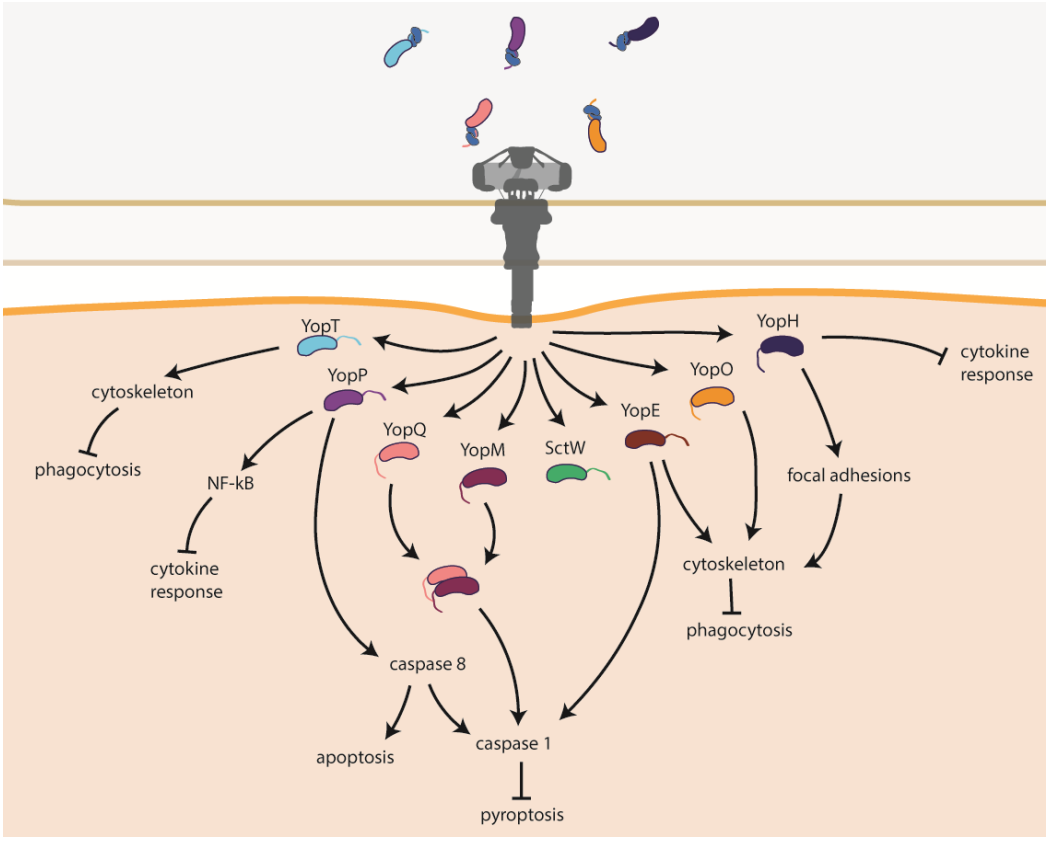

Figure 2: Function of effector proteins within an immune cell.
YopT modifies the actin cytoskeleton to prevent phagocytosis. YopP obstructs NF-κB and activates caspase 8 pathways, which initiates caspase 1 pathways and apoptosis. YopM, in the presence of YopQ, suppresses caspase 1 from initiating pyroptosis. YopE modifies the actin cytoskeleton, preventing phagocytosis, and suppresses caspase 1. YopO alters the actin cytoskeleton, prohibiting phagocytosis. YopH prohibits cytokine production and changes the focal adhesions, which prevents phagocytosis.

YopH is a protein-tyrosine phosphatase and is one of the first effectors translocated into the host. Specifically, YopH dephosphorylates focal adhesion complexes, which prevents phagocytosis (Bliska *et al*, 1991; Adkins *et al*, 2007) and inhibits cytokine responses to stop recruitment of immune cells (Philip *et al*, 2016). YopO is a serine/threonine protein kinase which modifies the actin cytoskeleton, inhibiting phagocytosis (Lee *et al*, 2015). YopT is described as a cytotoxin that targets Rho family GTPases, specifically RhoA (Zumbihl *et al*, 1999; Aepfelbacher *et al*, 2003), which interacts with the actin cytoskeleton (Shao *et al*, 2002, 2003; Navarro *et al*, 2005). YopP inhibits MAPK (mitogen-activating protein kinases) (Ruckdeschel *et al*, 1997a; Orth *et al*, 1999) and NF-κB (Ruckdeschel *et al*, 1998; Orth *et al*, 2000) pathways, as well as inducing apoptosis of immune cells (Monack *et al*, 1997; Mills *et al*, 1997; Erfurth *et al*, 2004). YopE is a cytotoxin (Rosqvist *et al*, 1990) and interacts with Rac proteins which halts phagocytosis (Andor *et al*, 2001), and induces apoptosis in immune cells (Ruckdeschel *et al*, 1997b). YopM, in the presence of YopQ, inhibits caspase 1 pathways which prevents inflammasome activation (Chung *et al*, 2014; Larock & Cookson, 2012). YopQ regulates the translocation rate of effectors during translocation (Garcia *et al*, 2006; Thorslund *et al*, 2011; Dewoody

et al, 2011). SctW holds both a regulatory and virulence role functioning as a gatekeeper, which prevents premature secretion activation, *yop* expression when secretion is inactivated, and is required for translocation of YopH and YopE (Forsberg *et al*, 1991; Cheng *et al*, 2001; Bamyaci *et al*, 2018, 2019).

1.5 Assembly of the T3SS

The assembly of the T3SS occurs in four distinct steps: assembly of the basal body and export apparatus; assembly of the cytosolic components; assembly of the inner rod and needle; and assembly of the tip and translocon. Two methods have been described for the assembly of the T3SS and this mainly stems around the insertion of the membrane rings, resulting in the inside-out method utilized by *Salmonella* (Wagner *et al*, 2010) or the outside-in used by *Yersinia* (Diepold *et al*, 2010, 2011). The inside-out method consists of the formation of the basal body and export apparatus within the inner membrane, beginning first with the assembly of the inner ring anchors, export apparatus and lastly the outer membrane ring (secretin, SctC). The outside-in model begins with anchoring the secretin protein in the outer membrane. The assembly of the inner membrane ring and the export apparatus occurs independently, although SctJ can bind to the export apparatus in the absence of SctC (Diepold *et al*, 2010, 2011). The formation of the inner rod and needle requires the export apparatus (Wagner *et al*, 2010) and the cytosolic components (Diepold *et al*, 2010). Once assembled, the injectisomes are able to export the tip and translocon, which allows translocation of effector proteins.

1.6 *Yersinia* virulence plasmid

All three pathogenic strains of *Yersinia* encode their T3SS on a virulence plasmid ranging from 66 to 72 kb in size (Gemski *et al*, 1980b, 1980a; Ben-Gurion & Shafferman, 1981; Ferber & Brubaker, 1981; Portnoy *et al*, 1984). Although the organization of the virulence plasmids differs between *Y. pestis*, *Y. pseudotuberculosis* and *Y. enterocolitica*, the genes that encode the T3SS components are conserved and highly similar (Hu *et al*, 1998). The T3SS genes can be categorized into machinery components (*yscB*-L, *yscN-U* and *lcrD*) and transcription and secretion regulation (*lcrR*, *lcrGVH*, *virF*, *sctW* and *yscM1*) (Hueck, 1998). Although the T3SS machinery is conserved, the distribution and location of the Yops on the pYV varies among the pathogenic species of *Yersinia* (Hu *et al*, 1998).

The *Yersinia* virulence plasmid (pYV) for *Y. enterocolitica* is shown in Figure 3. Expression of the T3SS is controlled by temperature and when the bacteria is exposed to 37°C, VirF is expressed and binds to multiple regions of the pYV, specifically: *yscA-L*, *lcrGVH*, *yopE* (Wattiau & Cornelis, 1994) and *yopH* (de Rouvroit *et al*, 1992). Although VirF is involved in the activation of the expression of the T3SS apparatus, it does not directly control the expression of the *yop* genes (de Rouvroit *et al*, 1992). *yop* expression is controlled by YscM1 (Michiels *et al*, 1991) and YscM2 (Stainier & Cornelis, 1997) via a

negative-feedback loop (Stainier & Cornelis, 1997). These proteins act in a concentration-dependent manner. In non-secreting conditions (high level of environmental calcium; no host contact), YscM1 and YscM2 are present in high concentration thus repressing the expression of the *yop* genes (Rimpilainen *et al*, 1992; Allaoui *et al*, 1994; Stainier & Cornelis, 1997). However, in secreting conditions (low level of environmental calcium; host cell contact), YscM1 and YscM2 are exported and this decrease in protein concentration allows for upregulation of the *yop* genes (Pettersson *et al*, 1996; Stainier & Cornelis, 1997).

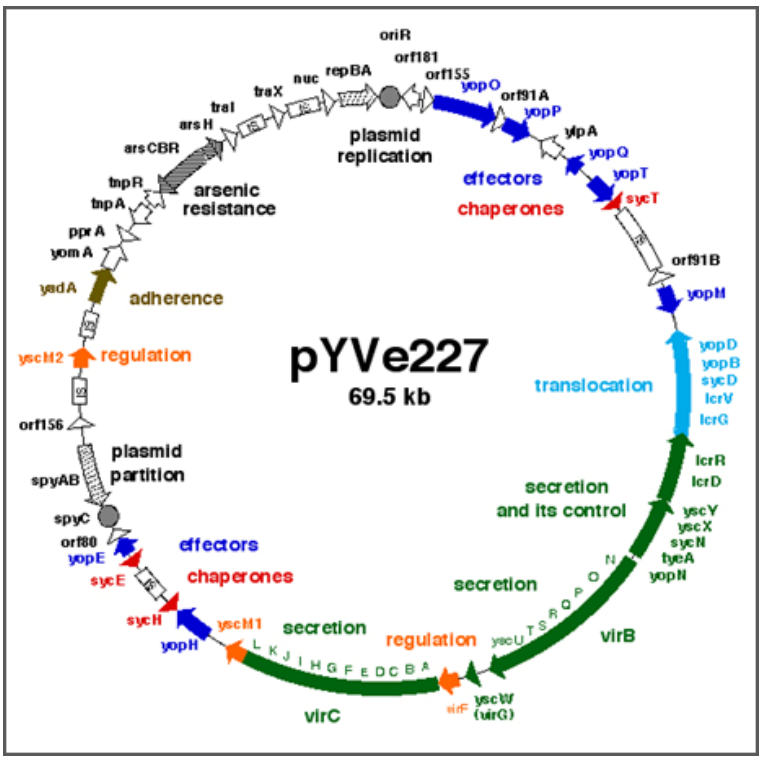

Figure 3: Genetic map of the pYVe227 virulence plasmid for *Y. enterocolitica* W22703.
Y. enterocolitica virulence plasmid that is closely related to MRS40 (pYVe40), which has been primarily throughout this study. Genes are organized by color to distinguish the part of the injectisome they encode for. Green – genes that encode the Ysc apparatus components. Light blue – genes that encode the translocators, Dark blue – genes that encode virulence effector proteins. Red – genes that encode effector chaperones. Brown – gene that encodes adhesin. Gray – genes that encodes arsenate resistance. Orange – genes that are involved in gene expression regulation. Taken from Iriarte & Cornelis, 1999.

1.7 Regulation of the T3SS in *Y. enterocolitica*

1.7.1 Thermoregulation of the injectisome

T3SS components are regulated on several levels and use different environmental cues to control regulation of injectisome assembly and effector expression. Injectisome assembly is controlled by temperature, specifically from the environment and host. In environmental conditions (temperatures below 30°C), *Yersinia* are motile and peritrichous (Bottone & Mollaret, 1977) and are not expressing

the injectisome. However, when the bacteria transition into the host, they begin to express and assemble the injectisome. This regulation is controlled by two mechanisms on transcriptional and translational levels, as shown in Figure 4. At environmental temperatures (25°C), the yscW-lcrF operon is partially repressed by YmoA homodimers and YmoA-N-HS heterodimers (Nieto et al, 2002) and lcrF mRNA that is transcribed is fully repressed by a two-stem-loop found on the 5' end (RNA thermometer, RNAT) that prevents the ribosome from translating (Böhme et al, 2012). However, when the bacteria are shifted to 37°C, YmoA is degraded by ClpP and Lon proteases, allowing full transcription of the operon (Jackson et al, 2004). Additionally, the two-stem-loop is melted at 37°C, resulting in efficient translation of LcrF (VirF in *Y. enterocolitica*) (Böhme et al, 2012). LcrF/VirF is the transcriptional activator for expression of the T3SS proteins on the pYV (Skurnik & Toivanen, 1992; Wattiau et al, 1994).

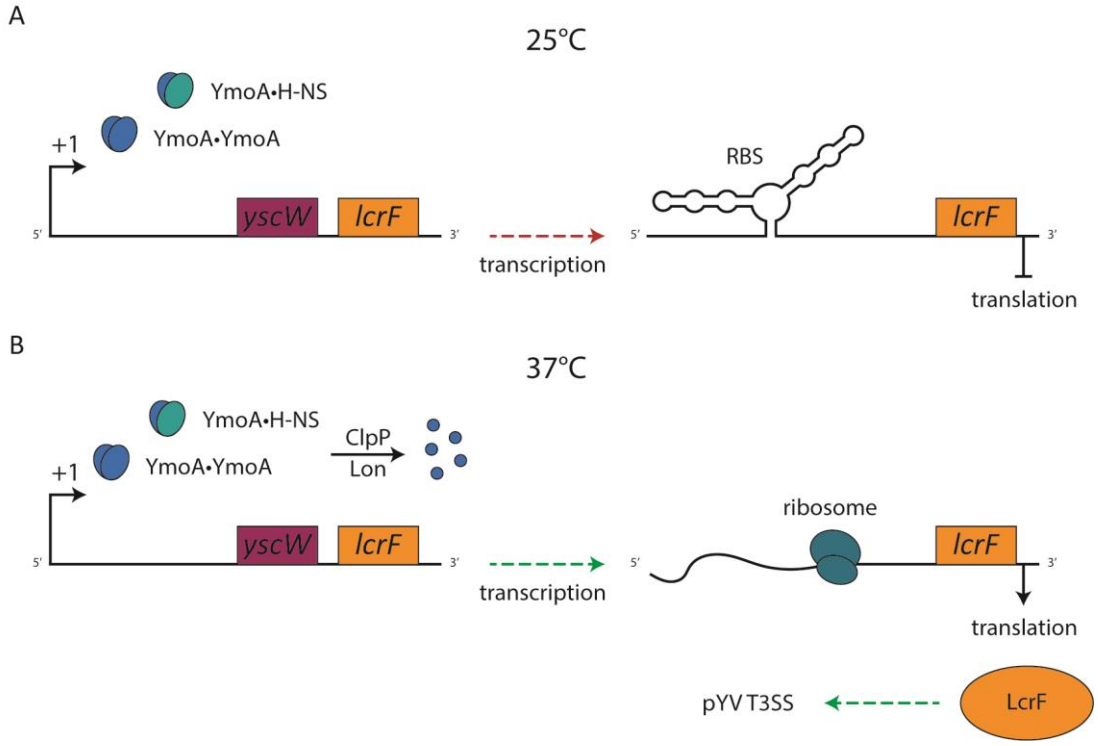

Figure 4: Thermo-regulation of LcrF (homologue to VirF in *Y. enterocolitica*) by YmoA and RNAT.
(A) At 25℃, the *ycsW-lcrF* operon is partially repressed by YmoA homodimers and YmoA-H-NS heterodimers, preventing transcription. Translation is fully prepressed by the RNAT, a two-stem-loop structure in the mRNA found on the *lcrF* mRNA. **(B)** At 37℃, YmoA homodimers and YmoA-N-HS heterodimers are cleaved by ClpP and Lon proteases allowing full transcription of the *lcrF* operon. The RNAT in the *lcrF* mRNA is melted at higher temperatures, allowing translation of LcrF, which activates transcription of the pYV. Based on De Nisco *et al* (2018).

1.7.2 Counter-regulation of motility and virulence

Temperature not only regulates the injectisomes, but also the flagella. Expression of these two systems is counter-regulated in *Y. enterocolitica*. In environmental conditions (temperatures below 30°C), the expression of the flagella is upregulated allowing the bacteria to be motile. However, in

host conditions (37°C), the flagellum becomes downregulated and existing flagella are shed (Darland et al, 1974; Bottone & Mollaret, 1977; Minnich Scott A. and Rohde, 2007), and the expression of injectisome components is upregulated (Skurnik et al, 1984; Michiels et al, 1991; de Rouvroit et al, 1992; Hoe & Goguen, 1993). This counter-regulation is controlled on a transcriptional level where the expression of the main transcription factors for the flagella (FlhDC) are active at environmental temperatures, but not host temperatures, and vice versa for the injectisome transcription factor (LcrF). This regulation corresponds to the switch from motility (in environmental conditions) to virulence (in host physiological conditions) (Bleves *et al*, 2002; Horne SM *et al*, 2006; Soscia *et al*, 2007). This temperature control between motility may also be involved in maintaining specificity between both flagellar and injectisome T3SS, as well as preventing host immune responses to the flagella (Diepold & Armitage, 2015).

1.7.3 Substrate specificity switches

The T3SS is composed of three substrate classes: early substrates (rod and needle subunits), middle substrates (translocators) and late substrates (effector proteins). The export of these substrates occurs in a hierarchical manner to allow for the formation of functional injectisomes, as shown in Figure 5. Once the basal body is assembled, the insertion of the inner rod (SctI) and the interaction of the ruler protein (SctP) with the base of the needle complex is vital for the export of the needle subunits (Kubori et al, 2000; Kimbrough & Miller, 2000). The priming of the needle complex with the inner rod and the ruler protein marks the switch to early substrate export. SctP is known to control the length of the needle, where the C-terminus is attached to the base of the needle complex and the N-terminus interacts with the end of the growing needle (Agrain et al, 2005; Botteaux et al, 2008). SctU has also been found to interact with SctP and both are believed to bring a stop to needle growth, leading to the switch between early and middle substrates (Botteaux et al, 2008; Feria et al, 2012; Ho et al, 2017), however, this interaction *in vivo* remains unclear. Needle growth ceases once SctP interacts with the distal end of the needle, this interaction initiates the switch for export of the middle substrates (Shen et al, 2012). By capping the distal end of the needle with SctA, export of the middle substrates is inhibited, thus stopping needle growth (Poyraz et al, 2010). The needle tip consists of the hydrophilic protein SctA, which forms a pentamer (Broz et al, 2007). At this stage, the needle is prepared to make host cell contact, which will mark the switch to the late substrates. Host cell contact is sensed by the needle tip (Veenendaal et al, 2007; Roehrich et al, 2013; Armentrout & Rietsch, 2016) resulting in the release of the gatekeeper, SctW (Day & Plano, 1998; Iriarte et al, 1998; Ferracci et al, 2005). The gatekeeper allows the export of SctB and SctE in *Salmonella*, *Shigella*, *Chlamydia*, and EPEC (Lara-Tejero et al, 2011; Cherradi et al, 2013; Archuleta & Spiller, 2014; Gaytán et al, 2018) and suppress effector export (Deng et al, 2004, 2005; Martinez-Argudo & Blocker, 2010; Cherradi et al,

2013). The translocator pore proteins (SctB and SctE) interact with the needle tip (Mueller et al, 2005; Broz et al, 2007; Johnson et al, 2007) and create a pore in the host plasma membrane (Håkansson et al, 1996; Neyt & Cornelis, 1999; Blocker et al, 1999; Goure et al, 2004; Picking et al, 2005; Nauth et al, 2018) to allow translocation of the effector proteins (Schlumberger et al, 2005; Enninga et al, 2005; Mills et al, 2008; Wolters et al, 2015).

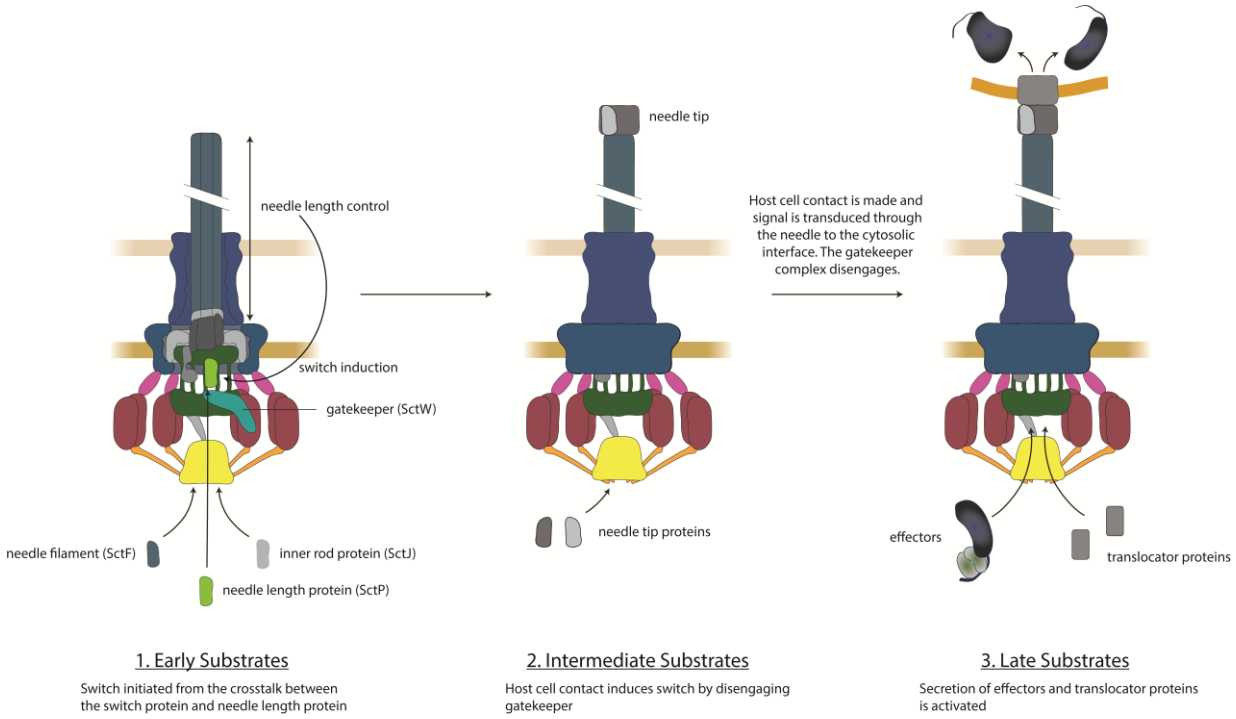

Figure 5: Substrate specificity switches of the T3SS.
The export of the early substrates allows for the formation of the needle until it has reached its specified length, which is determined by the ruler protein. The ruler protein then allows the switch from early to intermediate substrates, the needle tip proteins, through interactions with the switch protein (1). The needle tip is able to sense host contact and this signal is transduced through the needle to the cytosolic interface of the injectisome. This signal allows for the disengagement of the gatekeepers (SctW, main gatekeeper protein, and associated complex proteins) (2). Then the late substrates, which is made up of the effectors, are able to be translocated into the host cell (3). Based on Diepold & Wagner (2014).

1.7.4 Heterogeneity in T3SS expression

Many pathogens utilize their injectisomes to promote survival and enhance pathogenicity (Büttner, 2012; Deng et al, 2017), but how they express their injectisomes varies among different organisms. Some pathogens, such as *Salmonella enterica* and *Pseudomonas aeruginosa*, heterogeneously express their T3SS resulting in two subpopulations to promote successful infection (Rietsch & Mekalanos, 2006; Sturm et al, 2011; Rundell et al, 2016). Usually, heterogeneous expression allows for the survival of the clonal population at the expense of a subpopulation. This behavior is evident in T3SS-active *Salmonella*, which use their T3SS to infiltrate the intestinal epithelial and induce an inflammatory response that removes competition in the intestinal lumen (Stecher et al, 2007; Müller et al, 2009; Knodler et al, 2010; Behnsen et al, 2014). This allows the T3SS-inactive subpopulation to then colonize

the lumen. However, the T3SS-active bacteria experience growth retardation (Kupferberg & Higuchi, 1958; Mehigh *et al*, 1989; Fowler & Brubaker, 1994; Sturm *et al*, 2011), resulting in the T3SS-inactive population outgrowing the T3SS-active population (Sturm et al, 2011; Diard et al, 2013; Sánchez-Romero & Casadesús, 2018; Weigel & Dersch, 2018). Ultimately, this cooperative virulence demonstrates that the T3SS-active population sacrifice themselves to improve their genetic fitness and successful infection.

1.8 Growth retardation during secretion

During secretion, T3SS-utilizing bacteria experience growth retardation (Kupferberg & Higuchi, 1958). This behavior is well documented and is what led to the discovery of the T3SS in *Yersinia* (reviewed in Schneewind, 2016), however, the link remains unclear on why *Yersinia* inhibits division during secretion. Several hypotheses have been suggested consisting of: metabolic burden resulting from biosynthesis, assembly and operation of the T3SS (Brubaker, 1983, 2005; Sturm *et al*, 2011; Wilharm & Heider, 2014; Wang *et al*, 2016); the leakage of amino acids or ions that are co-exported with effectors (Fowler & Brubaker, 1994; Fowler *et al*, 2009); or a combination of both. The metabolic burden is currently the most common explanation for why secreting bacteria are unable to grow.

The assembly and maintenance of the T3SS is thought to be energetically taxing and may result in growth arrest. This transition from non-secreting to secreting conditions suggests the modification of metabolic pathways to support the biosynthesis related to T3SS activation (Schmid *et al*, 2009). YscM1 and YscM2 are not only involved in *yop* regulation (Pettersson *et al*, 1996; Bahrani *et al*, 1997; Stainier & Cornelis, 1997), but also metabolic regulations by repressing phosphoenolpyruvate carboxylase (PEPC) (Schmid *et al*, 2009). Under non-secreting conditions, YscM1 represses PEPC activity, however, when secretion is activated, YscM1 is secreted and is unable to reduce PEPC activity, thus allowing modification of the metabolism (Schmid *et al*, 2009). Schmid and colleagues proposed the "load and shoot" model, where the T3SS requires two phases: 1) loading – biosynthesis of Yop proteins in preparation of immune cell attack; 2) shooting – export of the pre-synthesized pool. Under the first stage, PEPC activity is required to replenish amino acids for synthesis from the tricarboxylic acid cycle. During stage two, the bacteria are required to maintain the energy charge level and Yop production over general biosynthesis and population growth by reducing PEPC activity (Schmid *et al*, 2009). The effect of secretion on the bacterium was found to induce a lower energy charge than that of non-secreting bacterium (Zahorchak *et al*, 1979), however, the relationship between secretion and metabolic burden still requires further study.

Ion and amino acid leakage during T3SS activation has been suggested to affect bacterial propagation. Fowler and colleagues suggest ions leaked or co-exported through the T3SS potentially affect their

ability to uptake essential nutritional components, resulting in growth arrest (Fowler *et al*, 2009). Also, the addition of ions and amino acids (such as Na^+, L-glutamate and L-aspartate) to the medium negatively affects bacterial growth and recovery in Ca^{2+} deficient media (Brubaker, 1967, 2005; Fowler & Brubaker, 1994; Fowler *et al*, 2009). They propose that Ca^{2+} alleviates Na^+ sensitivity in growth media and the extracellular environment within the host contains high levels of Ca^{2+}, whereas in visceral organs these ions are not present, thus alleviating any toxicity (Kugelmass, 1959; Fowler *et al*, 2009). This suggests that T3SS activation has a negative effect on the bacteria, however, the relationship between growth retardation and leakage of ions and amino acids remains unclear.

1.9 Translocation of T3SS effectors proteins in *Y. enterocolitica*

Effectors can be exported into the supernatant/environment or directly into the host cell, in processes called secretion or translocation, respectively. These events can be initiated by either host cell contact or can be artificially induced either by calcium depletion for *Yersinia* (Kupferberg & Higuchi, 1958), the addition of Congo red dye (Parsot *et al*, 1995; Bahrani *et al*, 1997) for *Shigella*, or the combination of decreased pH and nutrient deprivation for the *Salmonella* SPI-2 system (Deiwick *et al*, 1999; Beuzón *et al*, 1999; Rappl *et al*, 2003; Yu *et al*, 2010). Within the host, the extracellular fluid was shown to have high levels of, whereas the intracellular environment (within the host cells) were found to have low calcium levels (Carafoli, 1987). As a result, *Yersinia* does not secrete in an environment that mimics the extracellular calcium levels (high calcium concentrations; non-secreting conditions), however secretion is activated when the bacteria are exposed to conditions that mimic the intracellular calcium levels (low calcium concentrations; secreting conditions) (Grosdent *et al*, 2002; Philip *et al*, 2016).

1.9.1 Function of the gatekeepers

Reacting to the environmental levels of calcium is essential in allowing *Yersinia* to precisely time effector export, prevent the waste of effector proteins and avoid alerting the immune system. This vital job is carried out by the gatekeepers. This complex in *Y. enterocolitica* is made up of: SctW, the main gatekeeper that is exported into the host cell ; two chaperones, YscB and SycN; and the inhibitory protein TyeA (Iriarte et al, 1998; Cheng et al, 2001; Day et al, 2003) . When low calcium levels or host cell contact is sensed, SctW is disengaged from the complex and is exported out of the cell, followed by the subsequent effectors (Ferracci et al, 2004). The cue for deactivation of the T3SS remains unclear, but following sufficient secretion, the gatekeeper complex needs to be reestablished to prevent further secretion. All components of the gatekeeper complex are essential in responding to the change in calcium levels and without any of these components, the bacteria constitutively secrete regardless of the environmental calcium levels (Ferracci et al, 2004). Two mechanisms for the gatekeeper complex have been considered, one describing a physical “plugging” of the cytosolic

interface, which prevents the export of effectors in high calcium environments (Büttner, 2012; Fàbrega & Vila, 2012), and the other suggesting either an order of secretion or delocalized regulation (Cheng et al, 2001). The gatekeepers, SepD and SctW (SepL), of pathogenic *E. coli* (enteropathogenic and enterohemorrhagic *E. coli*, EPEC and EHEC, respectively) have been found to be physically bound to the cytosolic interface of the injectisome and are essential for regulating translocation export (Deng et al, 2005; Portaliou et al, 2017; Gaytán et al, 2018). Unlike *Yersinia*, *E. coli* utilizes its gatekeepers to control the switch between translocator and effector export. The gatekeepers allow for the export of the translocators in high calcium environments or prior to host cell contact, however, when low calcium environments or host cell contact is sensed, SepD and SctW suppress the export of the translocators and allow effector export (Deng et al, 2005; Younis et al, 2010; Deng et al, 2015; Shaulov et al, 2017; Portaliou et al, 2017; Gaytán et al, 2018). Although this two-step process in exporting the translocators and effectors in *E. coli* appears to demonstrate different regulation than *Yersinia*, the *Yersinia* gatekeepers are vital for sensing environmental cues and establishing control for translocator and effector export (Cheng et al, 2001; Ferracci et al, 2004, 2005; Deng et al, 2005). Nonetheless, the molecular interactions of the gatekeepers and the T3SS in *Yersinia* remains unclear.

1.9.2 Hierarchical export of the effectors

While studies suggest a high degree of regulation for effector export, the exact determination and adaptation of the coordination of effector secretion remains unknown in *Y. enterocolitica*. Activation of secretion and translocation events are highly controlled, where the export of the effectors is dependent on translational and transcriptional regulation, the use of other effectors to control translocation rate, as well as the presence of chaperones (Mills *et al*, 2008, 2013; Dewoody *et al*, 2011; Berger *et al*, 2012). These levels of regulation are thought to establish a secretion hierarchy among the effectors. This may allow the bacteria to precisely control host cell behavior, specifically by inhibiting host cell inflammatory pathways and inducing apoptosis at specific times. *Salmonella* utilizes a sorting platform, where translocators are exported prior to the effectors. Lara-Tejero and colleagues suggest that recognition of chaperone-substrate complexes with the sorting platform may be dependent on the interaction with the chaperone itself (Lara-Tejero et al, 2011). Whereas in *E. coli*, the gatekeeper complex interacts with the injectisome to selectively export the translocators prior to the effectors (Deng *et al*, 2005; Portaliou *et al*, 2017; Gaytán *et al*, 2018).

The chaperones have been found to play an integral role in translocation, where the chaperones keep the effectors partially unfolded (Stebbins & Galan, 2001), guide them to the cytosolic interface and ultimately increase the effector concentration prior to export (Rathinavelan *et al*, 2010; MacDonald *et al*, 2017). Interestingly, chaperone expression affects the export of effectors, specifically: the

overexpression of SycO (chaperone of YopO) reduces export of all substrates (translocators and effectors) (Dittmann *et al*, 2007); the overexpression of SycH promoted effector export of YscM1/2 (negative regulators of *yop* expressions), the needle tip (SctA) and SctB/E (translocators) in non-secreting conditions (Cambronne *et al*, 2000; Wulff-Strobel *et al*, 2002); and deletion of SycH resulted inhibition of YopH and YscM1 secretion (Cambronne *et al*, 2000). Additionally, the chaperones prevent mislocalization and premature degradation of the effectors prior to secretion (Wattiau *et al*, 1994; Frithz-Lindsten *et al*, 1995; Page & Parsot, 2002). Most effectors are co-expressed with their cognate chaperone (Wattiau *et al*, 1994; Button & Galán, 2011), and although chaperones promote more efficient translocation, they are not required by all effectors for export (Letzelter *et al*, 2006; Ernst *et al*, 2018). The chaperones bind to the effector proteins in dimers, resulting in a 2:1 chaperone to effector ratio (Cheng & Schneewind, 1999; Ghosh, 2004).

In order for effectors to be exported, a signal is needed to allow the proteins to translocate through the injectisome. These export signals are encoded on the N-terminal region of the effector and currently two different export signals are known – a short signal that allows for export of proteins in the environment and a long signal that grants translocation into host cells (Figure 6). The short signal is commonly called the secretion signal, which usually consists of the first ~20 amino acids. The longer signal termed the translocation signal contains the first ~50 amino acids (Sory *et al*, 1995; Schesser *et al*, 1996; Köberle *et al*, 2009; Autenrieth *et al*, 2010) and longer sequences (containing up to 140 amino acids) include the chaperone binding domain (CBD) (Cornelis & Gijsegem, 2000; Boyd *et al*, 2000). In *Yersinia*, the effectors and heterogeneous cargo (i.e. fluorescent or non-native proteins) can be secreted or translocated through the injectisome without the CBD (Sory *et al*, 1995; Cheng *et al*, 1997), however, this is not the case for all organisms. For *Salmonella*, the CBD is essential for injectisome-specific export and if the CBD is removed the proteins can then be exported through the flagellar T3SS (Lee & Galán, 2004). The export signals play a vital role in the export of effectors and heterogeneous cargo, but how these protein domains interact with the injectisome remains unclear.

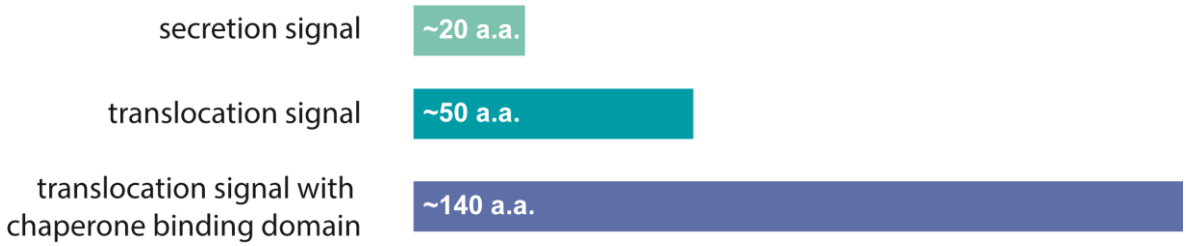

Figure 6: Export signals of T3SS substrates.
Export signals are located on the N-terminus of the type III secretion system effector, which allow these proteins to be exported through the injectisome. The secretion signal contains approximately the first 20 amino acids (a.a.) and allows export of cargo into the supernatant or environment. The translocation signal is composed of approximately the first 50 amino acids, including the export signal, and allows export of cargo into host cells and the environment. The translocation signal containing the chaperone binding domain makes up approximately the first 140 amino acids and has the ability to interact with the cognate chaperone of the effector.

1.9.3 Effector synthesis and export kinetics

Activation of the T3SS results in the export of up to a thousand effectors per minute per bacterium (Schlumberger et al, 2005; Enninga et al, 2005). How the bacteria manage to export their effectors remains unknown and has led to many questions on how bacteria prepare prior to activation. Does *Yersinia* utilize a pre-synthesized pool of effectors and, if so, how large is this pool? Is the translation and export of the effectors a one- or two-step process?

The pre-synthesized effector pool model would require a pool of effectors to be expressed prior to activation of the T3SS. Once export is initiated, the bacterium would deplete their intracellular pool and begin resynthesizing new effectors for export. Looking at the secretion rate, there would be two waves of effector export, with the first wave being the quick export of the pre-synthesized pool, followed by a decrease in secretion rate where the bacteria expresses and exports newly synthesized effectors (Figure 7.A). If a pre-synthesized pool is not produced, this would require rapid synthesis and export of effectors in order to quickly combat immune cells. In this case, the secretion rate of effectors would appear linear over time (Figure 7.B).

Translational regulation is vital in providing the necessary effectors to ensure survival when combating immune cells. Post-translation and co-translational synthesis and export offer two potential models explaining how the bacteria are able to quickly express and translocate proteins into host cells. The co-translational model describes a one-step mechanism where effectors are directly expressed into the injectisome for subsequent export. If effectors would be translated and exported in this way, it would require ribosomes to be located near the injectisomes (Figure 7.C). The post-translational regulation model describes a two-step process where effectors are synthesized in the cytosol followed by delivery to the injectisome, potentially with the aid of chaperones. In this model, synthesis would be cytosolic where translation by the ribosome would occur throughout the bacterium and in addition to coordinated delivery of the effectors to the injectisome (Figure 7.C).

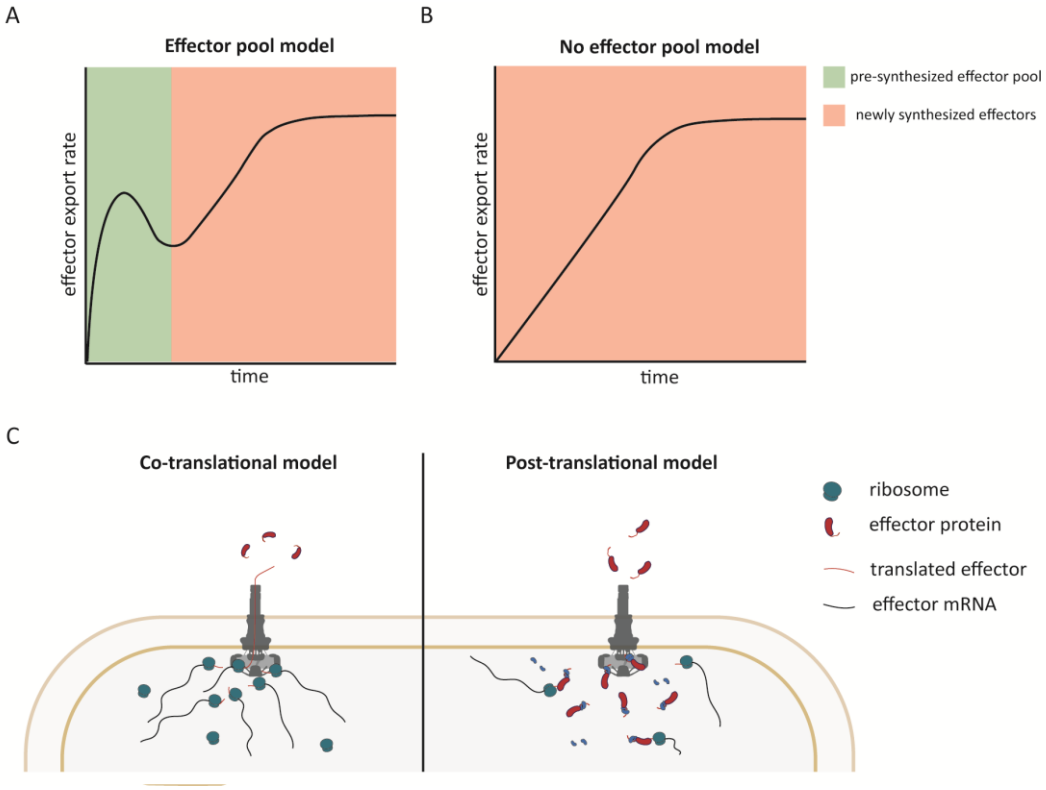

Figure 7: Effector export models.
(A) Pre-synthesized effector pool model describes a pool of effectors produced prior to export activation that are quickly exported demonstrating a rapid export rate, followed by a decrease in secretion rate. As effector biosynthesis is initiated, effectors are then exported as they are produced. **(B)** No effector pool model describes a linear export rate of effectors, where effectors are synthesized and subsequently exported. **(C)** Co-translational effector export model demonstrates translation of effector mRNA, followed by the newly synthesized protein being exported. Post-translational export model illustrates the expression of effectors that are then protected and guided by their cognate chaperones to the injectisome prior to export.

Translation and export is vital for successful infection; however, much remains to be elucidated in how these mechanisms are connected. Additionally, the role of the chaperones in this process and whether chaperones are needed more heavily at different points during secretion (Büttner, 2012; Finn *et al*, 2017).

1.9.4 Deactivation of secretion

The cue for deactivation also remains unclear, but it is suggested that down regulation of effector translocation is controlled by YopQ (YopK in *Y. pestis* and *Y. pseudotuberculosis*) (Garcia et al, 2006; Thorslund et al, 2011; Dewoody et al, 2011). YopQ regulates the translocation rate of the effectors and is suggested to be one of the first proteins exported following SctW. In *yopQ* mutants, *Yersinia* is unable to control export resulting in increased effector translocation, however, if YopQ is overexpressed, the bacterium is unable to translocate YopE and YopH. It is hypothesized that as the concentration of YopQ increases within the host, translocation of the effector proteins slows down

(Holmström et al, 1997). Although *yopQ* mutants demonstrate a higher translocation rate and cytotoxicity, these strains are attenuated by the host (Dewoody et al, 2011). Interestingly, YopQ interacts with the translocators and has been shown to play a role in pore size, where *yopQ* mutants create a larger pore in the host membrane (Holmström et al, 1997; Dewoody et al, 2011). As seen in Figure 8, two models have been described to explain how YopQ deactivates secretion: 1) signal transduction model – exported YopQ binds to the pore and initiates a confirmation change in the injectisome to inhibit secretion; 2) plug model – exported YopQ accumulates at the pore and mechanically prevents the effectors from entering the host cell (Dewoody et al, 2013). Effector proteins YopE and YopT also function to inhibit further pore formation by other injectisomes, thus preventing an overload of effectors in the host cell (Viboud & Bliska, 2001; Aili et al, 2008; Mejía et al, 2008).

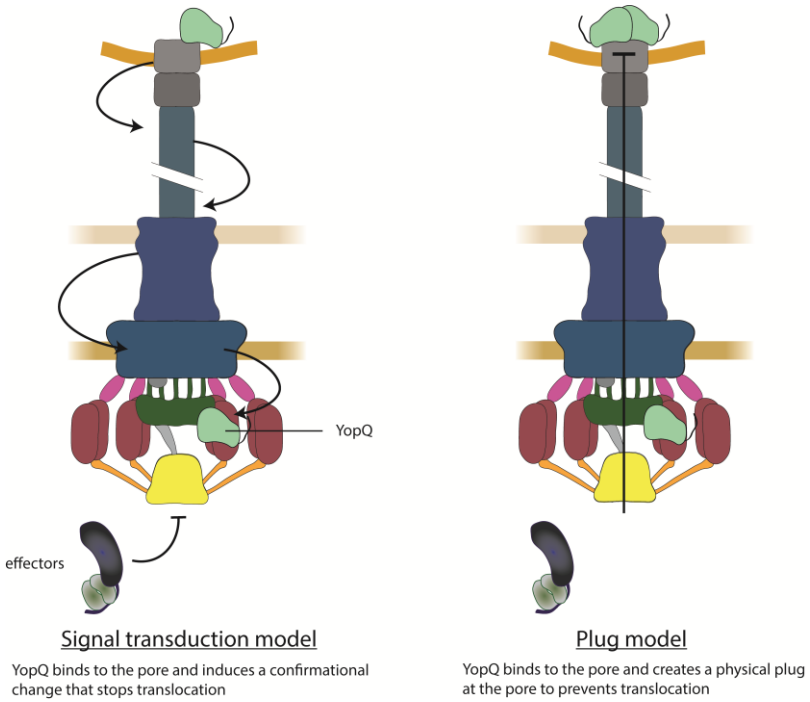

Figure 8: Models of YopQ (YopK in *Y. pestis* and *Y. pseudotuberculosis*) function for deactivation of effector export. Signal transduction model – YopQ interacts with the pore, which results in a conformational change in the pore. The changes in the pore initiates structural changes in the needle, then signaling to the basal body to stop effector export. Plug model – YopQ binds to the pore and physically seals the pore preventing further export of effectors. Based on Dewoody et al (2013).

2. Aims

Pathogenic bacteria utilize their injectisomes to manipulate the host immune system to promote infection. Over the last decades, studies have elucidated not only the intricate structure of the injectisome, but also the overall mechanism of how the injectisome works. In contrast, the molecular function and regulation of secretion, especially in relation to native infection, remains largely unclear. Using *Y. enterocolitica* as a model organism, I aimed to demonstrate the molecular mechanisms and regulation of the T3SS injectisome, specifically in relation to responding to different environments and exporting native and heterogeneous cargo during secretion.

In this work, I characterized the mechanisms that control secretion and translocation. Effector export is vital, however, what happens after secretion remained unknown. I explored the adaptivity of the T3SS in response to different environments, especially in relation to activating and deactivating the system and reestablishing division following secretion using sensitive enzymatic assays, fluorescence microscopy and growth curve experiments. Additionally, I sought to understand the link between secretion and growth retardation by employing metabolomic approaches to measure the levels of AMP, ADP, and ATP in secreting and non-secreting cultures over time to establish if the energy levels within the cells are the reason secreting cultures are unable to grow. To further understand host-pathogen interaction, I established eukaryotic cell lines within the lab to utilize infection assays and, in collaboration with Florian Lindner, examined the ability to utilize optogenetic systems to control cargo export into host cells. Lastly, I investigated the role of effector chaperones to promote secretion and understand how chaperone-effector complexes interact with the injectisome.

3. Results

3.1 Life after secretion - *Yersinia enterocolitica* rapidly toggles effector secretion and can resume cell division in response to changing external conditions

Y. enterocolitica utilizes its T3SS to counteract the immune response by preventing phagocytosis, inhibiting inflammatory responses, and promoting efficient dissemination throughout the host (Navarro *et al*, 2005; Cornelis, 2006; Galán, 2009; Pha & Navarro, 2016). During infection, *Y. enterocolitica* can encounter host cells and after the interaction dissociate, potentially interacting with other host cells. Although the initial interaction between host cells and T3SS-utilizing bacteria is well-described, post-secretion events remain unclear. These post-secretion events consist of deactivation, reestablishment of bacterial cell division, and possibly the reactivation of the T3SS. By understanding these events, we can gain more insight into how *Y. enterocolitica* is able to interact with its environment to promote survival and pathogenesis. Thus, we used fast and quantitative *in vitro* secretion assays to measure activation and deactivation of the T3SS, monitored cellular division and growth throughout these secretion events, and determined if previously secreting bacteria can reactivate secretion. Our results show that activation and deactivation of the T3SS occurs immediately in response to changes in secretion cues, and following deactivation the bacteria are able to reestablish division while maintaining functional T3SS that are able to be reactivated.

This study has been peer-reviewed and published in Frontiers Microbiology on 13 September 2019.

Milne-Davies B, Helbig C, Wimmi S, Cheng DWC, Paczia N, Diepold A. Life After Secretion-*Yersinia enterocolitica* Rapidly Toggles Effector Secretion and Can Resume Cell Division in Response to Changing External Conditions. Front Microbiol. 2019 Sep 13;10:2128. doi: 10.3389/fmicb.2019.02128. PMID: 31572334; PMCID: PMC6753693.

3.1.1 Authors contribution

I contributed to this published paper by conceiving the study, designing and performing experiments, analyzing data, and writing the paper.

Carlos Helbig contributed by generating and analyzing microscopy images and generating strains and plasmids (strains and plasmids labeled with CH or pCH, respectively).

Stephan Wimmi contributed by generating and analyzing microscopy images.

Dorothy W. C. Cheng contributed by generating microscopy images.

Nicole Paczia contributed by performing mass spectrometry for measuring AXP (AMP, ADP, and ATP) levels and analyzing data to determine energy charge of the samples.

Andreas Diepold contributed by conceiving the study, designing and performing experiments, analyzing data, and writing the paper.

3.1.2 Expression and assembly of the *Y. enterocolitica* T3SS is uniform and stable under different conditions

Earlier visualizations of T3SS components within *Y. enterocolitica* showed that most bacteria express the T3SS, and the injectisomes are localized in a non-random pattern of small patches visible as fluorescent foci at the bacterial surface (Diepold et al, 2010; Kudryashev et al, 2015; Diepold et al, 2017). To quantify the fraction of T3SS-positive *Y. enterocolitica*, we analyzed how many bacteria within a population displayed this standard pattern of fluorescence for functional EGFP-labeled fusions of a T3SS inner membrane ring protein (SctD), and a cytosolic protein (SctQ) at 37°C (Figure 9.A). Both under non-secreting conditions (presence of 5 mM Ca^{2+} in the medium) and secreting conditions (chelation of Ca^{2+} by addition of 5 mM EGTA), all or almost all bacteria were T3SS-positive (Figure 9.B and C). Even after long-term incubation under secreting conditions for three hours, the vast majority of bacteria (>98%) were T3SS-positive (Figure 9.D).

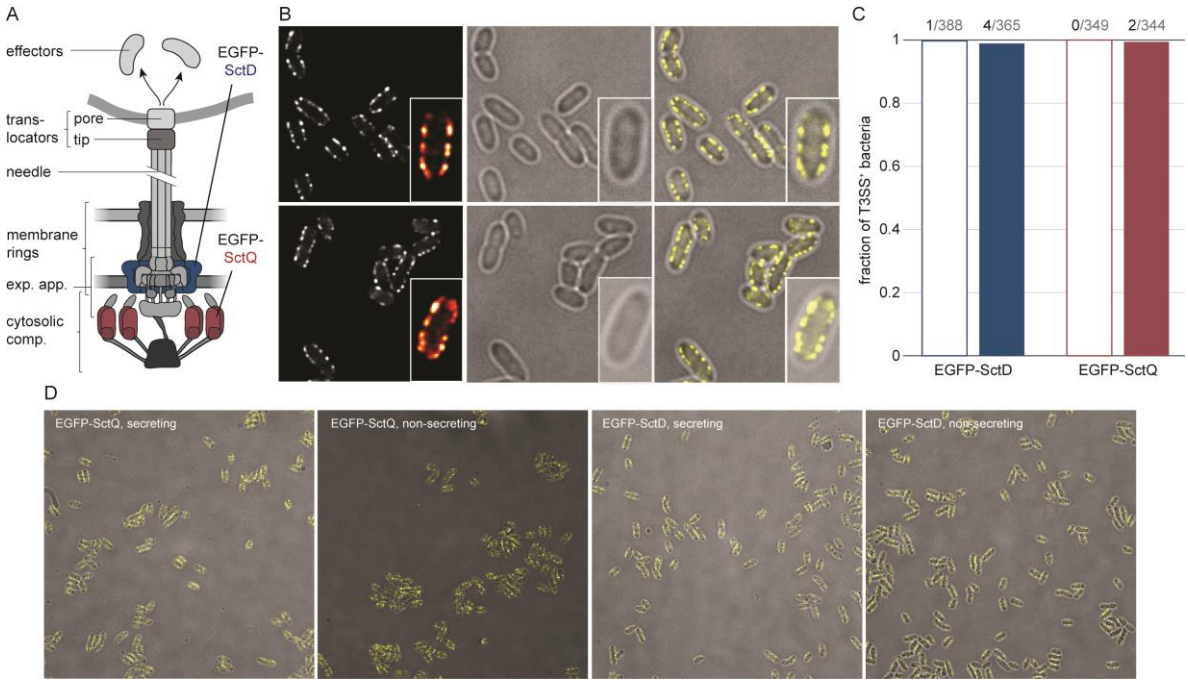

Figure 9: The type III secretion is expressed homogenously in almost all Y. enterocolitica in both secreting and non-secreting conditions.
(A) Schematic overview of the T3SS subcomponents (left). Positions analyzed in this study are indicated (right). **(B)** Micrographs of *Y. enterocolitica* ΔHOPEMTasd expressing EGFP-SctD (top panel) or EGFP-SctQ (bottom panel) from their native genetic locus. 3 hrs after induction of the T3SS expression (by temperature shift to 37°C) under non-secreting conditions, bacteria were subjected to secreting conditions, and imaged. Left, EGFP fluorescence (insets show fluorescence intensity for one enlarged bacterium in ImageJ red-hot coloring scale); center, corresponding phase contrast image images; right, overlay. **(C)** Fraction of bacteria with standard expression and distribution of T3SS (multiple membrane foci) for the indicated fusion protein, 3 hrs after induction of T3SS expression under non-secreting conditions (empty bars) or secreting conditions (filled bars) n = 344-388. Numbers on top indicate the number of bacteria that do not display multiple visible T3SS, and the number of analyzed bacteria. **(D)** Expression of labelled T3SS subunits under the indicated conditions. Overlays of phase contrast (grey) and fluorescence images in the green channel (yellow) for *Y. enterocolitica* strains expressing the indicated proteins from their native genetic locus. Bacteria were subjected to the indicated conditions 3 hrs after induction of T3SS expression by shift to 37°C under non-secreting conditions. Secreting and non-secreting conditions refer to incubation in medium with addition of 5 mM EGTA or $CaCl_2$, respectively. Experiment performed by Stephan Wimmi.

3.1.3 Activation kinetics of the *Y. enterocolitica* T3SS by Ca^{2+} chelation

The previous results showed that *Y. enterocolitica* populations almost uniformly assemble T3SS injectisomes. Next, we analyzed the activation and deactivation of these injectisomes in more detail, using an improved version of a previously published enzymatic export assay (Diepold et al, 2015), which measures the export of the reporter construct $YopH_{1-17}$-β-lactamase (Charpentier & Oswald, 2004; Marketon et al, 2005). Utilizing this method allows higher sensitivity for quantifying secretion within short time periods than the standard accumulative *in vitro* secretion assay (Figure 10.A). The updated protocol utilizes the pACYC184 plasmid rather than the pBAD plasmid, which removes β-lactamase background caused by pBAD expression (Figure 10.B). The higher signal/noise ratio of the modified assay allowed us to reliably quantify secretion in intervals down to five minutes, and we confirmed that the enzymatic assay itself is not influenced by the used concentration of $CaCl_2$ or EGTA

(Figure 10.C). We therefore were able to quantify the initiation of secretion in *Y. enterocolitica* within the first 15 minutes after Ca^{2+} chelation. For the reporter export assay, bacteria were grown at 37°C under non-secreting conditions for two hours, allowing for assembly, but not activation of the T3SS. Bacteria were then collected and secretion was activated by resuspension in pre-warmed secreting medium. For the next 15 minutes, samples were taken every five minutes, and measured for export of the reporter substrate into the supernatant within the following five minutes. The results of the reporter assay clearly show that secretion is fully active at the earliest time range after activation (0-5 min) (Figure 10.D), suggesting that effector secretion is initiated immediately upon Ca^{2+} chelation. Notably, the level of reporter substrate secretion remained constant throughout the first hour after secretion was activated (Figure 10.D).

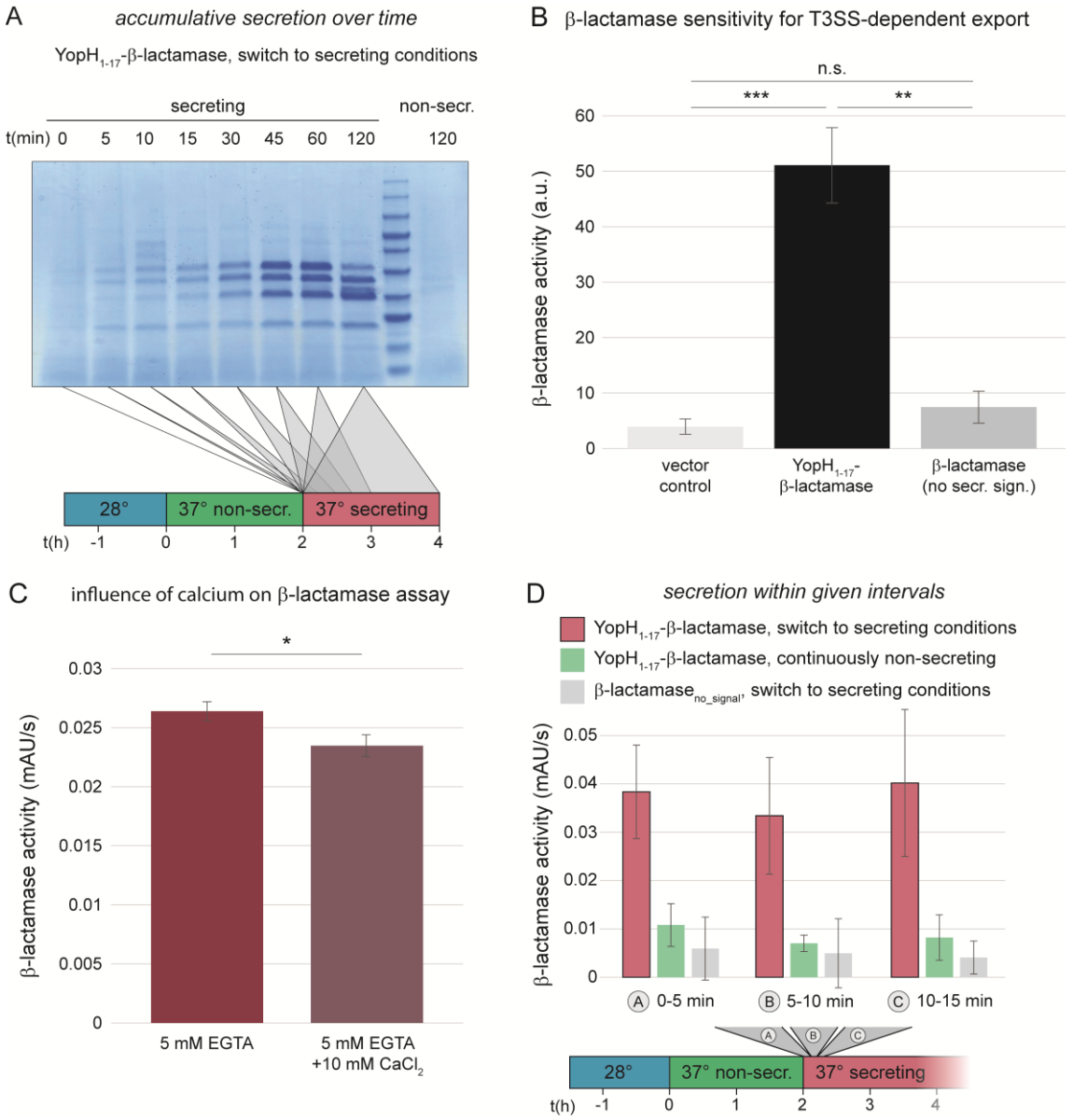

Figure 10: Immediate activation of the T3SS can be measured by an in vitro β-lactamase assay.
(A) Accumulative effector secretion into the culture supernatant during a standard *in vitro* secretion assay using *Y. enterocolitica* MRS40. At the time points indicated (0 min = activation of T3SS secretion by resuspension of bacteria in secreting, see also time line at bottom), the culture supernatant 3 x 10^9 bacteria was removed and visualized by Coomassie staining of an SDS-PAGE gel. Control (far right), bacteria resuspended in non-secreting medium. **(B)** Quantification of β-lactamase activity, measured by the increase in Fluorocillin florescence, in the supernatant of strains expressing the indicated proteins for 60 min after resuspension of bacteria in secreting medium. *Y. enterocolitica* ΔHOPEMTasd harboring an empty pACYC184 vector (vector control, light grey), pACYC184::$YopH_{1-17}$-β-lactamase (black), or pACYC184::β-lactamase (no secretion signal, grey). Error bars indicate the standard deviation of a technical triplicate of one experiment. **/***, p<0.01/0.001; n.s. difference not statistically significant in a two-tailed homoscedastic t-test. **(C)** Test for direct influence of the Ca^{2+} concentration on the β-lactamase assay. The supernatant of bacteria incubated for 10 min after resuspension in secreting medium (containing 5 mM EGTA) was analyzed in a standard β-lactamase assay with or without the addition of 10 mM Ca^{2+}, mimicking the conditions of the β-lactamase assay for non-secreting samples, directly prior to the assay. Error bars indicate the standard deviation of a technical triplicate of one experiment. *, statistical significant difference (p=0.03 in a two-tailed homoscedastic t-test). **(D)** Quantification of effector export in the indicated time ranges after resuspension of *Y. enterocolitica* ΔHOPEMTasd in secreting medium (see also time line at bottom). Red bars, β-lactamase activity indicative of export of the reporter T3SS substrate $YopH_{1-17}$-β-lactamase; green bars, non-secreting control; gray bars β-lactamase lacking a T3SS secretion signal under secreting conditions. Error bars indicate standard deviation of the averages of technical triplicates between three biological replications. *p < 0.05 vs. the $YopH_{1-17}$-β-lactamase, switching to secreting conditions, samples (red bars) in a two-tailed homoscedastic t-test. Secreting and non-secreting (non-secr.) conditions refer to incubation in medium with addition of 5 mM EGTA or $CaCl_2$, respectively. Experiments performed by Bailey Milne-Davies.

3.1.4 T3SS secretion activity ceases within minutes after removal of the activating signal

Next, we measured if and how fast the T3SS is inactivated upon reintroduction of calcium into the medium. Bacteria that had been secreting for two hours were resuspended in non-secreting medium, and the export of the reporter substrate was measured in ten minute intervals afterwards. Already within the first period after calcium addition, the export of the reporter dropped significantly compared to the control that was left under secreting conditions (Figure 11.A). Based on the amount of exported reporter substrate under non-secreting conditions over time (green bars in Figure 11.A), deactivation is likely to occur within the first minutes after the removal of the activating signal.

Additionally, we were interested in determining which factor, temperature or calcium concentration, has a greater effect on the export of different substrate classes. As a result, we analyzed the export of different substrate classes: an effector (YopE), the needle protein SctF, the hydrophilic translocator SctA (= LcrV), and the ruler protein SctP. Cultures were grown in secreting conditions and after three hours, the previously secreting cultures were exposed to: non-secreting conditions at 26°C or 37°C and secreting conditions at 26°C or 37°C. Strikingly, our results show that while export of the effector was strongly repressed by the addition of calcium, it was secreted in the absence of calcium, irrespective of the temperature, the effect of which we tested in parallel (Figure 11.B and C). Export of the needle, translocator, and ruler protein, in contrast, were more strongly influenced by the temperature than the calcium level (Figure 11.B and C). In all cases, differences in expression levels cannot explain the observed export phenotype (Supplementary Figure 1; Supplementary Figure 2; Supplementary Figure 3).

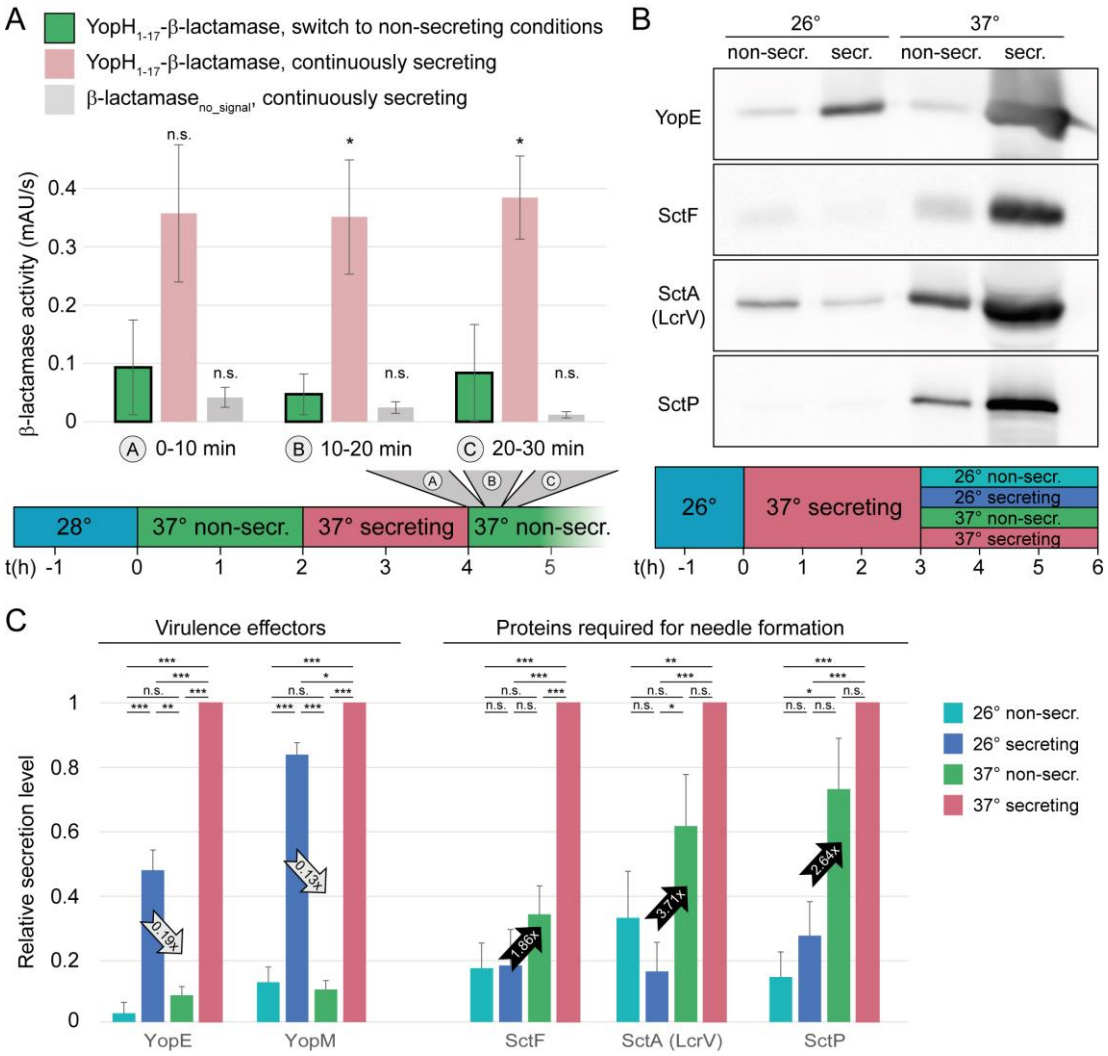

Figure 11: Type III secretion, but not needle formation, is stopped within short time in the absence of activating signal. **(A)** Quantification of effector export in the indicated time ranges after resuspension of *Y. enterocolitica* ΔHOPEMTasd in non-secreting medium (see also time line at bottom). Green bars, β-lactamase activity indicative of export of the reporter T3SS substrate $YopH_{1-17}$-β-lactamase; red bars, secreting control; gray bars, β-lactamase lacking a T3SS secretion signal under secreting conditions. Error bars indicate standard deviation of the averages of technical triplicates between three biological replicates. *p < 0.05 vs. the $YopH_{1-17}$-β-lactamase, switch to non-secreting conditions, sample in a two-tailed homoscedastic t-test; n.s., difference not statistically significant. **(B)** The export of different substrate classes is influenced differently by the temperature and the external calcium concentration. Wild-type *Y. enterocolitica* expressing all effectors (MRS40) were grown at 26°C for 1.5 hrs, and subsequently at 37°C under secreting conditions for 3 hrs. Afterwards, they were resuspended in different conditions, as indicated (top and time line at bottom) for another 3 hrs. Proteins secreted by 3 x 10^9 bacteria were separated on an SDS-PAGE gel and analyzed by immunoblot using antibodies against the indicated proteins, the effector YopE, the needle subunit SctF, the hydrophilic translocator SctA (LcrV), and the ruler protein SctP (n = 4, image representative). The respective analysis for bacteria directly subjected to the indicated conditions after incubation at 26°C, Coomassie-based analysis of all secreted proteins, and protein expression controls are displayed in Supplementary Figure 3.1.2**. (C)** Relative secretion levels of indicated virulence effectors (left) and proteins required for needle export (right) under the indicated conditions [see time line in (B)]. Secretion levels were quantified by densitometric analysis of the bands for the respective proteins in Coomassie-stained SDS-PAGE gels for YopE and YopM (n = 3) and immunoblots for YopE (one additional analysis), SctF, SctA (LcrV), and SctP (n = 4 in each case), and normalized to the respective secretion level at 37°C under secreting conditions. Error bars display the standard error of the mean; arrows indicate the difference between the influence of the temperature (28°C, secreting conditions) and calcium levels (37°C, non-secreting conditions) and the ratio of secretion under these conditions. Secreting and non-secreting (non-secr.) conditions refer to incubation in medium with addition of 5 mM EGTA or $CaCl_2$, respectively. *p < 0.05, **p < 0.01, ***p < 0.001 in a two-tailed homoscedastic t-test; n.s., difference not statistically significant. Experiments performed by Bailey Milne-Davies and Andreas Diepold.

3.1.5 *Y. enterocolitica* can resume growth or engage in new secretion activity after secretion has ended

Having analyzed the activation and deactivation of type III secretion by external signals, we turned our interest to the events after secretion. Specifically, we wanted to find out whether and when post-secretion *Y. enterocolitica* can resume division and/or reinitiate secretion. To answer the first question, we compared the optical culture density of bacteria that had previously been secreting, and were then either kept under secreting conditions, or subjected to non-secreting conditions. Compared to the non-secreting control, secreting bacteria slow down their division (Figure 12.A and B, "first incubation"). Notably, previously secreting bacteria that were subjected to non-secreting conditions resumed division within a short time (Figure 12.A and B, "second incubation"). This phenotype is linked to T3SS activity, as indicated by the steady division of T3SS-negative (ΔSctD) bacteria under all tested conditions (Figure 12.A and B). Similar results were obtained on solid medium, where T3SS-positive bacteria did not divide and only slightly increased their cell volume under sustained secreting conditions, in contrast to T3SS-negative bacteria (Figure 12.C; Supplementary Figure 4). Under non-secreting conditions, both populations displayed a higher rate of growth and division (Figure 12.C; Supplementary Figure 4). Taken together, these results indicate that individual *Y. enterocolitica* cells not only can disengage from secretion within a short time, but also quickly resume division in the absence of further stimulating signals.

To determine if *Y. enterocolitica* can also undergo repeated cycles of secretion activation and deactivation, we tested the reactivation of secretion in bacteria that had been secreting for two hours, and where secretion was stopped afterwards by addition of $CaCl_2$. These bacteria were incubated in the presence of calcium for 15 minutes at 28°C to suppress the formation of new injectisomes (Figure 12.B), and then again subjected to secreting conditions (37°C, absence of calcium). The secretion of effectors started within the first five minutes after the renewed incubation under secreting conditions (Figure 12.D), which shows that type III secretion can be reactivated, and that this occurs within a similarly short time as the initial activation of secretion.

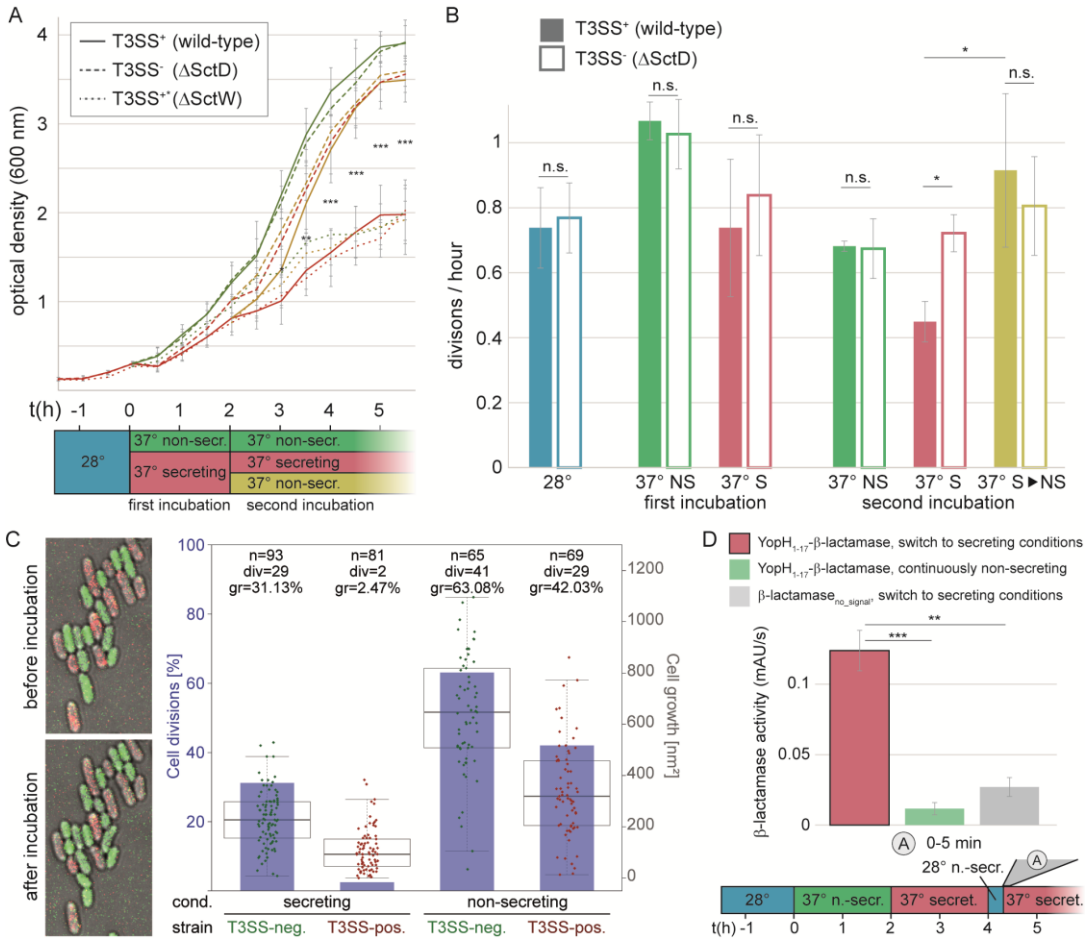

Figure 12: Bacteria can resume division, or engage in another round of secretion after deactivation of secretion.
(A) Growth curves (optical culture density at 600 nm) of T3SS-positive *Y. enterocolitica* wild-type MRS40 expressing all virulence effectors (T3SS+, continuous lines), T3SS-negative bacteria (T3SS−, dashed lines), and Ca^{2+}-blind constantly secreting bacteria (T3SS+*, dotted lines) incubated under the conditions indicated in the time line (bottom). **(B)** Number of bacterial divisions per hour during the different phases, colors as in (A). Filled bars, T3SS-positive bacteria; open bars, T3SS-negative bacteria. Error bars indicate the standard deviation of the averages of technical triplicates between three independent biological replicates. **(C)** Growth and division of T3SS-positive (mCherry-SctL, red) and T3SS-negative (EGFP-SctL ΔSctD, green) *Y. enterocolitica* ΔHOPEMTasd on LB-agarose pads under secreting conditions during the first 2 hrs of the second incubation period [see (A)]. Left, fluorescence micrographs showing growth and division of green (T3SS-negative), but not of red (T3SS-positive) bacteria within the analysis period. Right, quantification of fraction of cell divisions (blue bars and axis on left side) and cell growth (increase in two-dimensional cell area on micrographs) per initial bacterium (box charts and single data points, right axis) for the indicated strains and conditions. Each data point represents a single measurement. The boxes show the median and quartiles (75^{th} and 25^{th} percentile). The whiskers extend 1.5 times the interquartile range until the furthest data point within this range. No standard deviation is displayed. n, number of analyzed bacteria; div, number of bacteria dividing within analysis period; gr, average growth (increase of cell area) within analysis period. Cell growth is statistically significantly different ($p < 0.001$ in a two-tailed homoscedastic t-test) for all pairwise comparisons of strains and conditions. **(D)** Quantification of effector export in the indicated time range after resuspension of *Y. enterocolitica* ΔHOPEMTasd in secreting medium after a 15 min incubation in non-secreting medium at 28°C (see time line at bottom). Red bar, β-lactamase activity indicative of export of the reporter T3SS substrate $YopH_{1-17}$-β-lactamase; green bar, non-secreting control; gray bar, β-lactamase lacking a T3SS secretion signal under secreting conditions. Error bars indicate standard deviation of the averages of technical triplicates between three biological replicates. Secreting and non-secreting conditions refer to incubation in medium with addition of 5 mM EGTA or $CaCl_2$, respectively. The incubation steps at 28°C (blue bars) are performed in medium with 5 mM $CaCl_2$. *$p < 0.05$; ** $p < 0.01$; *** $p < 0.001$ in a two-tailed homoscedastic t-test; n.s., difference not statistically significant. For (A), this statistical analysis applies to the difference between wild-type and ΔSctD under secreting conditions (continuous and dashed red lines), other time points were not statistically significantly different. Experiments performed by Bailey Milne-Davies (A, B, and D) and Carlos Helbig (C).

3.1.6 *Yersinia* are not energetically exhausted during secretion

Inhibition of division during secretion has been thoroughly described and actually led to the discovery of the T3SS (reviewed in Schneewind, 2016). Why secreting bacteria stop division remains unclear. It has been hypothesized that secretion requires such a large amount of energy that the bacteria deplete their ATP. As a result, these exhausted bacteria are unable to divide. To determine if the activation of effector export negatively impacts the ATP levels, we measured the AXP (AMP, ADP, and ATP) levels within ΔHOPEMTasd background *Y. enterocolitica* to determine the adenylate energy charge (([ATP]+0.5[ADP]/([ATP]+[ADP]+[AMP])). The bacteria were incubated at 28°C for 1.5 hours and shifted to 37°C under non-secreting conditions for two hours, the bacteria were transitioned into secreting conditions. Samples were taken 10 minutes after activation. The energy charge shows that secreting cultures were not significantly decreased (Figure 13.A) and secretion of effectors remains constant over time (Figure 13.B; Supplementary Figure 5). Interestingly, when a secreting culture is then exposed to non-secreting conditions the energy levels are not higher than the continuously secreting cultures (Figure 13.A). These results indicate that contrary to the current hypotheses, the energy charge levels are not the link between secretion and inhibition of growth.

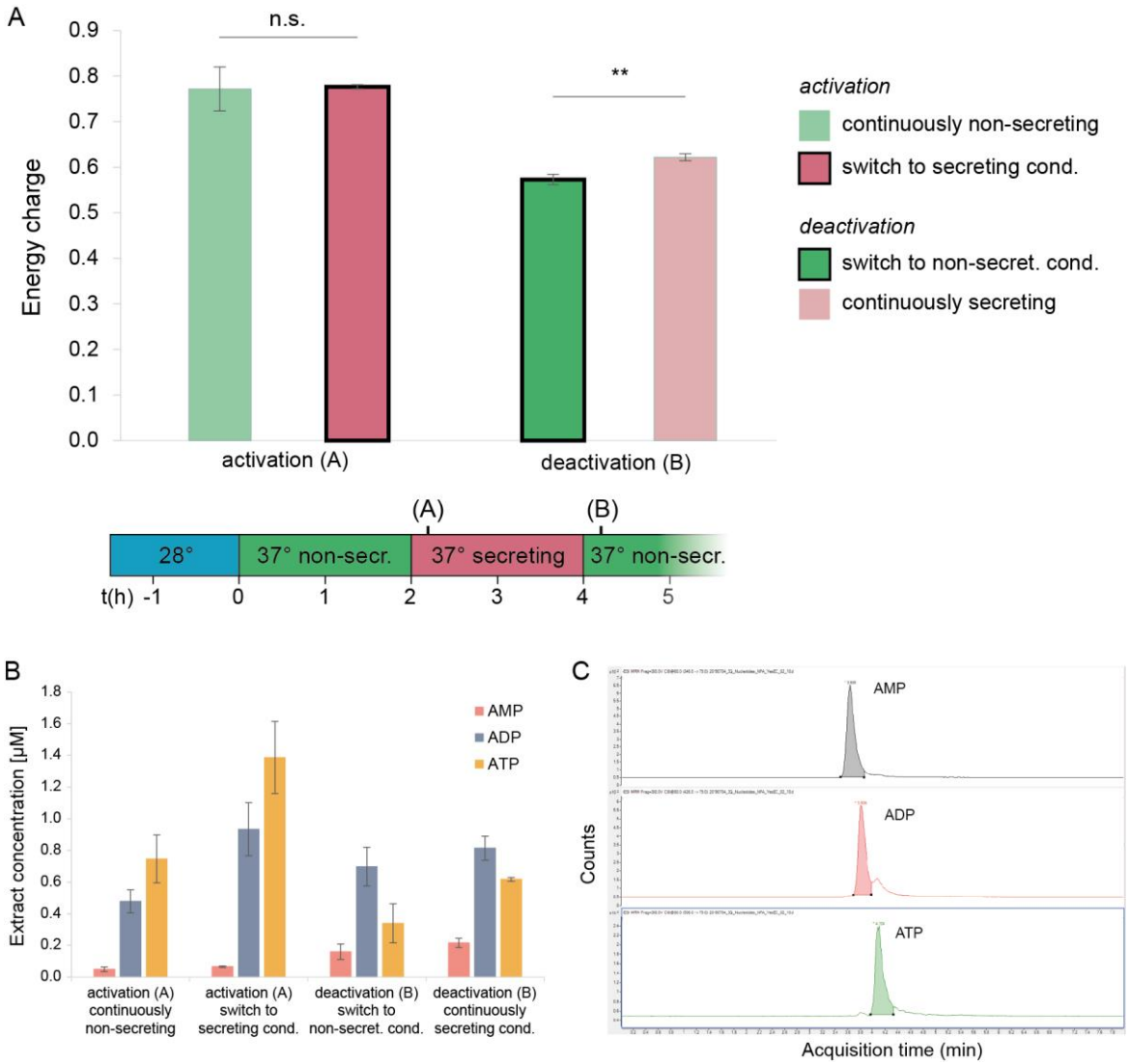

Figure 13: The ATP energy charge of *Y. enterocolitica* is not increased under non-secreting conditions within the time range used in the activation and deactivation experiments.

(A) Energy charge, defined as [ATP]+0.5[ADP])/([ATP]+[ADP]+[AMP]) for activation of secretion (left, relates to Figure 10.D) and deactivation of secretion (right, relates to Figure 11.A). Light green column, continuously non-secreting *Y. enterocolitica* ΔHOPEMTasd; dark red column, switch to secreting conditions; dark green column, switch to non-secreting conditions; light red column, continuously secreting conditions, at the time points indicated in the time line (bottom). Error bars indicate standard deviation of three biological replicates. n.s., no statistical significant difference (p=0.87 in a two-tailed homoscedastic t-test); **, statistical significant difference (p=0.004). **(B)** Measured AXP concentrations for the experiment shown in (A). **(C)** Chromatographic peak separation of ATP, ADP, and AMP. Secreting and non-secreting (non-secr.) conditions refer to incubation in medium with addition of 5 mM EGTA or $CaCl_2$, respectively. Experiment performed by Andreas Diepold.

3.1.7 Supplementary results

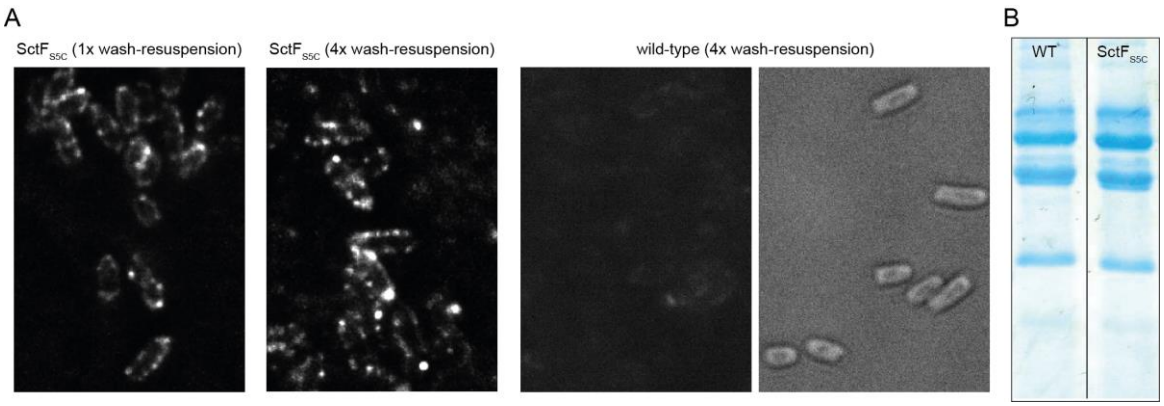

Supplementary Figure 1: T3SS needles are not significantly affected by gentle resuspension of bacterial cultures. **(A)** Stability of fluorescently marked T3SS needles over several wash-resuspension cycles. To label needles extracellularly, we replaced a serine residue in the unstructured N-terminal region of SctF with a cysteine (SctF$_{S5C}$) in a *Y. enterocolitica* MRS40 wild-type strain. Extracellular SctF was labeled covalently with a fluorescent dye, maleimide-CF633. The amount and intensity of fluorescent foci, representing needles or needle clusters, did not visually differ between strains that were centrifuged and resuspended once (the minimal number for this treatment; left), and four times (center). In contrast, a wild-type strain did not show any clearly discernible foci (right; corresponding transmitted light image on far right for detection of bacteria). **(B)** The strain expressing SctF$_{S5C}$ from the native genetic locus, used in (A), is functional for protein secretion. Coomassie-stained SDS-PAGE gel showing exported proteins (supernatants from 3 x 10^9 bacteria) in a wild-type strain and an otherwise identical SctF$_{S5C}$ strain. Experiment performed by Dorothy Cheng and Carlos Helbig.

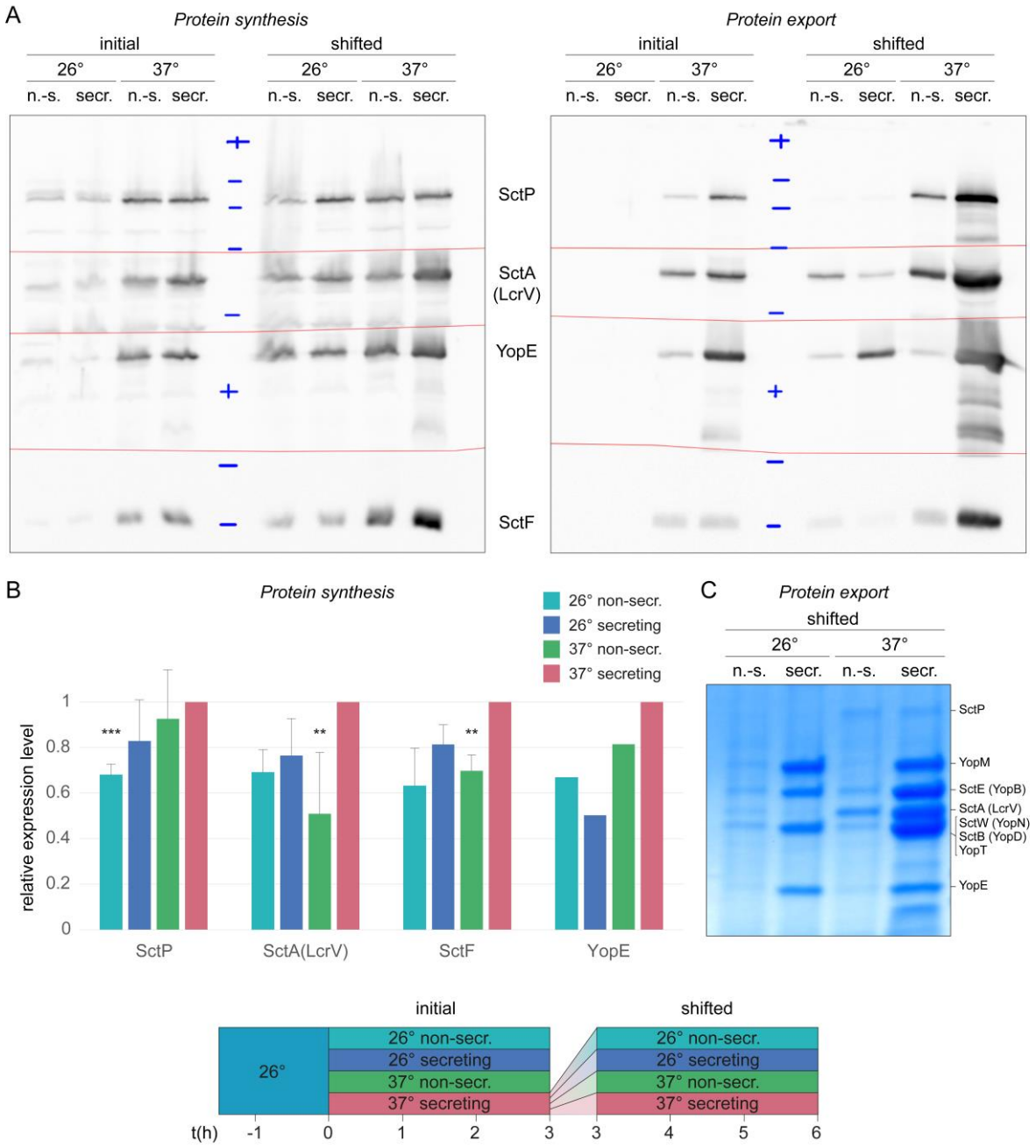

Supplementary Figure 2: Protein expression and export by the T3SS in response to different external conditions.
(A) Immunoblots using antibodies against the indicated proteins to detect protein synthesis (total cell samples from 10^9 bacteria, left) and protein export (supernatants from 3 x 10^9 bacteria, right). Initial cultures were subjected to the indicated conditions (n.-s., non-secreting; secr., secreting) directly after 1.5 hrs at 28°C (0-3 hrs in the schematic below); shifted cultures were subjected to the indicated conditions after 3 hrs under secreting conditions at 37°C (3-6 hrs in the schematic below). Red lines indicate where the membrane was cut to allow incubation with different primary antibodies. Blue crosses indicate position of protein marker (148, 98, 64, 50, 36, 22, 16, 10 kDa from top to bottom). Expected protein sizes, SctP, 57.7 kDa; SctA (LcrV), 37.3 kDa; YopE, 22.9 kDa; SctF, 9.5 kDa. **(B)** Quantification of protein synthesis for the indicated proteins and conditions (see schematic below). Four independent experiments (one for YopE), performed as in (A), were quantified by densitometry; error bars represent standard errors of the mean. **(C)** Coomassie-stained SDS-PAGE gel of protein export (supernatants from 3 x 10^9 bacteria, equivalent to (A)) and tentative assignment of secreted proteins. Experiments performed by Bailey Milne-Davies and Andreas Diepold.

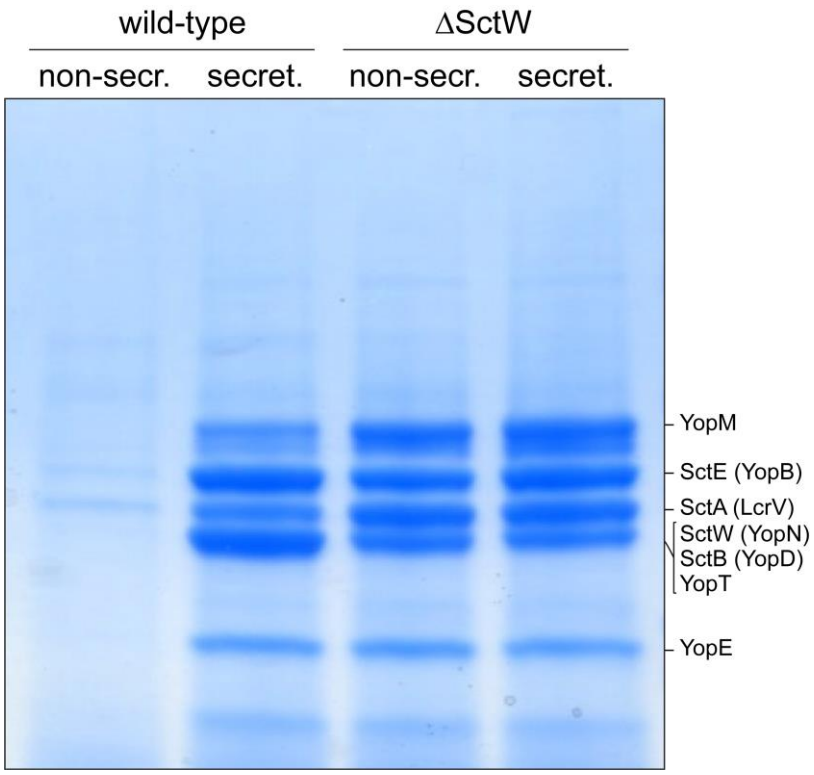

Supplementary Figure 3: Secretion profiles of wild-type MRS40 and the calcium-blind ΔSctW strain.
Coomassie-stained SDS-PAGE gel showing exported proteins (supernatants from 3 x 10^9 bacteria) in a wild-type strain expressing all virulence effectors (MRS40) and an otherwise identical ΔSctW (YopN) strain. Right side, tentative assignment of secreted proteins (based on (Diepold *et al*, 2010)). n = 3, representative image. Secreting (secret.) and non-secreting (non-secr.) conditions refer to incubation in medium with addition of 5 mM EGTA or $CaCl_2$, respectively. Experiment performed by Bailey Milne-Davies.

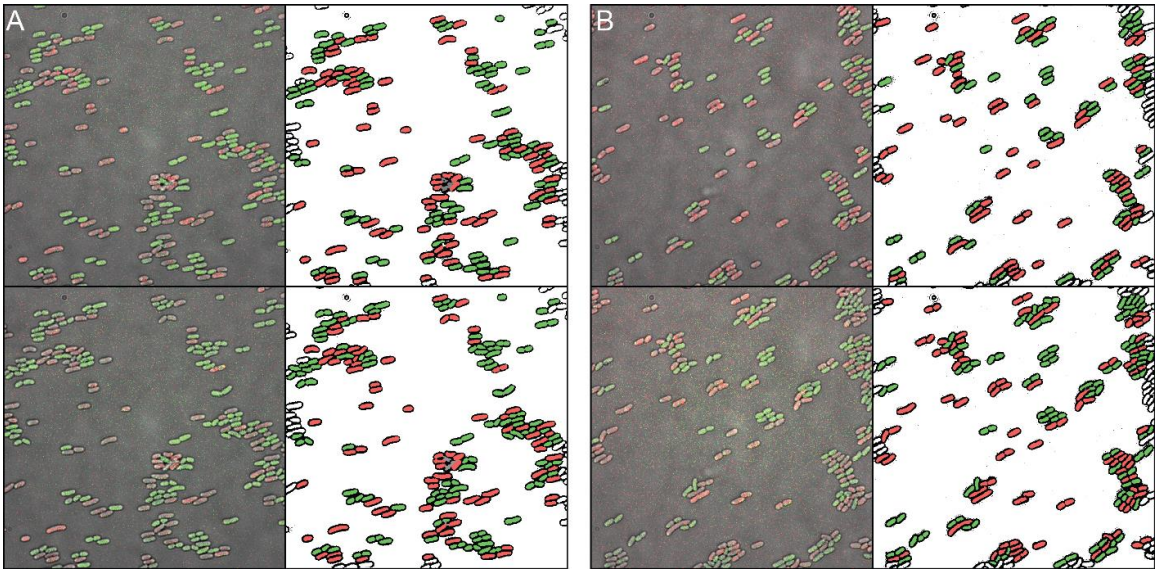

Supplementary Figure 4: Growth and division of T3SS-positive and negative bacteria under secreting and non-secreting conditions.

T3SS-positive bacteria (ΔHOPEMTasd mCherry-SctL) and T3SS-negative bacteria ((ΔHOPEMTasd EGFP-SctL ΔSctD) from liquid cultures grown under secreting conditions were collected, and mixed in equal ratio, **(A)** under secreting conditions (presence of 5 mM EGTA in the medium), or **(B)** under non-secreting conditions (presence of 5 mM $CaCl_2$ in the medium). The mixed bacteria were immediately spotted onto pre-warmed agarose pads of the respective medium and imaged over time at 37°C. The images displayed were taken immediately after transfer to the agarose pad (top), and 2 hrs afterwards (bottom). Left, overlay of phase contrast images (grey) and fluorescence micrographs (red/green) to distinguish T3SS-positive and negative bacteria. Right, processed images used for strain discrimination and determination of cell growth and divisions. Experiment performed by Carlos Helbig.

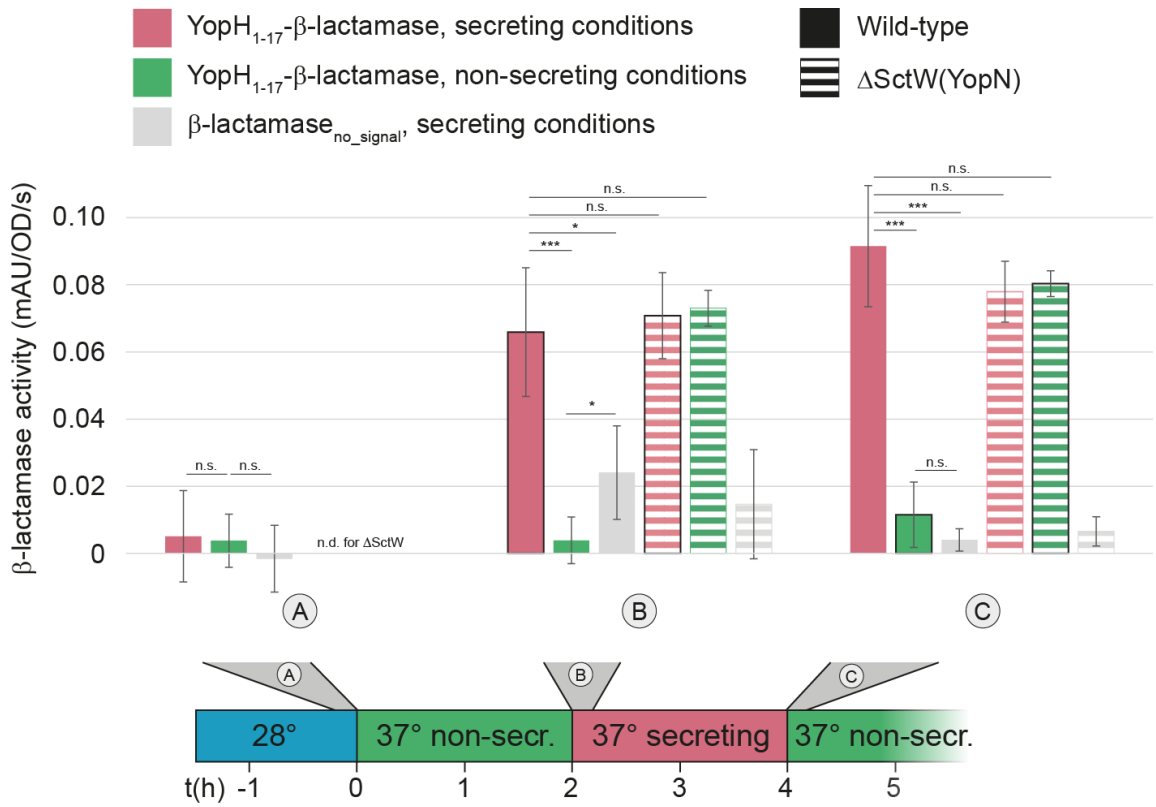

Supplementary Figure 5: Comparison of secretion activity at different time points used in this study.
Quantification of effector export in the indicated 10-minute time ranges (see also time line at bottom) in wild-type (filled) and ΔSctW (YopN) (striped) strains in a ΔHOPEMTasd strain background. β-lactamase activity, indicative of export of the reporter T3SS substrate $YopH_{1-17}$-β-lactamase, normalized by OD_{600} of culture. Red bars, under secreting conditions; green bars, under non-secreting conditions; grey bars, β-lactamase lacking a T3SS secretion signal under secreting conditions. Black boxes indicate samples shifted into new conditions. Error bars indicate standard deviation of two (ΔSctW strains) to four (wild-type strains) biological replicates. */**/***, $p<0.05/0.01/0.001$ in a two-tailed homoscedastic t-test; n.s., no statistical significant difference. Secreting and non-secreting conditions refer to incubation in medium with addition of 5 mM EGTA or $CaCl_2$, respectively. Experiment performed by Bailey Milne-Davies.

3.2 LITESEC-T3SS – Light-controlled protein delivery into eukaryotic cells with high spatial and temporal resolution

The T3SS is a highly efficient export machine capable of responding to different environmental conditions and export a variety of non-native proteins into host cells. Although these studies have demonstrated the flexibility of the system to deliver cargo into host cells and the environment, the lack of controlled export has brought limitations for potential biotechnology and healthcare applications. The T3SS is a highly dynamic system that depends on rapid exchange of cytosolic components (Figure 14.A) (Diepold *et al*, 2010, 2015). If some components could be sequestered, specifically any cytosolic components, secretion could be inhibited. As a result, we devised optogenetic systems to control the T3SS by binding the cytosolic component, SctQ, to the membrane upon illumination called LITESEC-T3SS (Light-induced translocation of effectors through the sequestration of endogenous components of the T3SS). Two optogenetic switches, LITESEC-act and LITESEC-supp, were utilized to activate or suppress secretion under light conditions, respectively (Figure 14.B). The optogenetic interaction switches utilize a membrane-bound anchor protein and a bait fused to SctQ, when the anchor and bait interact cargo export is inhibited (Figure 14.C). By utilizing these switches, cargo export could be controlled in not only *in vitro* conditions, but also *in vivo*. Ultimately, the LITESEC system demonstrates the potential applications of optogenetic systems in bacteria for both academic and industrial settings.

This study has been peer-reviewed and published in Nature Communications on 13 May 2020, except for the results pertaining to the pro-apoptotic proteins PUMA, HSVTK and p53 (including Figure 16).

Lindner F, Milne-Davies B, Langenfeld K, Stiewe T, Diepold A. LITESEC-T3SS - Light-controlled protein delivery into eukaryotic cells with high spatial and temporal resolution. Nat Commun. 2020 May 13;11(1):2381. doi: 10.1038/s41467-020-16169-w. PMID: 32404906; PMCID: PMC7221075.

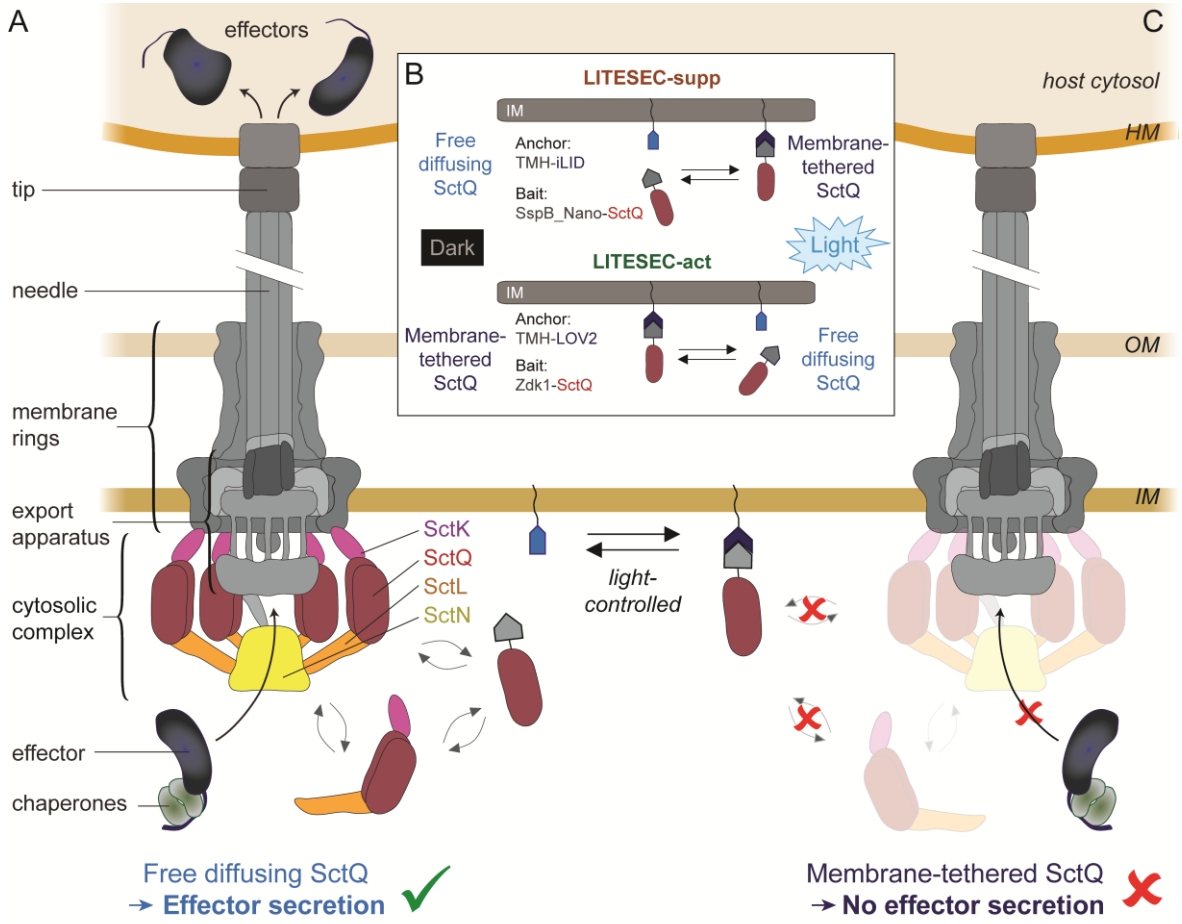

Figure 14: Schematic of the LITESEC systems – light-controlled activation and deactivation of protein translocation by the type III system.
(A) Active T3SS schematic. Major subcomplexes on the left side; dynamic cytosolic components labelled on the right side. Effector export by the T3SS is dependent on the interaction of the unbound bait-SctQ fusion and the T3SS. **(B)** Different states of the bait and anchor proteins in light and dark illumination conditions. The LITESEC-supp system (top), SctQ is fused to a small interaction switch domain SspB-Nano and binds to an iLID interaction partner fused to a transmembrane helix (TMH) located in the inner membrane. Under light conditions, the SctQ bait is bound to the anchor, sequestering the protein from the cytosol and inhibiting effector export. In dark conditions, the anchor and bait are unbound and effector export can be facilitated. The LITESEC-act system (bottom), the bait protein SctQ fused to small interaction switch Zdk1 interacts with the larger interaction partner domain LOV2 fused to a TMH located in the inner membrane. Under light conditions, the bait and anchor are unbound and effector export can be facilitated. In dark conditions, SctQ is tethered to the membrane anchor and effector export is inhibited. **(C)** Sequestration of the bait-SctQ fusion by the TMH-anchor under select illumination prevents effector secretion. HM, host membrane; OM, bacterial outer membrane; IM, bacterial inner membrane.

3.2.1 Author's contribution

Florian Lindner generated and characterized the LITESEC strains and performed a majority of experiments and data analysis. Data for the figures contributed in this thesis was generated by: Supplementary Figure 6, F. Lindner only; Figure 14, 15 and 17 and Supplementary Figure 7 and 8, F. Lindner and B. Milne-Davies collaboration.

I contributed in the establishment of the infection assays and participated in experiments and data analysis. Data for the figures contributed in this thesis was generated by: Supplementary Figure 6, F. Lindner only; Figure 14, 15 and 17 and Supplementary Figure 7 and 8, F. Lindner and B. Milne-Davies collaboration.

Katja Langenfeld propagated cell lines, seeded cells prior to experiments, and established and participated in infection assays.

Thorsten Stiewe provided input on methodology and reagents for apoptosis analysis.

Andreas Diepold conceived the study and experimental design, participated in data analysis and wrote the manuscript.

All authors reviewed the manuscript.

3.2.2 Light-induced protein translocation into eukaryotic host cells

We wanted to determine if the LITESEC system allows to control the export of non-native T3SS substrates and if this process is reversible by measuring the secretion kinetics of exported $YopE_{1-53}$-NanoLuc overtime. Secretion activity was quantified using a luciferase-based luminescence assay, which is an enzymatic assay where the NanoLuc reporter cleaves the luciferin substrate allowing the enzymatic activity to then be measured by luminescence in a plate reader. The secretion assay determined that NanoLuc secretion in LITESEC-act and -supp can be controlled by light and that this process is reversible (Supplementary Figure 6).

Having found that secretion of non-native T3SS substrates can be strongly controlled by the LITESEC system, we utilized the LITESEC-act system to control translocation of a reporter protein, $YopE_{1-53}$-β-lactamase, into eukaryotic host cells upon illumination with blue light. Visualization of β-lactamase translocation into the host was facilitated by a Förster resonance energy transfer (FRET) reporter substrate, CCF2 (Charpentier & Oswald, 2004). Cells that had successful translocation of the reported protein shift from green to blue fluorescence, via the cleavage of the CCF2 within the host cell; on the other hand, non-infected cells maintain green fluorescence. To quantify light-dependent translocation of the T3SS substrate, 671-2694 host cells were analyzed per bacterial strain and condition. As predicted, the wild-type strain translocated $YopE_{1-53}$-β-lactamase into a high fraction of host cells regardless of illumination conditions. The negative control (the same strain expressing β-lactamase without an export signal) displayed significantly lower blue fluorescence, demonstrating that translocation is T3SS-dependent (Figure 15.A). The LITESEC-act strain translocated the reporter protein in a light-dependent manner, resulting in a significantly high population of translocation-

positive host cells in light conditions rather than dark conditions (fractions were close to positive and negative controls, respectively; Figure 15.B; Supplementary Figure 7). On the other hand, the LITESEC-supp strain demonstrated the opposite phenotype (Figure 15.B; Supplementary Figure 7). No visible morphological changes indicating cell death were observed between incubation of host cells and T3SS-inactive bacteria, even following extended incubation times (Supplementary Figure 8), thus showing no or low T3SS-independent effects of bacteria on the eukaryotic cells. Altogether, the results affirm that T3SS-dependent translocation of non-native proteins into eukaryotic cells can be controlled by external light.

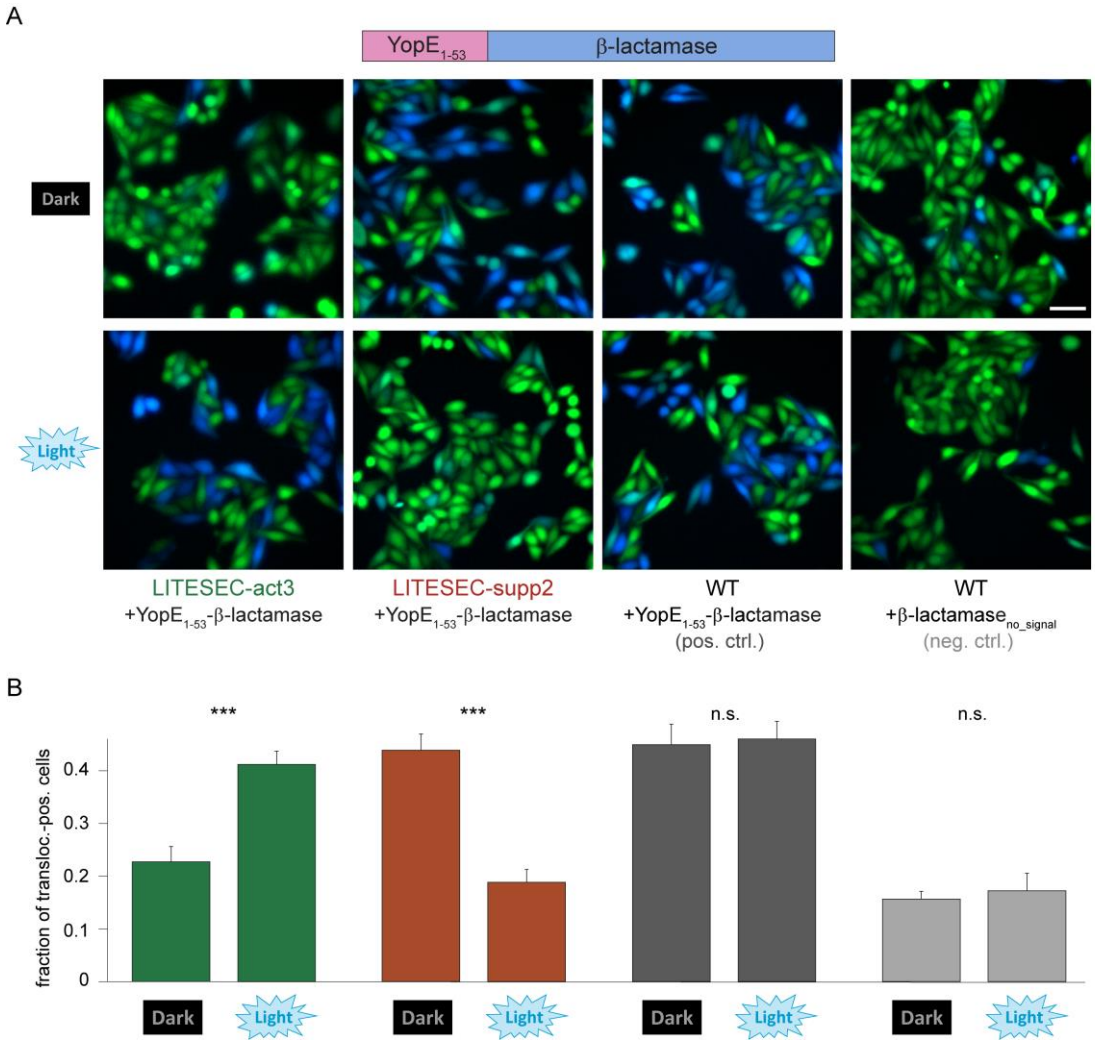

Figure 15: Light-dependent translocation of β-lactamase cargo into eukaryotic cells.
(A) Fluorescence micrographs depicting cultured HEp-2 cells that were incubated with the indicated strains expressing either a heterologous T3SS substrate, $YopE_{1-53}$-β-lactamase, or β-lactamase without a secretion signal as a negative control, for 1 hr. Translocation of β-lactamase is detected by cleavage of the intracellular β-lactamase substrate CCF2 (leading to loss of FRET, and a transition from green to blue fluorescence emission). Scale bar, 50 µm. **(B)** Fraction of β-lactamase-positive HEp-2 cells in (A) (blue fluorescence). 2343/2423/2226/2694 cells from 26/28/25/27 fields of view from three independent experiments were analyzed for the LITESEC strains under the given conditions from left to right (809/671/995/823 cells from 8/8/10/9 fields of view from three independent experiments for the controls). Single data points (percentage of positive cells per field of view) indicated by circles; error bars display the standard error of the mean. ***$p < 0.001$ in a two-tailed homoscedastic *t* test; n.s., difference not statistically significant (exact values from left to right, $6 \times 10^{-6}/2 \times 10^{-8}$/0.80/0.65). Experiment performed by Bailey Milne-Davies and Florian Lindner.

3.2.3 Light-activated induction of apoptosis in eukaryotic cells

We then became interested in exploring the possibilities where the LITESEC systems could be employed, specifically focusing on the utilization of these systems to combat disease. If the bacteria could be controlled to specifically export proteins into host cells, it may be possible to introduce proteins into the host cell and modify their behavior in a controlled way. We set out to establish light-induced apoptosis in host cells by fusing the YopE translocation signal without ($YopE_{1-53}$) and with ($YopE_{1-138}$) the chaperone binding domain (CBD) to selected pro-apoptotic proteins. Utilizing these signals had proven successful in exporting fluorescent reporters into host cells (Wölke et al, 2011), thus we expanded this to include pro-apoptotic cargo: HSVTK (Herpes Simplex Virus – Thymidine kinase), PUMA, and p53. HSVTK is a suicide protein that results in not only the cell death of the infected cell, but also of neighboring cells by passing through gap junctions (Mesnil & Yamasaki, 2000). PUMA is a pro-apoptotic protein that is induced by p53, this protein binds to Bcl2 proteins resulting in the initiation of apoptosis by releasing other pro-apoptotic genes (Nakano & Vousden, 2001). p53 is a transcription factor that suppresses the tumor formation, by inducing cell death. Mutation or loss of p53 results in uncontrollable cell growth (Bykov et al, 2018; Stiewe & Haran, 2018). The pro-apoptotic cargo could be exported in a T3SS-dependent manner into the supernatant during an *in vitro* secretion assay (Figure 16). We observed that HSVTK, PUMA and p53 were exported into the supernatant. All pro-apoptotic cargos appear to be successfully exported, although $YopE_{1-138}$-HSVTK has significant cleavage which may impair protein functionality. However, when using these translocation signals for the infection assay, no changes in cell morphology or cell death were visible in our infection plates. Since no phenotype could be visualized in the host cells, questions arose to why these proteins were unsuccessful. Our hypothesis is that the coexpression of the cognate chaperone promotes more efficient export of the cargo into host cells, demonstrating that for efficient translocation of functional proteins the chaperone is needed to be coexpressed. As a result, we used the truncated human BH3 interacting-domain death agonist (tBID) as a T3SS substrate ($YopE_{1-138}$-tBID) coexpressed with the cognate chaperone, SycE. This pro-apoptotic cargo has been shown to be successfully translocated into host cells and induce host cell death (Ittig *et al*, 2015).

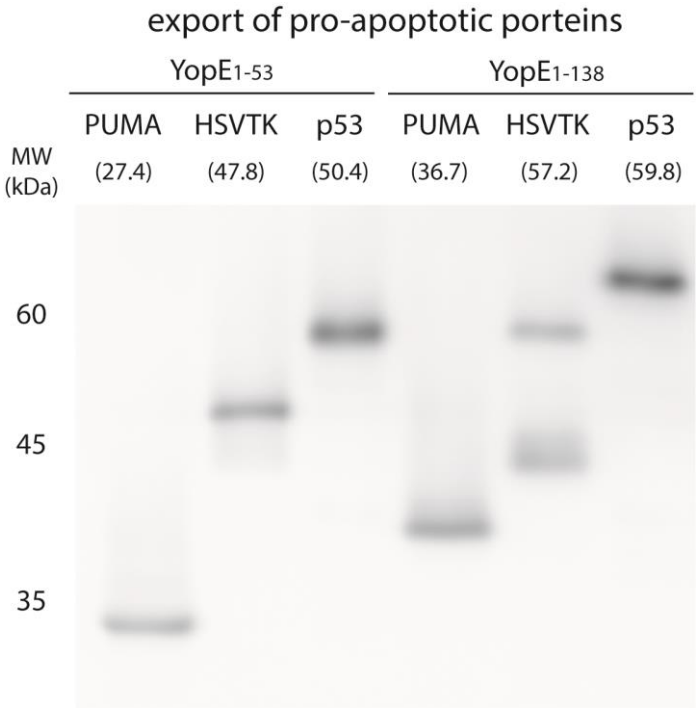

Figure 16: Export of pro-apoptotic proteins in *Y. enterocolitica* ΔHOPEMTasd background strains.
Accumulative effector secretion into the culture supernatant during a standard *in vitro* secretion with *Y. enterocolitica* ΔHOPEMTasd strains expressing PUMA, HSVTK, and p53 fused to $YopE_{1-53}$ and $YopE_{1-138}$ export signals on a pBAD expression plasmid. Pro-apoptotic proteins were also tagged with a flag tag for immunoblot detection. Cultures were induced with 0.2% arabinose and secreted for 3 hrs. Culture supernatant of 3 x 10^9 bacteria was removed and visualized by Coomassie staining on an SDS-PAGE gel (n=1). Molecular weight (MW) ladder is given below and in parentheses below the specified protein is the expected protein size. Both ladder and approximate size is given in kDa. Experiment performed by Bailey Milne-Davies.

The tBID cargo was then incorporated into the LITESEC strains. For controls, we utilized wild-type and T3SS-deficient ΔSctQ strains expressing the same pro-apoptotic plasmid. Notably, within one hour following infection strong HEp-2 cell death was induced, specifically in the host cells incubated with the LITESEC-act bacteria under light conditions, the LITESEC-supp under dark conditions, and the positive control (regardless of illumination conditions) (Figure 17.A and B). To confirm apoptosis induction in the host cells, we detected Poly (ADP-ribose) polymerase (PARP), an apoptosis marker, via Western blot (Figure 17.C). Additionally, we wanted to determine the spatial resolution of the LITESEC-act system by obstructing light access to the bacteria during infection and imaging host cells after infection. We observed high spatial resolution for the activation of the LITESEC-act strains where apoptosis was induced in illuminated areas, as well as a small (0.25 mm) intermediary area which was exposed to some diffracted light (Supplementary Figure 9). Ultimately, these results show specific translocation and induction of apoptosis of host cells by LITESEC strains under activating conditions, demonstrating a clear example for the potential application possibilities for the LITESEC system in both biotechnology and cell biology.

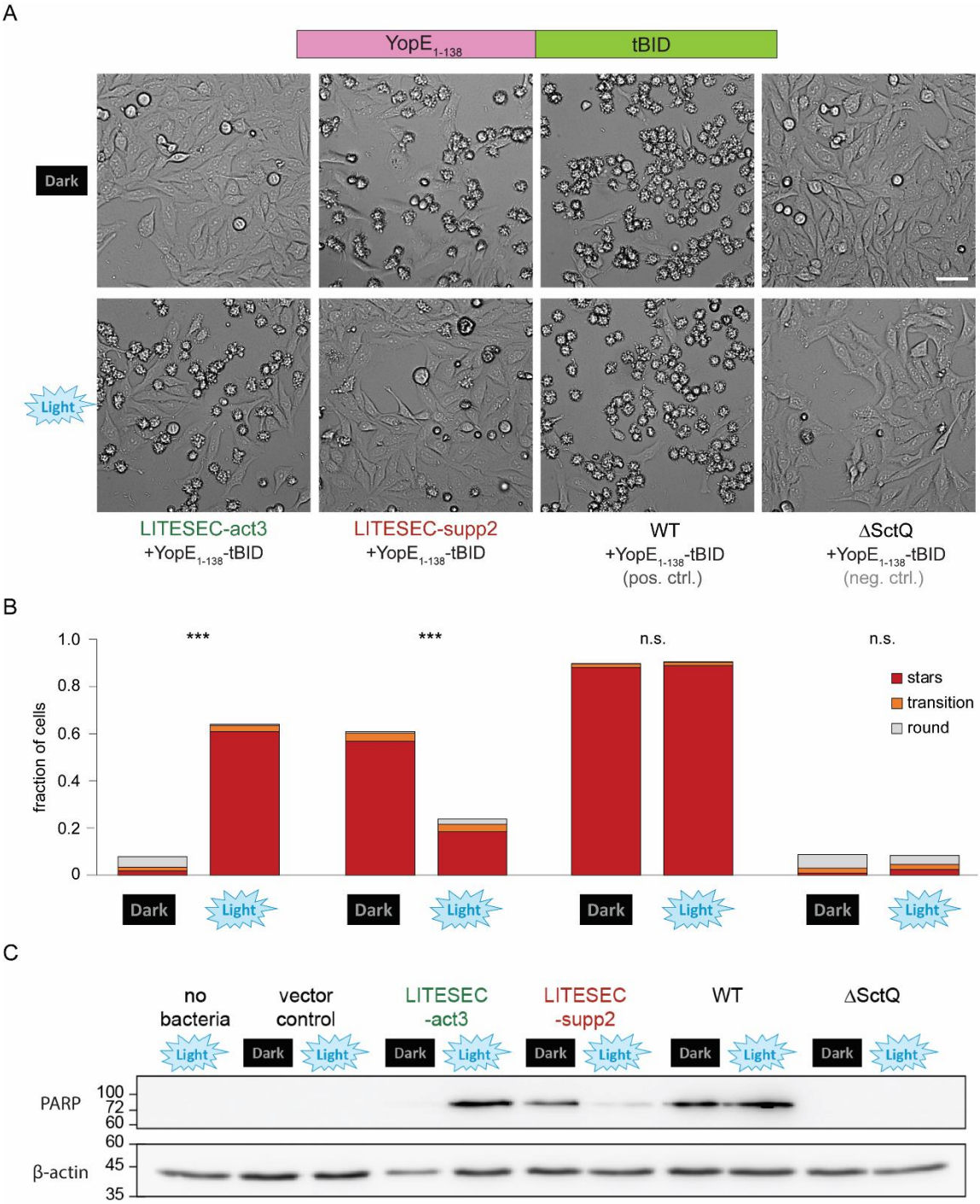

Figure 17: Light-dependent translocation of pro-apoptotic cargo into eukaryotic cells.
(A) Micrographs depicting cultured HEp-2 cells that have been incubated with the indicated strains expressing a heterologous T3SS substrate, YopE$_{1-138}$-tBID for 1 hr. Translocation of tBID induces apoptosis, which leads to a condensed star-shaped host cell morphology. Scale bar, 50 µm. **(B)** Visual classification of HEp-2 cells used in **(C)** after infection. 1522/1914/1510/1600/2299/1218/1468/1194 cells from 17/18/17/19/14/13/14/12 fields of view from five independent experiments were analyzed per strain and condition (from left to right). Single data points (percentage of apoptotic cells per field of view) indicated by circles; error bars display the standard error of the mean among fields of view. */***$p < 0.05/0.001$ in a two-tailed homoscedastic *t* test; n.s., difference not statistically significant (exact values from left to right, $2 \times 10^{-25}/1 \times 10^{-15}$/0.40/0.038). **(C)** Translocation of tBID induces cleavage of poly (ADP-ribose) polymerase (PARP), which was monitored by Western blot analysis of HEp-2 cells used in (**c**). β-actin was used as a loading control. Left, molecular weight in kDa. Experiment performed by Bailey Milne-Davies and Florian Lindner.

3.2.4 Supplementary results

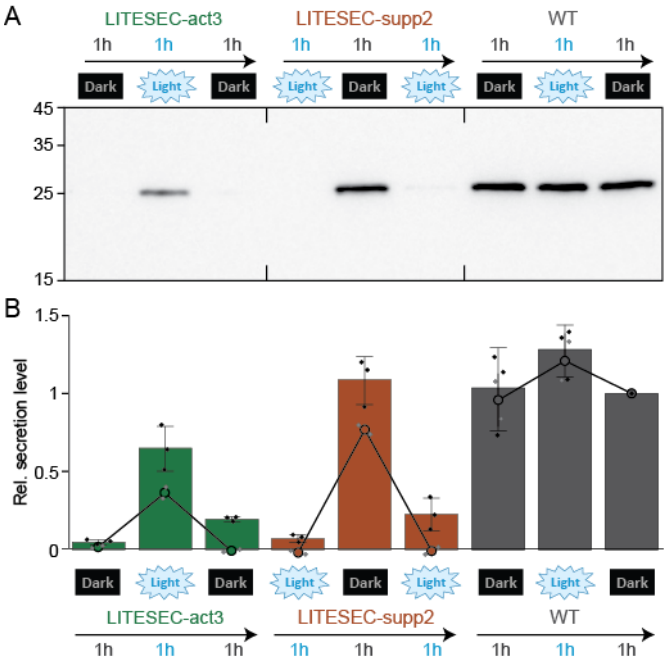

Supplementary Figure 6: Secretion of effector proteins can be controlled by light over time.
(A) Export of $YopE_{1-53}$-NanoLuc-Flag in indicated LITESEC strains. Secretion-competent bacteria were incubated in inactivating, activating, and inactivating light conditions for 1 hr each, as indicated. Culture supernatant of 3 x 10^8 bacteria was analyzed by immunoblot against Flag. Left side, molecular weight in kDa. **(B)** Quantification of the relative secretion levels (normalized to the wild-type level in the third incubation interval) of the strains and conditions shown in (A) for export of $YopE_{1-53}$-NanoLuc-Flag as determined by immunoblot analysis (bars; n=3 densitometry values from independent experiments, single data points shown in black dots) and immunoblot (circles, continuous lines; n=2, single data points shown as gray dots); bars show mean values; error bars denote standard deviation. Values for negative control (ΔSctQ expressing $YopE_{1-53}$-NanoLuc-Flag) were too small to display in the NanoLuc immunoblot assay (<0.001 for all time points). Experiment performed by Florian Lindner.

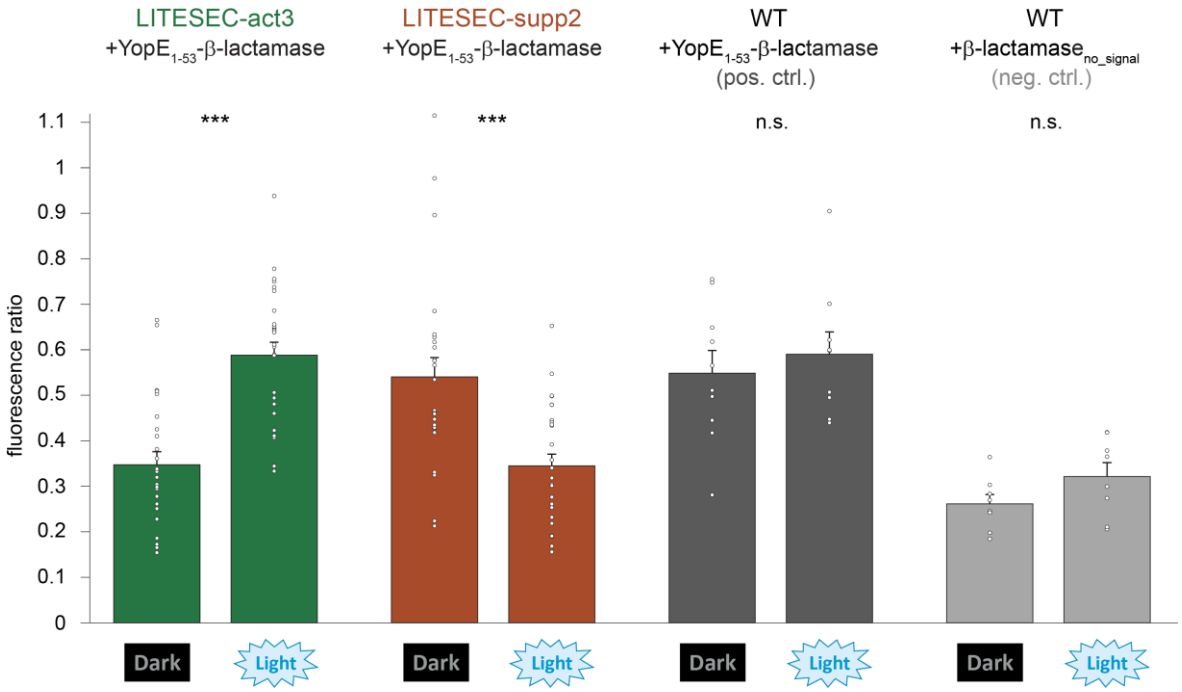

Supplementary Figure 7: Additional quantification of light-dependent translocation efficiency.
Quantification of the fluorescence ratio of CCF2 donor fluorescence (indicative of β-lactamase translocation) and FRET fluorescence for the infection experiment shown in Fig. 3.2.2. 2343/2423/2226/2694 cells from 26/28/25/27 fields of view from 3 independent experiments were analyzed for the LITESEC strains under the given conditions from left to right (809/671/995/823 cells from 8/8/10/9 fields of view from 3 independent experiments for the controls). Fluorescence ratios per single fields of view are displayed as circles; error bars display the standard error of the mean. ***, $p<0.001$ in a two-tailed homoscedastic t-test; n.s., difference not statistically significant (exact values from left to right, $6*10^{-7}/2*10^{-4}$/0.54/0.13. Experiment performed by Bailey Milne-Davies and Florian Lindner.

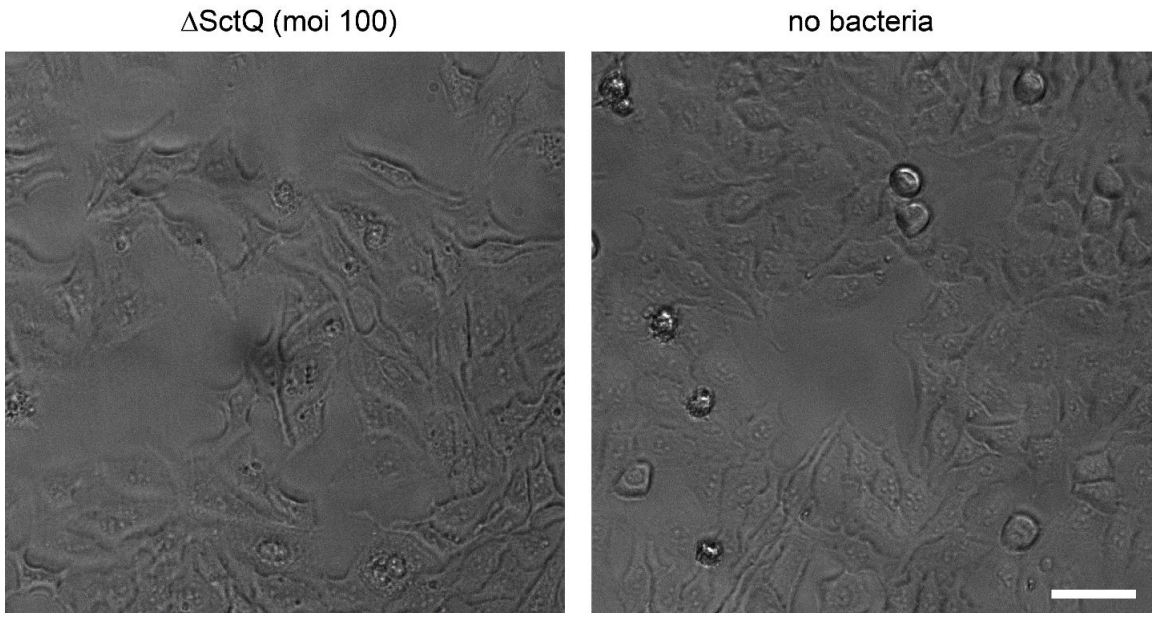

Supplementary Figure 8: Host cells show no visible reaction to T3SS-inactive *Y. enterocolitica*.
Left, HEp-2 cells were infected with ΔSctQ bacteria for 1 hr at a multiplicity of infection of 100, as in Figure 15 and Figure 17. After removal of the bacteria, cells were incubated in medium containing gentamicin for another 17 hr to detect possible long-term effects of the presence and contact of bacteria. Right, control incubated under the same conditions without bacteria. Scale bar, 50 µm. Experiment performed by Bailey Milne-Davies and Florian Lindner.

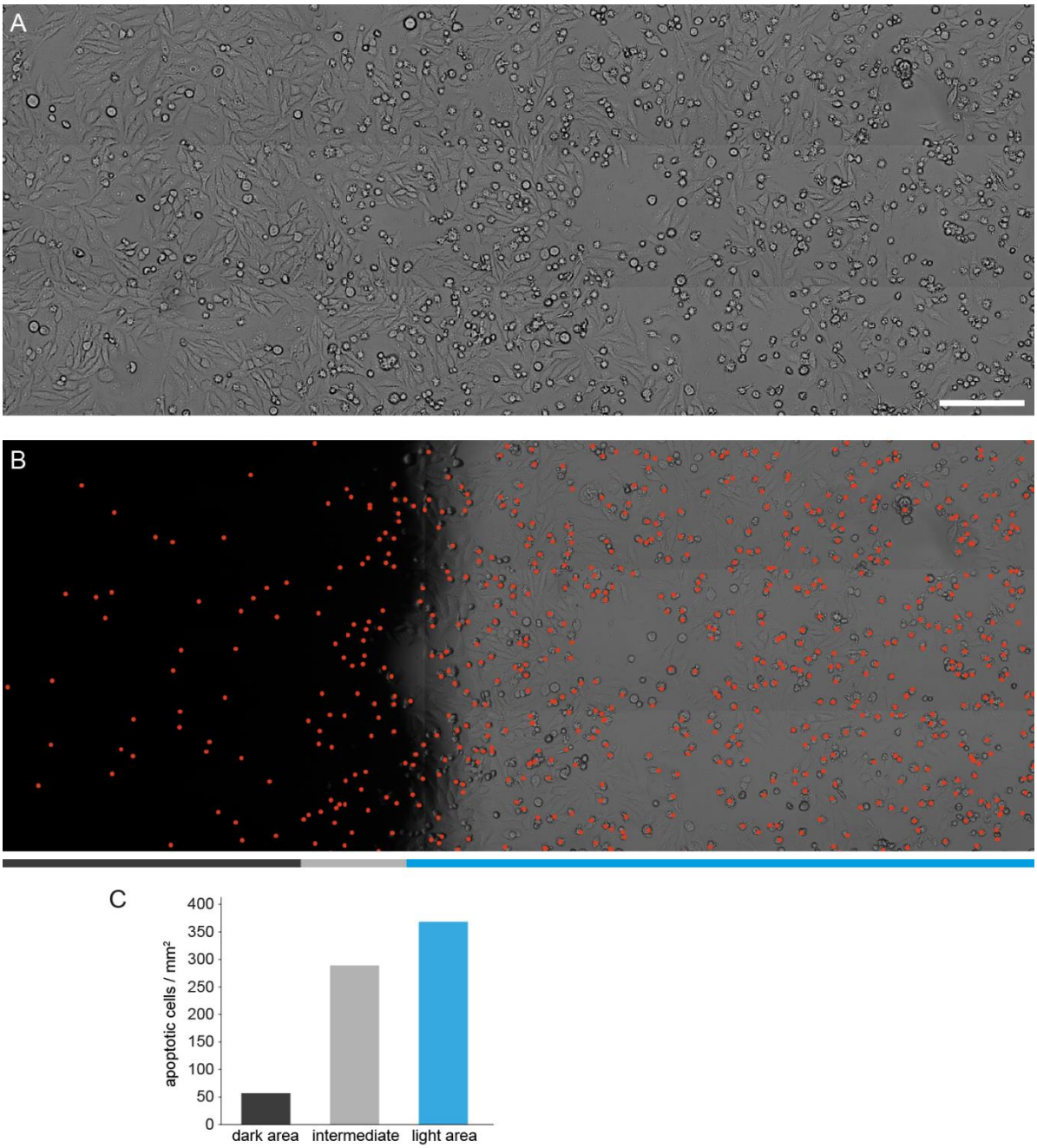

Supplementary Figure 9: Spatial resolution of apoptosis induction by LITESEC-act3 bacteria.
HEp-2 cells were infected with LITESEC-act3 bacteria expressing $YopE_{1-138}$-tBID, as in Fig. 3.2.4, under light conditions. In a part of the plate, light was blocked by an intransparent plastic inset. After infection, the region around the edge of the plastic sheet was imaged with and without the inset and apoptotic cells were determined by shape. **(A)** Light micrograph in the absence of the inset. Three adjacent rows of eight neighboring fields of view, using a 20x objective images each were stitched combined using the softWoRx 5.5 software. Fields of view, using a 20x objective (Scale bar, 0.2 mm). **(B)** Light micrograph of the same area in presence of the inset, showing the approximate area of illumination during infection, as well as the localization of apoptotic cells determined in (A) (red points). Bottom, areas assigned as dark (dark grey bar), intermediate (0.25 mm wide adjacent area, light grey bar) and light (blue bar). **(C)** Number of apoptotic cells per mm^2 in each of the areas determined in (B). Experiment performed by Andreas Diepold.

3.3 Role of the chaperones prior and during secretion

The T3SS chaperones play a vital role in the coordination of effector export by the T3SS. Chaperones have been found to prevent effector mislocalization within the bacteria and guide them to the cytosolic interface of the injectisome (Rathinavelan *et al*, 2010; MacDonald *et al*, 2017). Additionally, they keep the effectors partially unfolded which allows for more efficient translocation through the injectisome (Wattiau *et al*, 1994; Frithz-Lindsten *et al*, 1995; Page & Parsot, 2002) and prevent premature degradation of the effectors (Stebbins & Galan, 2001). Although it is apparent that chaperones hold many functions prior to export, their role in effector export remains unclear. Do the chaperones allow the formation of a pool of effectors around the cytosolic interface of the injectisome? Do they aid in establishing an order of secretion? How are the export signals involved in the export mechanism? By exploring the role of the export signals and effects of chaperone overexpression and deletion, we aim to gain more insight into their essential role in protein export.

3.3.1 Chaperone overexpression does not affect effector export

To dissect the multiple roles of the chaperones in preparing and protecting effectors prior to export we tested if the overexpression of specific chaperones affects effector secretion by either promoting or inhibiting export. Specifically, we hypothesized several possibilities where overexpression of the chaperone could: improve the export of the cognate effector, while preventing the export of other effectors; unbound chaperones could abolish secretion; increase export of the cognate effector; or no effect on effector export. To determine the effects of excess chaperones, SycD, SycE, SycH, SycT and SycO were overexpressed from a pBAD vector plasmid in the wild-type *Yersinia* (MRS40) strain, which encodes all effector chaperones and effectors. Using an accumulative secretion assay, we grew the bacteria at 28°C for 1.5 hours and then shifted the cultures to 37°C. Upon shifting, we induced the expression of the chaperones with 0.5% arabinose from plasmid and collected the supernatant following two hours of secretion.

As shown in Figure 18.A, compared to the pBAD control there is no increase or loss of effector export with the overexpression of the chaperones. Since we did not see a distinct phenotype in effector export, we wanted to determine if this was a result of not being able to overexpress the chaperones to a high enough degree compared to the basal level of chaperones. Since there are no specific antibodies, we decided to measure the chaperone levels by mass spectrometry. Additionally, this method allowed for protein detection at very low levels, which may not be detected by immunoblot. Total cell proteome analysis was able to show that SycT, SycE, SycH, SycD and SycO were overexpressed approximately 14.5, 1.4, 5.5, 1.6 and 9.3-fold, respectively (Figure 18.B). However,

chaperone overexpression did not appear to have a negative effect on effector expression. Therefore, this suggests that the presence of unbound chaperones does not inhibit or increase the export of effectors.

We then decided to investigate if the overexpression of the chaperones demonstrated any effects on effector export in non-secreting cultures. Previous studies have shown that the overexpression of SycH induces effector export in non-secreting conditions by interacting with YscM1/2. We therefore completed an accumulative secretion assay comparing non-secreting and secreting conditions. The cultures were induced with 0.5% arabinose and secreted for two hours prior to collection. The resulting secretion patterns were compared to the pBAD control and demonstrated an increased export when SycH, SycE and SycO were overexpressed in non-secreting conditions. Although the effect of SycH is known, it was surprising to see that SycE and SycO appears to result in effector export (Figure 18.C). This could suggest that SycE and SycO, like SycH, have a regulatory role for *yop* expression either by interacting with YscM1/2 or another regulatory mechanism.

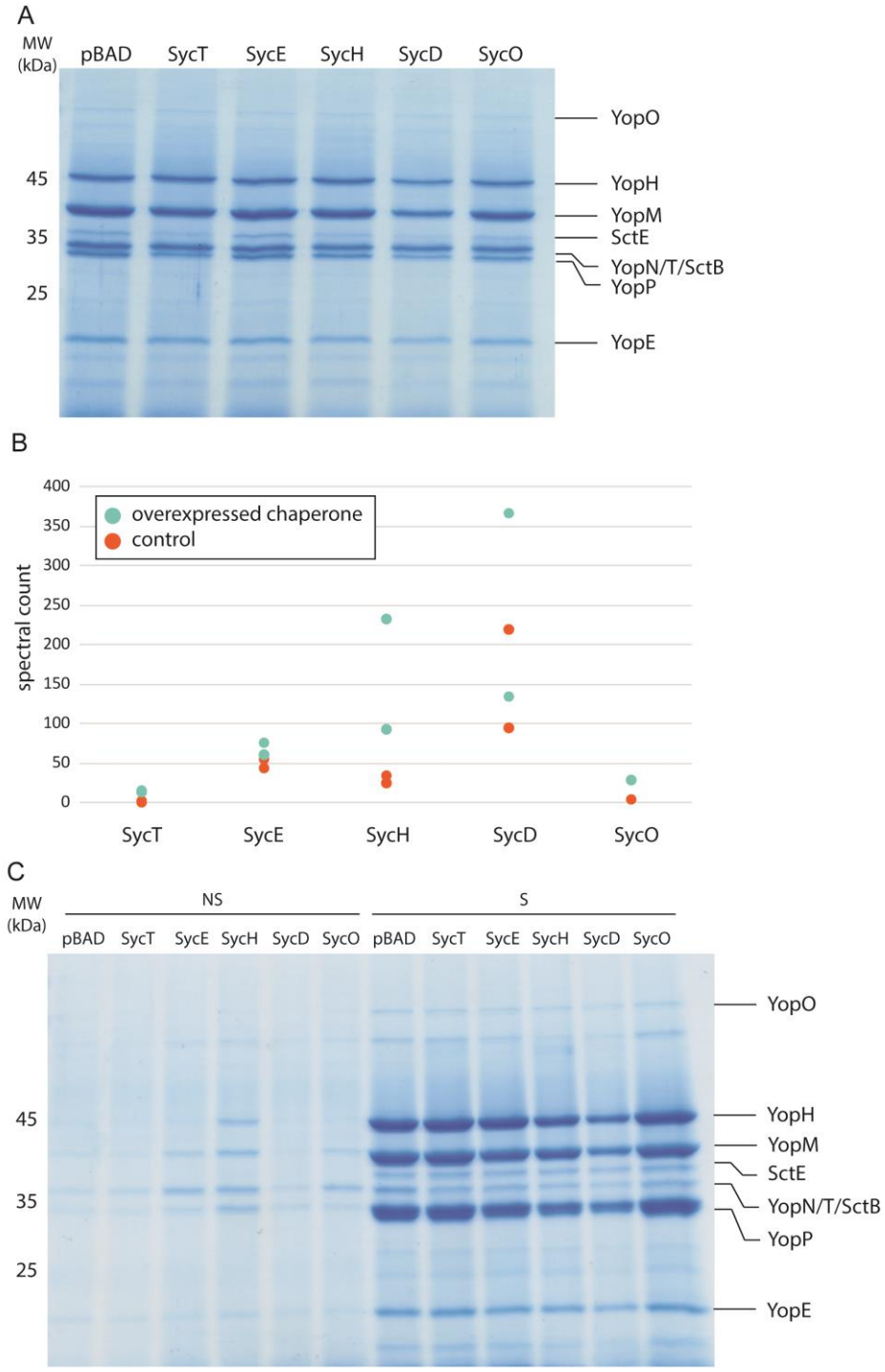

Figure 18: Effect of overexpressing chaperones on export of effector proteins in *Y. enterocolitica* MRS40 strain.
Accumulative effector secretion into the culture supernatant during a standard *in vitro* secretion with pBAD derived plasmids containing either SycT, SycE, SycH, SycD, or SycO. Cultures were induced with 0.5% arabinose and grown in either secreting or non-secreting conditions. **(A)** Culture supernatant of 3 x 10^9 bacteria from secreting cultures were removed and visualized by Coomassie staining on an SDS-PAGE gel. Control (far left) represents negative control (for pBAD, SycT, SycE, SycH and SycD, n=6; including SycO, n=3). **(B)** Ratio of total cell spectral counts of chaperones between overexpressed chaperones and pBAD vector control (for pBAD, SycT, SycE, SycH and SycD, n=2; including SycO, n=1). **(C)** Culture supernatant of 3 x 10^9 bacteria from secreting and non-secreting cultures were removed and visualized by Coomassie staining on an SDS-PAGE gel. Control (far left) represents negative control (for pBAD, SycT, SycE, SycH, SycD, and SycO, n=1). NS, non-secreting conditions – contains 5 mM $CaCl_2$. S, secreting conditions – contains 5 mM EGTA. Experiments performed by Bailey Milne-Davies.

3.3.2 Chaperone deletion has negative effects on substrate export

To determine the effects of chaperone deletion on effector export, SycH and SycE were deleted from the pYV virulence plasmid by allelic exchange. SycH and SycE overexpression plasmids were transformed into the respective deletion strains to complement the chaperone deletion. We performed an accumulative secretion assay to determine the effects of chaperone deletion, complementation, and comparison to the overexpression plasmids in wild-type *Y. enterocolitica* MRS40 strains. The secretion patterns show that deletion of the chaperones does have negative effects, where the ΔSycH strain is secretion deficient and the ΔSycE strain has significantly reduced export of translocators and effectors when compared to the control (Supplementary Figure 10.A). With the addition of the respective chaperone expression plasmids we do not observe complementation, but rather secretion-deficient strains. Since we were unable to complement the deletion strains, we checked to determine if the secretion deficiency was due to the lack of functional injectisomes. We performed a Western blot of the total cell pellet to measure the cellular concentrations of SctQ, a cytosolic component of the T3SS. The Western blot demonstrated that SctQ is efficiently expressed in wild-type MRS40 strain background, but no or highly reduced SctQ detection was visible in the ΔSycH and ΔSycE background, respectively (Supplementary Figure 10.B). This could suggest the loss of the pYV during homologous recombination, a large deletion of essential T3SS components that occurred during recombination, or that the chaperone is heavily involved in proper expression of the injectisome apparatus. We then amplified SctV, which is an essential component of the T3SS, by PCR from extracted pYV plasmid from the strains to determine if the pYV was present. PCR amplification demonstrated no amplification in the ΔSycH strains and amplification in the ΔSycE strain, but very low or no amplification in the complemented strain (Supplementary Figure 10.C). These PCR results suggest that either the pYV was lost or there was a major deletion within the pYV plasmid, however, how this occurred is not clear. The efforts to delete the chaperones from the virulence plasmid to further determine the function of the chaperones on effector export were inconclusive and thus not pursued further.

3.3.3 Establishing the role of export signals

To explore the role of the export signals on secretion, the translocation signal ($YopE_{1-53}$) and translocation signal containing the CBD ($YopE_{1-138}$) of YopE were fused to the reporter proteins, EGFP and NanoLuc. For $YopE_{1-138}$, we also included a construct that coexpresses the cognate chaperone SycE to determine if the addition to the chaperone affects secretion. These non-native cargos, EGFP and NanoLuc, were selected due to their different stability. Cargo stability has been shown to strongly affect export with more stably folded proteins being unable to be efficiently exported (Wilharm et al,

2004, 2007). EGFP has been shown to fold stably and even block the injectisome preventing not only export of the EGFP, but also other cargo (Radics et al, 2013), whereas the NanoLuc reporter has been shown to be easily exported out of the cell (Westerhausen et al, 2020), suggesting the reporter is less stably folded and thus easier to export than EGFP.

Accumulative secretion assays were performed to determine the effect of heterogeneous cargo export on secretion. Sample cultures were incubated at 28°C for 1.5 hours and then shifted to 37°C and plasmid expression was induced. We tested the cargo export at overexpression (0.2% arabinose) and native (0.03% arabinose) levels to determine effects on secretion. The arabinose concentration for native expression levels was determined based on the levels found in the $YopE_{1-138}$-EGFP coexpressed with the cognate chaperone, which utilizes the native promoter and is not arabinose inducible (Figure 19). Cultures then secreted for three hours prior to sample collection for SDS-PAGE Coomassie staining or Western blot.

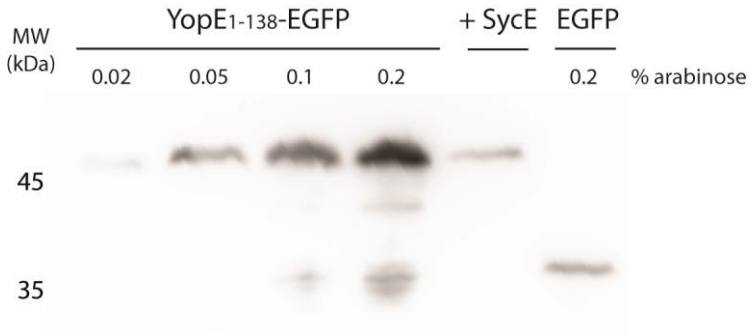

Figure 19: Induction of plasmid expression at different arabinose concentrations.
Total cell pellet analysis of EGFP expression levels at different arabinose induction levels and samples were collected after 3 hrs of secretion. $YopE_{1-138}$-EGFP was induced at 0.02%, 0.05% 0.1% and 0.2% arabinose, expression levels were compared to SycE, $YopE_{1-138}$-EGFP (+ SycE) expression levels (which utilize a native promoter rather than the arabinose promoter). EGFP control (far right) is a positive control for EGFP expression. 3 x 10^9 bacteria were separated on an SDS-PAGE gel and analyzed by immunoblot using antibodies against GFP (n=1).

When the EGFP cargo was overexpressed, there was no visible difference in the secretion pattern between the control and $YopE_{1-15}$-EGFP. However, $YopE_{1-53}$-EGFP export was significantly reduced and with $YopE_{1-138}$-EGFP export was even further reduced. Strikingly, the addition of SycE results in significant export of translocators at a levels similar to the control (Figure 20.A). Based on the expression levels in the total cell Western blot (Figure 20.B), the expression of $YopE_{1-138}$-EGFP coexpressed with SycE was lower than our arabinose-inducible cargo. Overexpression of the EGFP cargo resulted in a decrease in overall secretion when the translocation signals increased in length from $YopE_{1-53}$ to $YopE_{1-138}$. Interestingly, the coexpression of the chaperone SycE resulted in increased overall secretion at a level similar to the pBAD control, but the EGFP cargo is not visible (Figure 20.A).

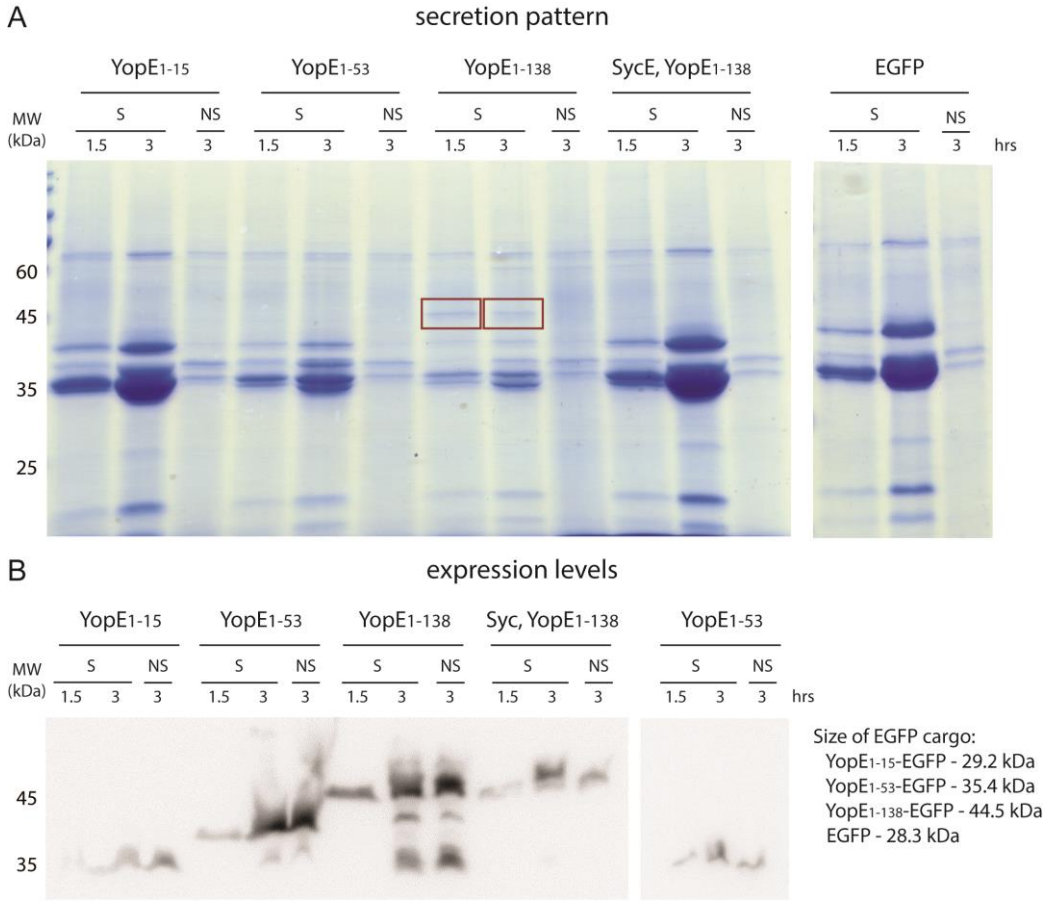

Figure 20: Secretion of overexpressed EGFP utilizing different secretion signals.
Accumulative effector secretion assay into the culture supernatant during a native in vitro secretion utilizing *Y. enterocolitica* ΔHOPEMTasd strain background expression EGFP cargo fused to different export signals ($YopE_{1-15}$-EGFP, $YopE_{1-53}$-EGFP, $YopE_{1-138}$-EGFP, and SycE, $YopE_{1-138}$-EGFP) on a pBAD vector plasmid. Secretion control (far right) demonstrates positive control and was utilized to demonstrate native secretion levels since cytosolic EGFP and that EGFP export is T3SS-dependent. Cultures were grown in secreting (S) or non-secreting (NS) conditions containing EGTA and $CaCl_2$, respectively. Plasmids were induced with 0.03% or 0.2% arabinose and samples for secretion were taken at 1.5 and 3 hr time points. **(A)** Cultures were induced with 0.2% arabinose and samples were taken at 1.5 and 3 hr time points. Culture supernatant of 3 x 10^9 bacteria was removed and visualized by Coomassie staining on an SDS-PAGE gel (n=3). $YopE_{1-15}$-EGFP, $YopE_{1-53}$-EGFP, $YopE_{1-138}$-EGFP, and SycE, $YopE_{1-138}$-EGFP were run on a differed SDS-PAGE gel than EGFP control samples. **(B)** Cultures were induced with 0.2% arabinose and samples were taken at 1.5 and 3 hr time points. Total cell pellet analysis of EGFP expression. 3 x 10^9 bacteria were separated on an SDS-PAGE gel and analyzed by immunoblot using antibodies against EGFP (n=3). Hr, time in hours. MW, molecular weight marker.

Since the main focus of this study was the export of cargo with the translocation signals (with and without the CBD) at native induction levels, we focused the experiments on $YopE_{1-53}$-EGFP, $YopE_{1-138}$-EGFP, and SycE, $YopE_{1-138}$-EGFP. We measured EGFP expression and secretion levels by immunoblot analysis against GFP since we wanted specific detection and secreted EGFP has a similar molecular weight and therefore cannot be differentiated from other proteins exported by the T3SS in a Coomassie-stained gel. Unfortunately, the immunoblot analysis varied between experiments for unknown reasons, however, we were able to gather some trends from the data. $YopE_{1-53}$-EGFP and $YopE_{1-138}$-EGFP, with and without SycE, are expressed at similar levels as the cytosolic EGFP (Figure 21.A). However, $YopE_{1-138}$-EGFP coexpressed with SycE was expressed at distinctly lower levels. We

also measured EGFP cargo secretion and found that YopE$_{1-53}$-EGFP is exported more than YopE$_{1-138}$-EGFP and the addition of SycE demonstrated even lower secretion levels (Figure 21.B). Since we could see that the EGFP cargo was secreted, we wanted to determine if EGFP export has a negative effect on overall secretion. The secretion pattern demonstrates that export of YopE$_{1-53}$-EGFP and YopE$_{1-138}$-EGFP does not affect the secretion of other substrates. Interestingly, the addition of SycE appears to improve secretion and enhance translocator export into the supernatant (Figure 21.C).

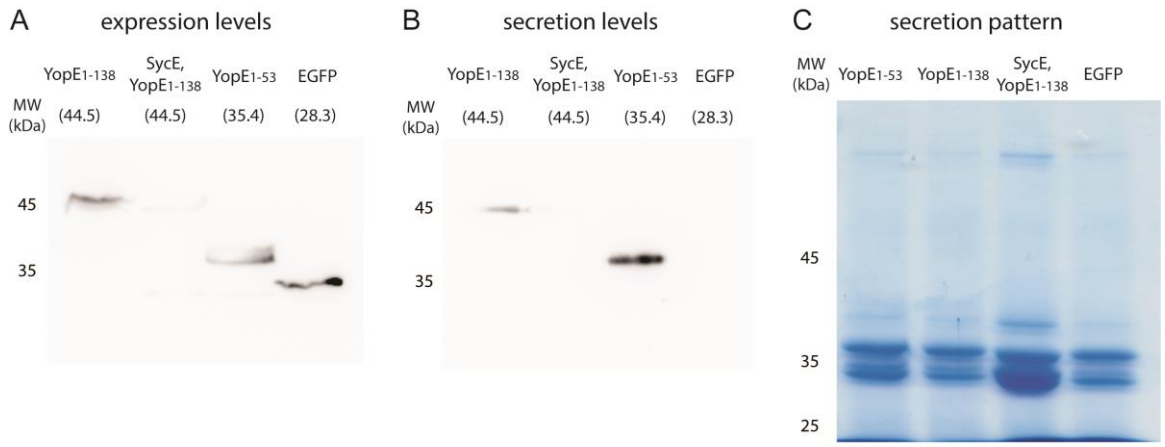

Figure 21: Secretion of EGFP at native level utilizing different secretion signals.
Accumulative effector secretion assay into the culture supernatant during a native in vitro secretion utilizing *Y. enterocolitica* ΔHOPEMTasd strain background expression EGFP cargo fused to different export signals (YopE$_{1-15}$-EGFP, YopE$_{1-53}$-EGFP, YopE$_{1-138}$-EGFP, and SycE, YopE$_{1-138}$-EGFP) on a pBAD vector plasmid. Secretion control (far right) demonstrates positive control and was utilized to demonstrate native secretion levels since cytosolic EGFP and that EGFP export is T3SS-dependent. Cultures were grown in secreting conditions with medium containing EGTA. Plasmids were induced with 0.03% and samples for secretion were taken at 3 hr time points. **(A)** Total cell pellet analysis of EGFP expression levels from 3 x 10^9 bacteria were separated on an SDS-PAGE gel and analyzed by immunoblot using antibodies against GFP (n=3). **(B)** Supernatant analysis of EGFP secretion levels from culture supernatant of 3 x 10^9 bacteria was removed and visualized by Coomassie staining on an SDS-PAGE gel (n=3). **(C)** Culture supernatant of 3 x 10^9 bacteria was removed and visualized by Coomassie staining on an SDS-PAGE gel (n=3). Numbers below MW (molecular weight) marker represent the molecular weight ladder. Numbers below the lane names represents the approximate protein size, with size given in kDa.

For the less stably folded NanoLuc, longer export signals resulted in more restricted secretion. Upon overexpression (0.2% arabinose), we visualized efficient secretion of substrates in YopE$_{1-15}$-NanoLuc. For YopE$_{1-53}$-NanoLuc, substrate secretion was reduced and using the longer translocation signal with the CBD there is more significant inhibition of overall secretion. Notably, the addition of the chaperone abolished secretion (Figure 22.A), rather than increasing export as seen for the EGFP cargo (Figure 20 and Figure 21).

Since we were most interested in the effect of the different translocation signals, we focused our experiments on the export of these proteins under native induction levels. Using native level arabinose induction (0.03% arabinose), a similar secretion pattern was observed where YopE$_{1-53}$-NanoLuc was exported more than the NanoLuc cargo including the translocation signal, CBD and coexpressed with

SycE – which resulted in complete inhibition of secretion (Figure 22.B). This phenotype was highly unexpected considering NanoLuc is expected to be the less stably folded cargo. Next, we utilized a luciferase assay which allowed us to quantify NanoLuc export in the supernatant and total cell pellet. The luciferase assay determined that within the total cell fraction (Figure 22.C), luciferase activity was lower for $YopE_{1-53}$-NanoLuc. However, this cargo was highly exported which could account for the lower cytosolic levels. Cytosolic levels of $YopE_{1-138}$-NanoLuc were lower than for $YopE_{1-138}$-NanoLuc coexpressed with SycE, however this does not coincide with higher export. It is possible that the chaperone may prevent degradation of the $YopE_{1-138}$-NanoLuc within the bacterial cytosol and this could be why the coexpression of SycE results in higher cellular concentration of $YopE_{1-138}$-NanoLuc. The assay determined that $YopE_{1-53}$-NanoLuc is exported distinctly more in the supernatant than $YopE_{1-138}$-NanoLuc and the addition of SycE did not improve NanoLuc export (Figure 22.D).

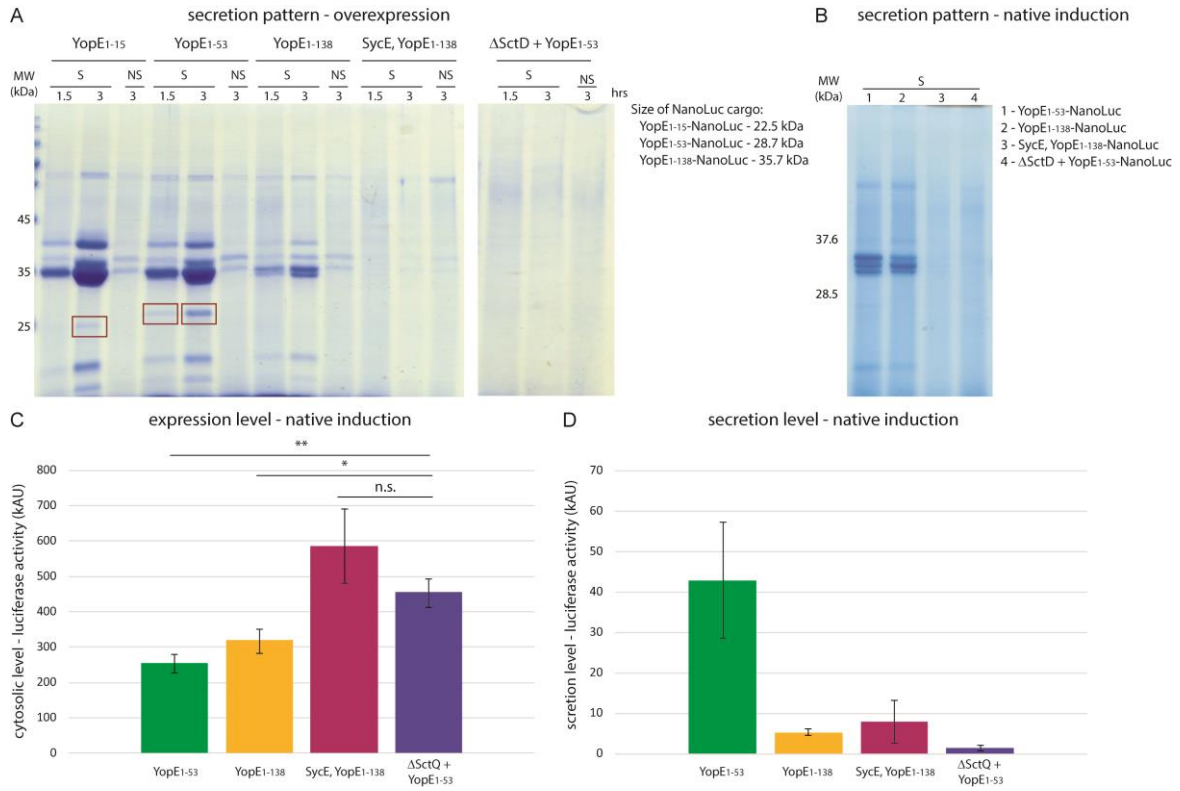

Figure 22: Influence of secretion signals and coexpression of chaperone on the secretion of the NanoLuc report substrate.

Accumulative effector secretion assay into the culture supernatant during a native *in vitro* secretion utilizing *Y. enterocolitica* ΔHOPEMTasd strain background expression NanoLuc cargo fused to different export signals ($YopE_{1-15}$-NanoLuc, $YopE_{1-53}$-NanoLuc, $YopE_{1-138}$-NanoLuc, and SycE, $YopE_{1-138}$-NanoLuc) on a pBAD vector plasmid. Secretion control (far right) demonstrates negative control (n=3). Cultures were grown in secreting (S) or non-secreting (NS) conditions containing EGTA and $CaCl_2$, respectively. Plasmids were induced with 0.03% or 0.2% arabinose and samples for secretion were taken at 1.5 and/or 3 hr time points. **(A)** Cultures were induced with 0.2% arabinose and samples were taken at 1.5 and 3 hr time points. Culture supernatant of 3 x 10^9 bacteria was removed and visualized by Coomassie staining on an SDS-PAGE gel (n=3). **(B)** Cultures were induced with 0.03% arabinose and samples were taken at the 3 hr time point. Culture supernatant of 3 x 10^9 bacteria was removed and visualized by Coomassie staining on an SDS-PAGE gel (n=3). **(C)** Quantification of NanoLuc cargo expression, samples were grown under secreting conditions following 0.03% arabinose induction and 3 hrs of secretion (n=3). **(D)** Quantification of NanoLuc cargo export into the supernatant under secreting conditions following 0.03% arabinose induction and 3 hrs of secretion (n=3). Once samples were collected, the total cell pellet was resuspended in non-secreting medium to inhibit export of NanoLuc into the supernatant. For C and D, green bar, $YopE_{1-53}$-NanoLuc; Yellow bar, $YopE_{1-138}$-NanoLuc; Pink bar, SycE, $YopE_{1-138}$-NanoLuc; Purple bar, ΔSycQ + $YopE_{1-53}$-NanoLuc.

3.3.4 Supplementary results

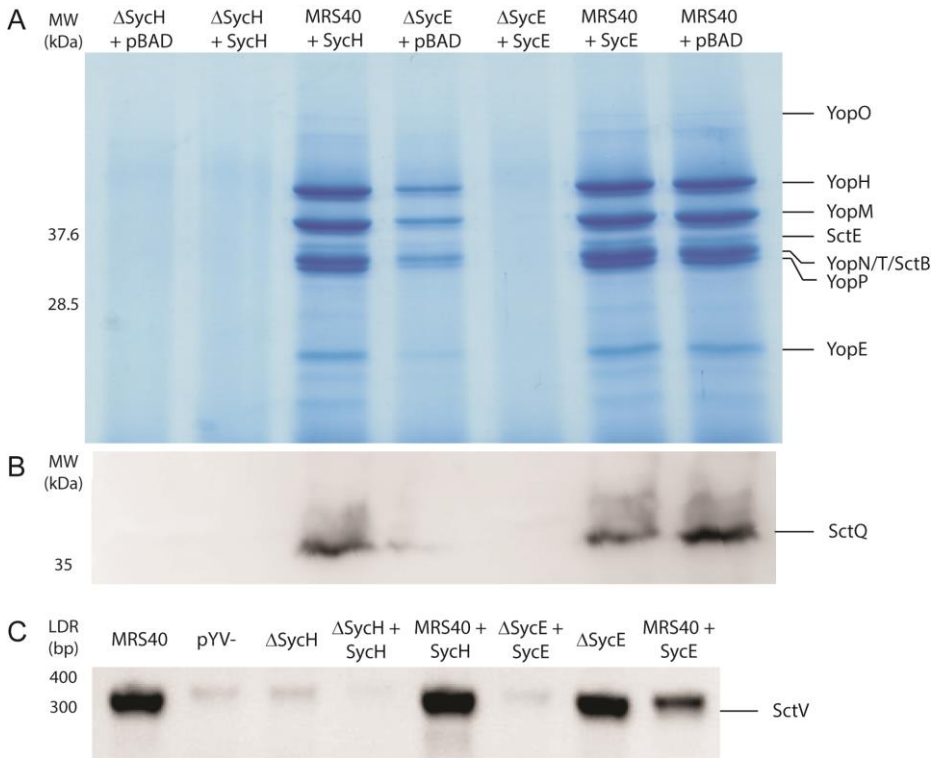

Supplementary Figure 10: Chaperone deletion and complementation in *Y. enterocolitica* MRS40 background strains. Accumulative effector secretion into the culture supernatant during a standard in vitro secretion with ΔSycH and ΔSycE mutants and wild-type MRS40 strains. Deletion mutants were transformed with a pBAD vector control and respective chaperone plasmids for deletion complementation. Plasmid controls in MRS40 strains were utilized to demonstrate overexpression does not negatively affect export. Control (far right) represents positive control (n=3). Cultures were induced with 0.5% arabinose and secreted for 3 hrs. **(A)** Culture supernatant of 3 x 10^9 bacteria was removed and visualized by Coomassie staining on an SDS-PAGE gel (n=3). **(B)** Total cell pellet analysis of chaperone mutants and controls. 3 x 10^9 bacteria were separated on an SDS-PAGE gel and analyzed by immunoblot using antibodies against SctQ (n=3). Sample order is the same as indicated by the lane titles in A. The respective analysis of the bacteria are from the same experiments and are subjected to the same conditions. **(C)** Detection of the pYV to ensure strains still contain the pYV. Plasmids were extracted from overnight cultures of indicated strains and used for PCR amplification of SctV, a vital component of the T3SS. Bands indicate amplification of the gene using gene specific primers (n=1). MW, molecular weight marker; LDR, ladder; bp, base pairs.

3.3.5 Characterizing the effector pool of *Yersinia*

Effector export has been shown to begin almost immediately once secretion is activated (Schlumberger et al, 2005; Enninga et al, 2005; Barber & Stark, 2014; Milne-Davies et al, 2019). Although export is well studied, it remains unclear whether *Yersinia* utilizes a pre-synthesized pool of effectors, and if effectors are exported co-translationally or post-translationally during ongoing secretion. Utilizing a pre-synthesized pool would require a small pool of effectors ready to be synthesized prior to activation and once this pool is depleted, new effector biosynthesis would allow effectors to be produced and subsequently exported. Co-translational export describes expression of the effectors directly into the injectisome for immediate export; whereas post-translational export

would consist of the expression of the effectors, followed by the guiding of the protein to the injectisome potentially with the aid of a chaperone.

To determine if *Yersinia* synthesizes a pool of effectors prior to activation, we grew two cultures, either in non-secreting or secreting conditions (containing either Ca^{2+} or EGTA, respectively), at 28°C for 1.5 hours to bring the cultures to exponential phase and then shifted the cultures to 37°C for 2.5 hours to induce expression and assembly of the T3SS. The cultures were then split into two and chloramphenicol (15 µg/ml) was added to one culture in each environment to prevent further biosynthesis of effectors. Following 10 minutes of chloramphenicol exposure, a baseline sample at -5 minutes was taken for all cultures prior to activation of the non-secreting cultures (activated bacteria). Non-secreting cultures were activated with EGTA (10 mM) to create a low Ca^{2+} environment equal to the secreting cultures at the 0-minute time point. Samples were then taken 15, 30, 45 and 60 minutes afterwards and analyzed by SDS-PAGE and Coomassie staining.

As shown in Figure 23.A, the continuously secreting bacteria exported effectors consistently over time. With the addition of chloramphenicol, the bands decreased over time. This demonstrates that biosynthesis is significantly decreased and effectors in the supernatant are likely degraded overtime. The activated bacteria demonstrate effector export in both conditions treated with and without chloramphenicol (Figure 23.B). The bacteria not treated with chloramphenicol consistently exported effectors over time, resulting in an increase in effector concentration, which is indicated by the darker bands. However, bacteria treated with chloramphenicol showed an increase in exported effectors between the -5 minutes' baseline (non-secreting conditions) and 15 minutes' post-activation (15 minutes following the addition of EGTA to culture to induce secretion), which could be the pre-synthesized pool. A small amount of exported effectors could be visualized in the first 15 minutes of secretion and over time the bands appeared to be more distinct. This slight increase over time could indicate that the pool is being exported over a longer time range or that biosynthesis of new effectors was not completely inhibited. Interestingly, in the activated bacteria we can see a distinct difference between bacteria treated with and without chloramphenicol, where the majority of the early export is dependent on effector synthesis. This emphasizes that the pool of pre-synthesized effectors is rather small and the bacteria rely on rapid synthesis of new effectors that need to be quickly exported once or while the pre-synthesized pool is depleted.

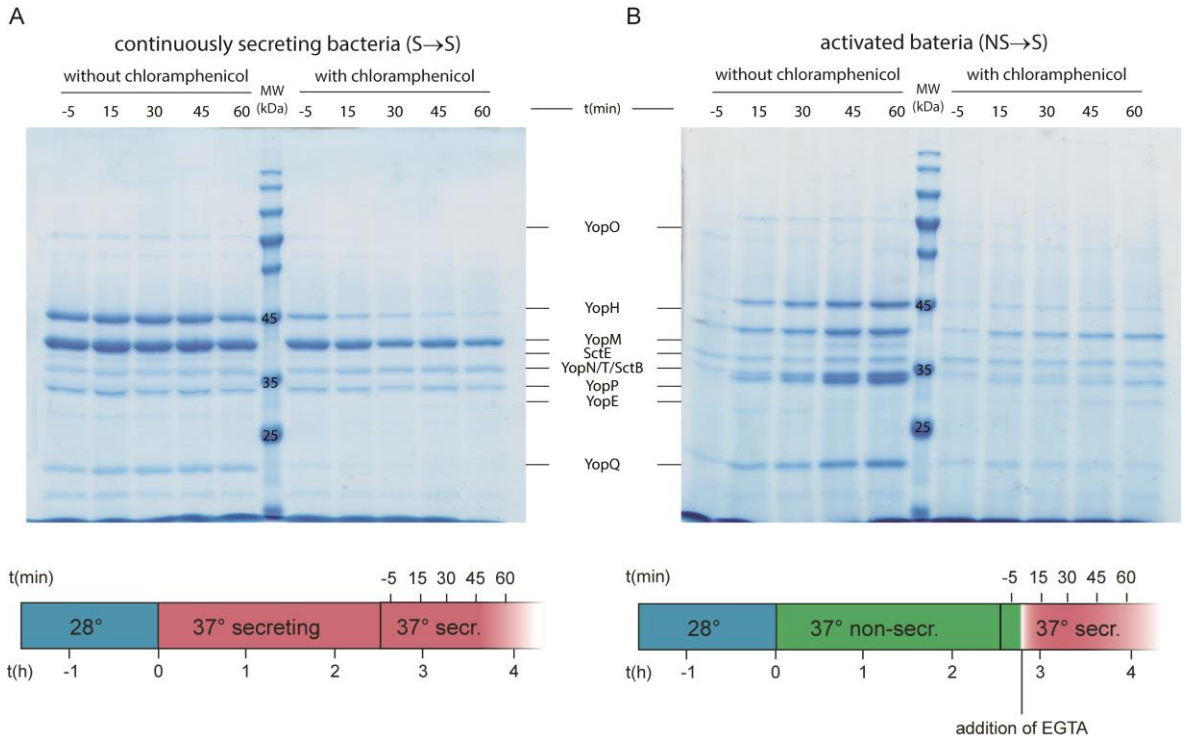

Figure 23: Pre-synthesized pool of effectors exported upon activation.
Accumulative secretion assay of wild-type *Y. enterocolitica* (MRS40) secreting into culture supernatant with and without chloramphenicol to determine the presence of a pre-synthesized pool of effectors. Cultures were initially grown at 28°C for 1.5 hrs in either non-secreting or secreting conditions containing $CaCl_2$ and EGTA, respectively. Cultures were then shifted to 37°C for 2.5 hrs. Each culture was split into two and chloramphenicol (15 µg/ml) was added one of the two cultures in each condition. After 10 min of chloramphenicol incubation, baseline samples were taken 5 min prior to activating secretion of non-secreting cultures. Previously non-secreting cultures were activated by the addition of 10 mM EGTA directly to the culture to induce secretion at the 0-min time point. Samples were then collected at 15, 30, 45 and 60 min. **(A)** Continuously secreting control and **(B)** activated bacteria culture supernatant of 3 x 10^9 bacteria was removed and visualized by Coomassie staining on an SDS-PAGE gel (n=3). Experimental timeline can be seen below. Baseline samples at -5 min were taken as control for each culture.MW, molecular weight; NS/non-secr., non-secreting conditions; S/secr., secreting conditions; min, minutes; h, hours.

3.4 Role and location of the gatekeepers

It has been established that the gatekeepers (YscB/SycN/SctW/TyeA) are responsible for reacting to changes in environmental calcium levels and controlling the secretion switch (Day & Plano, 1998; Day *et al*, 2003; Iriarte *et al*, 1998). As a result, these proteins play an essential role in controlling the activation and deactivation kinetics. Although we understand that these proteins have an important regulation function, how the gatekeepers work and their location during these events have not been established (Cheng *et al*, 2001). As a result, we fluorescently tagged YscB, SycN and TyeA to either EGFP or sfGFP to visualize the location of the gatekeepers in secreting and non-secreting conditions via fluorescent microscopy. SctW was not selected to be tagged, since SctW is exported and it is known that tagging exported proteins can negatively affect successful export; additionally, this protein interacts with other proteins at both the N- and C-terminus which could affect the complex functionality.

3.4.1 Gatekeepers are functional and stable

YscB and SycN are chaperones that bind to the N-terminus of SctW (the main gatekeeper) and TyeA is the calcium regulator in the complex. If any of these components are not functional, the bacterium permanently secretes regardless of the calcium levels. EGFP-YscB, SycN-sfGFP and TyeA-sfGFP were inserted into the ΔHOPEMTasd pYV via allelic exchange. YscB was tagged at the N-terminus since the N-terminus doesn't interact with SctW. For SycN and TyeA, the N-terminus of both proteins interacts with SctW and to avoid affecting the function, the C-terminus was tagged. Once successfully integrated, the functionality of the gatekeepers was tested. EGFP-SctQ, ΔSctD, ΔHOPEMTasd and ΔSctW were included as controls: EGFP-SctQ was utilized as a GFP positive control; ΔSctD serves as a T3SS-deficient control that is unable to secrete; ΔHOPEMTasd serves as a positive secretion control; and ΔSctW is a constitutively secreting control to demonstrate loss of gatekeeper function. Bacteria were grown in secreting and non-secreting conditions and were first incubated at 28°C for 1.5 hours. Following incubation, the cultures were shifted to 37°C for three hours. Samples were collected and the supernatant and total cell were analyzed by SDS-PAGE Coomassie staining and Western blot, respectively. The secretion pattern of the Coomassie stained supernatant, indicates that the gatekeepers are functional. If the gatekeepers were not functional, secretion would be uncontrolled in non-secreting conditions as depicted by ΔSctW in Figure 24.A. Although the gatekeepers are functional, it appears that EGFP-YscB is slightly leaky with a darker secretion pattern than the control. To determine GFP stability of the fusions, the total cell samples were analyzed by Western blot against GFP. The results show that GFP is not significantly cleaved in the sample and the fusion proteins are stable (Figure 24).

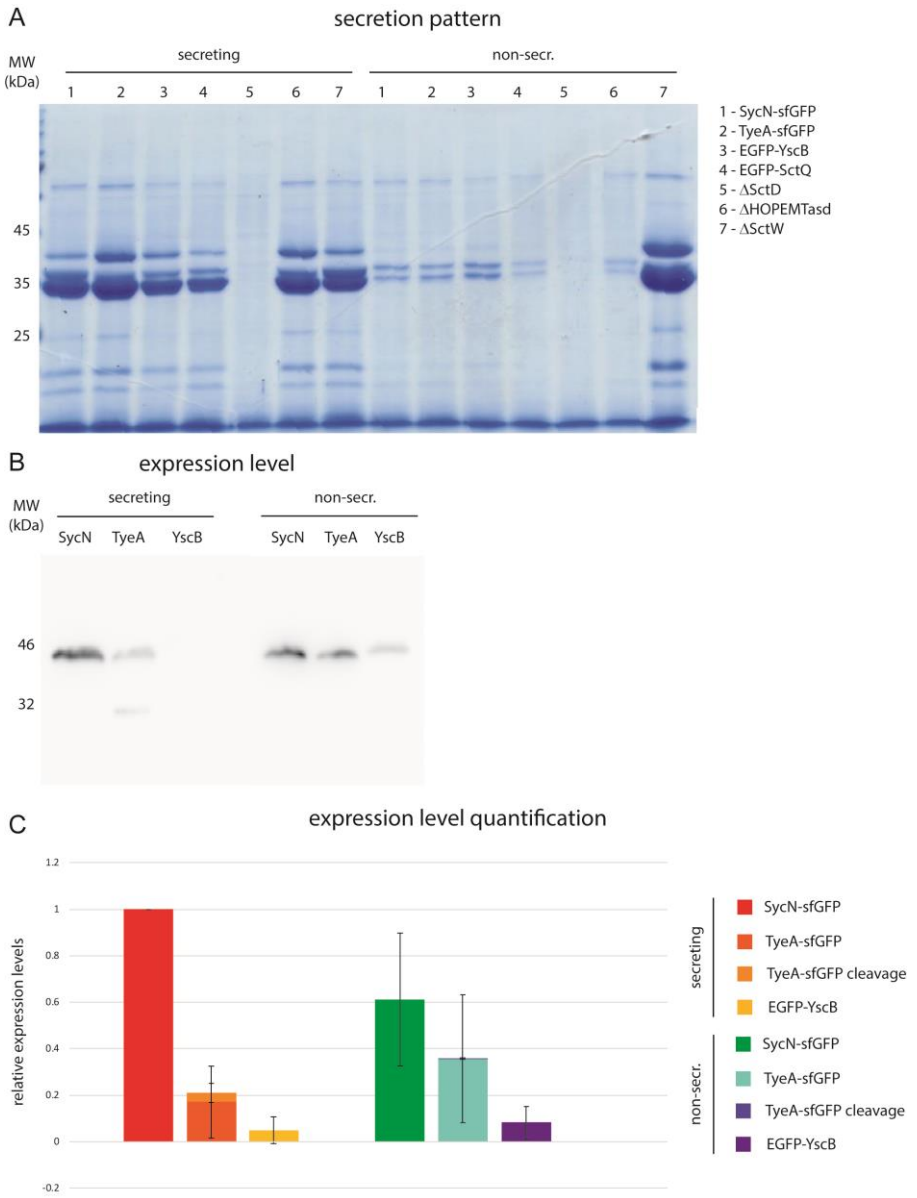

Figure 24: Functionality and stability of gatekeepers.
Accumulative secretion assay utilizing *Y. enterocolitica* ΔHOPEMTasd strains with EGFP-YscB, SycN-sfGFP and TyeA-sfGFP expressed from their native locus. Cultures were grown in either secreting or non-secreting cultures and first incubated at 28°C for 1.5 hrs and then shifted to 37°C. Samples were taken after 3 hrs and prepared for SDS-PAGE electrophoresis. **(A)** Culture supernatant of 3 x 10^9 bacteria was removed and visualized by Coomassie staining on an SDS-PAGE gel. EGFP-SctQ is utilized as a GFP control; ΔSctD is secretion deficient and utilized as the negative control; ΔHOPEMTasd is a native secretion control, demonstrating native secretion regulation; and ΔSctW is the positive control, demonstrating uncontrolled secretion regardless of the calcium levels (n=3). **(B)** Total cell pellet analysis of EGFP stability. 3 x 10^9 bacteria were separated on an SDS-PAGE gel and analyzed by immunoblot using antibodies against EGFP. EGFP-SctQ is utilized as a positive GFP control (n=3). **(C)** Relative expression levels of gatekeeper and GFP fusions. Expression levels were quantified by densitometric analysis of bands from immunoblot analysis against GFP. Bands were normalized by the average export of SycN-sfGFP (n=3). Error bars display standard deviation of the mean. Secreting and non-secreting (non-secr.) conditions refers to secretion conditions in medium containing EGTA or $CaCl_2$, respectively. Experiments performed by Bailey Milne-Davies and Anna-Lena Koida.

3.4.2 The gatekeeper proteins are localized in the cytosol

To determine the localization of the gatekeepers, we visualized the gatekeepers under secreting and non-secreting conditions. YscB, SycN, and TyeA were localized in the cytosol with no distinct foci at the membrane as seen for EGFP-SctQ in both secreting and non-secreting conditions. Since no foci were observed at the membrane, the gatekeepers don't appear to directly bind to the injectisome as previously hypothesized. Instead, cytosolic localization demonstrates a potentially different mechanism which may rely on a decentralized regulation rather than physically plugging the injectisome (Figure 25.A). To ensure that the GFP fusions are not more stable than the native proteins, we measured the plug proteins via mass spectrometry, since we lack antibodies to detect these proteins by immunoblot. Additionally, this method provides higher sensitivity, allowing detection of proteins at very low levels. YscB spectral counts were distinctly lower than native levels, which may explain the leakiness in the accumulative secretion assay. The SycN spectral counts were slightly lower than native levels, whereas TyeA levels were slightly higher. Overall, the stability of the fluorescent fusions is unlikely to explain the cytosolic localization (Figure 25.B). Thus, it appears that the gatekeepers function in the cytosol and not directly, as seen in *E. coli*.

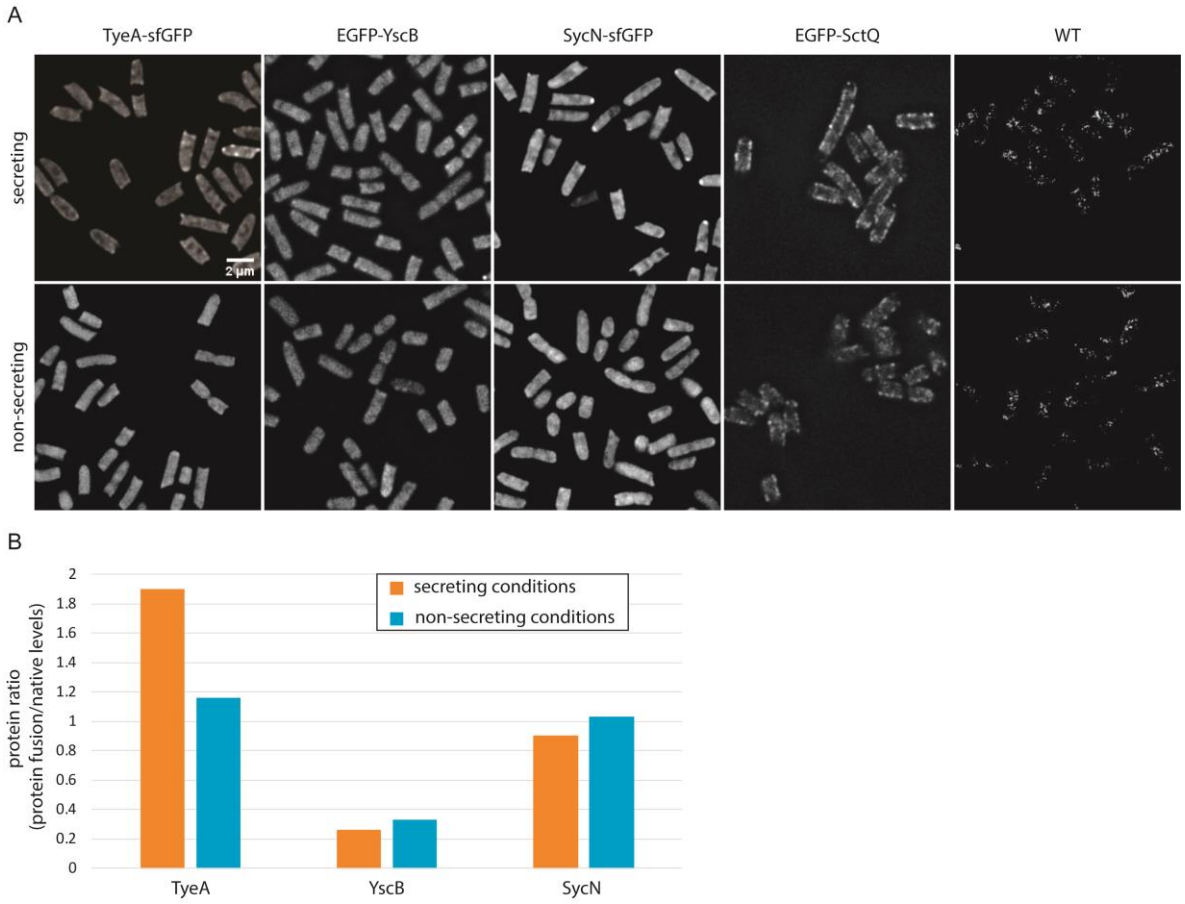

Figure 25: Gatekeepers localize in the cytosol in secreting and non-secreting conditions.
Y. enterocolitica ΔHOPEMTasd strains with SycN-sfGFP, TyeA-sfGFP, EGFP-YscB, and EGFP-YscQ expressed from their native locus. Cultures were grown in either secreting or non-secreting cultures and first incubated at 28°C for 1.5 hrs and then shifted to 37°C. Samples were taken after 3 hrs for analysis. **(A)** Micrographs of *Y. enterocolitica* ΔHOPEMTasd localization of SycN-sfGFP, TyeA-sfGFP, EGFP-YscB, EGFP-SctQ, and WT (ΔHOPEMTasd) in secreting (upper panel) and non-secreting (lower panel) conditions. Bacteria were visualized under 100x magnification using the green channel. 1-2 micrographs were analyzed per strain and condition, n=234-514. **(B)** Proteomic analysis of the total cell measuring the spectral count levels of SycN, YscB, and TyeA fusions compared to native levels in fusion strains and EGFP-SctQ, ΔSctD, ΔSctW, and WT (ΔHOPEMTasd). Native levels were averaged in each strain excluding protein fusions and protein fusion levels were divided by native level averages (n=1). Experiments performed by Bailey Milne-Davies and Anna-Lena Koida.

4. Discussion

4.1 Life After Secretion - *Yersinia enterocolitica* rapidly toggles effector secretion and can resume cell division in response to changing external conditions

Events following secretion – the deactivation of the T3SS, the recovery of division, and the possible future encounters with host cells – were unclear in *Yersinia*, regardless of their essential role in pathogenesis. In this project, we explored the kinetics of activation and, most interestingly, deactivation of secretion by external cues, as well as the potential for *Y. enterocolitica* to reestablish division and reactivate secretion afterwards. During infection, when *Y. enterocolitica* enters through the Peyer's Patches, the bacteria may come into contact with immune cells. In these circumstances, activation of effector export must occur rapidly to defend the bacteria from phagocytosis and inflammatory responses (Grosdent *et al*, 2002; Navarro *et al*, 2005; Philip *et al*, 2016; Galán, 2009; Pha & Navarro, 2016). Fast initiation of the type III secretion has been observed in other bacteria (Schlumberger *et al*, 2005; Enninga *et al*, 2005; Mills *et al*, 2008). Following an encounter with an immune cell, it is conceivable that *Y. enterocolitica* would benefit from inhibiting effector export and resuming division and subsequent dissemination throughout the host (where the bacteria may face another immune cell encounter). To explore T3SS kinetics, specifically activation and deactivation, in a fast and quantitative manner, we utilized an *in vitro* secretion assay for the reporter substrate β-lactamase in *Y. enterocolitica* fused to a short secretion signal from the native *Y. enterocolitica* effector YopH (Sory *et al*, 1995). Low and high calcium levels, as used in the assay, have been hypothesized to mimic the intracellular conditions within host cells (low calcium) and the extracellular host conditions (high calcium), respectively. Our results show that just like activation of secretion (Figure 10.D), deactivation (Figure 11.A) occurs immediately when introduced into secreting or non-secreting media, respectively.

The ability to quickly respond to external stimuli suggests that *Y. enterocolitica* has one or several highly sensitive regulation mechanisms controlling secretion. How the bacteria are able to sense host cell contact and environmental changes, like calcium levels, remains unclear. Several studies, mostly performed in *Shigella flexneri*, suggests that host cell contact is sensed by the needle tip (Veenendaal *et al*, 2007; Roehrich *et al*, 2013), where the signal is then transduced by rearrangements of needle subunits to the cytosolic interface of the T3SS (Torruellas *et al*, 2005; Kenjale *et al*, 2005; Davis & Mecsas, 2006). Other external cues, such as calcium, and other T3SS inducing stimuli, such as Congo Red, might be sensed by the needle tip and transmitted the same way. However, the cytosolic complex

of the *Y. enterocolitica* T3SS has been observed to be influenced by external calcium levels in strains lacking SctD (and therefore no assembled needles), suggesting a direct mechanism to sense external stimuli (Diepold *et al*, 2017). On the other hand, a calcium-dependent interaction between SctP (ruler protein) and SctW (cytosolic gatekeeper) in EPEC supports a different model where effector export is inhibited when a constant local influx of calcium ions enters the bacterium through the T3SS (Shaulov *et al*, 2017).

Interestingly, our deactivation experiments demonstrated that not all substrate classes are equally affected by concentration of calcium in the environment. The export of effectors was strongly suppressed by the increase in calcium levels, whereas the export of early and middle substrates – which are required for needle assembly – continues, although at a lower rate. In contrast, the decrease in temperature to 26°C, at continued low calcium levels, resulted in almost complete inhibition of early and middle substrate export, but allowed continued effector export (Figure 11.B and C; Supplementary Figure 2). Similar differential regulation between export of different substrate classes has been shown for *P. aeruginosa* (Cisz *et al*, 2008) and EPEC (Shaulov *et al*, 2017), suggesting a conserved mechanism among different T3SS.

Coordinating secretion events in *Y. enterocolitica* is essential since unlike other pathogens, *Yersinia* homogeneously expresses the T3SS at 37°C (Figure 9) and the complete population actively secretes in *in vitro* conditions (Wiley *et al*, 2007). The low fraction of T3SS-negative bacteria, even following long term secretion and regardless of decreased replication rate of T3SS-positive bacteria, demonstrates the essential role of the T3SS during infection. What happens after the bacterium survives an encounter with an immune cell? Following effector secretion, *Y. enterocolitica* benefit from reestablishing faster division, while remaining prepared to counter another immune cell attack. It would appear obvious that *Y. enterocolitica* would be able to reinitiate replication *in vivo*, however, it has remained unresolved since in *in vitro* conditions all injectisomes are activated (Wiley *et al*, 2007), which may differ from native infection conditions and other possible adaptations during infection (Heroven & Dersch, 2014; Avican *et al*, 2015). We found that *Y. enterocolitica* can swiftly restart cell division when reintroduced into a non-secreting environment following previous exposure to secretion-inducing conditions (Figure 12.A-C). This would demonstrate that new encounters with host cells, specifically with immune cells, is feasible. We showed that previously secreting *Y. enterocolitica* continue to assemble new needles (Figure 11.B), and when reintroduced into secreting media from non-secreting media can reactivate the T3SS (Figure 12.D). Being able to reestablish secretion likely allows the bacteria to defend themselves during future immune cell interactions. This indicates that *Y. enterocolitica* do not combat immune cells in an altruistic manner, but rather attempt to increase individual fitness.

Other pathogens deviate from this strategy and employ their T3SS differently. The *Salmonella* Typhimurium SPI-1 T3SS is expressed in a subpopulation of the bacterium, which induces an inflammatory response to reduce competition of the established microbiome. As a result of the inflammation and the reduced growth rate of the SPI-1 positive population, the SPI-1 negative population is able to outgrow both the SPI-1 positive subpopulation and residential bacteria (Sturm *et al*, 2011; Weigel & Dersch, 2018). This strategy allows for cooperative virulence amongst the *Salmonella* population, which allows SPI-1 negative bacteria to colonize the small intestine and increases the population fitness while promoting efficient invasion of the host (Ramos-Morales, 2012).

The link between secretion and cessation of growth and division remains unclear; however, it is hypothesized that this phenotype may be the result of: the leakage of ions and amino acids through the needle (Fowler *et al*, 2009; Fowler & Brubaker, 1994); the metabolomic burden impressed on the bacteria to maintain biosynthesis, assembly, and operation of the T3SS (Brubaker, 2005; Wilharm & Heider, 2014; Wang *et al*, 2016; Sturm *et al*, 2011); unknown specific regulator mechanisms; or a combination of different factors. Our findings show that cell division is restored within a short period following the inhibition of secretion, which is more compatible with a direct effect of ion leakage or an active regulatory mechanism. In agreement, when we explored the relationship between secretion and metabolic burden, we found that secreting bacteria are not energetically exhausted and the energy charge of activated bacteria demonstrate an energy charge that is not significantly different from continuously non-secreting bacteria (Figure 13.A).

The results from this project emphasize important aspects of *Y. enterocolitica*'s life after secretion. They demonstrate the bacteria's ability to quickly adapt to inhibit type III secretion, reestablish growth and division following the loss of the secretion cue, while remaining capable of fighting future immune attacks and disseminating throughout the host. Ultimately, it is evident that *Y. enterocolitica* employs the T3SS to promote individual fitness.

4.2 LITESEC-T3SS – Light-controlled protein delivery into eukaryotic cells with high spatial and temporal resolution

The LITESEC systems allow for highly controlled regulation of translocation by directly sequestering an essential component of the T3SS, SctQ, to the bacterial membrane. By altering the dynamics of SctQ, secretion can be activated or inhibited by external light. My involvement in establishing human cell culture and infection assays allowed us to demonstrate that the LITESEC systems not only allow control of secretion, but more importantly, control of translocation. This method offers a unique opportunity to understand protein interaction within bacteria and applications for industry.

As a proof of principle, we translocated the $YopE_{1-53}$-β-lactamase reporter into HeLa cells in either light or dark conditions using LITESEC strains. We were able to show (Figure 15), in both the LITESEC-act and -supp, that the reporter was efficiently translocated into the host cells under activating conditions (light or dark, respectively). The level of translocation was significantly higher in active conditions than under inactive conditions and the negative control. To demonstrate that the LITESEC systems could be used to induce cell death, we translocated $YopE_{1-138}$-tBID into the host cells using the LITESEC strains. We were able to successfully induce apoptosis of the host cells using both LITESEC strains under inducing conditions (Figure 17).

The LITESEC systems is a unique tool that can be applied in a variety of fields, specifically in cell biology and the biomedical industry. Generally, the T3SS translocates cargo in an uncontrolled manner, thus making application – especially in healthcare – highly uncontrollable and subsequently unusable. By overcoming this obstacle, the T3SS can be employed in a controlled and specific manner. Previously, the T3SS was mainly controlled by inducible promoters (Song *et al*, 2017; Schulte *et al*, 2019), however, these methods did not specifically control activation and deactivation of the T3SS and induction of expression and assembly of the system is slow (Diepold *et al*, 2010; Song *et al*, 2017; Schulte *et al*, 2019). These drawbacks prevent the use of inducible promoters from applying the secretion in a highly controlled and specific manner. However, by utilizing external light to induce or inhibit secretion, the T3SS can be efficiently controlled. We have demonstrated that translocation can be activated at a specific time and location by illuminating specific areas of interest. Also, this activation and deactivation of the LITESEC systems is reversible, which allows translocation to be inhibited within a few minutes when introduced to inactive illumination conditions. However, an important consideration when looking to apply the LITSEC-T3SS systems for protein translocation into eukaryotic cell is that the bacterial vector could initiate toxic or immunological responses (Walker *et al*, 2017; Felgner *et al*, 2017). During this study, we utilized *Y. enterocolitica* from ΔHOPEMTasd background,

which lack the main virulence effectors (YopH, O, P, E, M, and T) and are auxotrophic for diaminopimelic acid – preventing the bacteria from replicating without the addition of this amino acid. We were able to show that our inactive LITESEC strains did not induce negative side effects among the host cells when incubated for an extended period (Supplementary Figure 8). Nonetheless, if the LITESEC systems are to be further applied, it would be essential to determine bacterial vectors that induce less immunological side effects through the engineering bacteria that with less pathogen-associated virulence mechanisms (Bai *et al*, 2018; Neeld *et al*, 2014; Felgner *et al*, 2017; Walker *et al*, 2017).

Prior to utilizing $YopE_{1-138}$-tBID to induce apoptosis in the host cells, we attempted to utilize other pro-apoptotic proteins (PUMA, HSVTK and p53) to induce cell death. These proteins have been previously found to induce cell death, although not in this application. We fused these proteins to the $YopE_{1-53}$ and $YopE_{1-138}$ and could observe successful secretion into the supernatant with these translocation signals (Figure 16). However, these constructs were unsuccessful in inducing host cell death. Unfortunately, we were unable to determine why these proteins were not inducing host cell death since the translocation of these proteins could not be measured in the host cell lysate by Western blot. Are they being successfully translocated into the host cells? Are these proteins functional? Were the HEp-2 host cells resistant to all pro-apoptotic protein candidates? Our hypothesis is that the coexpression of the cognate chaperone promotes more efficient export of the cargo into host cells, demonstrating that for efficient translocation of functional proteins the chaperone needs to be coexpressed. As a result, we utilized the $YopE_{1-138}$-tBID cargo which had been previously shown to induce apoptosis (Ittig *et al*, 2015). We saw that this cargo was also coexpressed with the cognate chaperone, which brought the question whether the chaperone was needed to successfully translocate functional proteins into the host cell. Florian Lindner continued this project and was able to determine that coexpression of the chaperone with our pro-apoptotic proteins allowed for translocation and induction of cell death (results not shown). This demonstrates that chaperones appear to play a vital role in translocation of complex proteins, since the translocation of the β-lactamase cargo is not dependent on coexpression of the chaperone.

4.3 Role of the chaperones prior and during secretion

Although some T3SS chaperones are not required for protein export, they have been found to increase efficiency. To determine if the chaperones are involved in accumulation of effectors at the cytosolic interface of the injectisome and/or directly interact with the injectisome, we explored the effect of overexpression of chaperones on secretion, the role of the export signals on the export of non-native cargo, and the role of chaperones prior and during secretion. Our results demonstrate that effector chaperones play a vital role of export, specifically by preparing and improving export of effectors prior and during secretion, respectively. This emphasizes that the chaperones appear to be essential in promoting export of stable cargo. Additionally, we showed that *Y. enterocolitica* has a small pre-synthesized pool of effectors which allows for quick activation of effector export.

By overexpressing the chaperones, we aimed to discriminate between different scenarios: if the chaperones are involved in a secretion hierarchy, we expected to see specific export of the cognate effector while preventing the export of other effectors; if the chaperones directly interact with the injectisome, we would observe the loss or significant decrease of secretion by either the cognate effector or all effectors; if chaperones ensure secretion efficiency, we would see that overexpression would promote export of the cognate effector but not affect the export of other effectors; and if chaperones are not directly involved in secretion hierarchy or direct injectisome interaction, we would expect to see no effects on secretion. Our results observed that overexpression of the chaperones does not have an effect on effector export under secreting conditions, which would imply that the chaperones don't facilitate a secretion hierarchy or direct interaction. This suggests that the chaperone's role is linked to preparing effectors for export, but not directly interacting with the injectisome since "empty" chaperones do no compete with chaperone effector complexes.

Previous studies have shown that increased expression of SycH and SycO does have effects on effector export, specifically by interacting with YscM1 and YscM2 (Wulff-Strobel *et al*, 2002; Cambronne *et al*, 2004; Dittmann *et al*, 2007). The effects of SycH and SycO demonstrate that these chaperones are involved in several aspects of regulation outside the export of effectors, especially in relation to *yop* expression (Pettersson *et al*, 1996; Bahrani *et al*, 1997) and metabolism regulation (Schmid *et al*, 2009). When we overexpressed SycT, SycE, SycH, SycD or SycO we did not see any changes in the secretion pattern compared to the control (Figure 18.A). Overexpression of SycO has been found to reduce effector export at high levels of induction (Dittmann *et al*, 2007), however, we did not visualize a reduction in secretion. This could be the result if we did not induce to a high enough degree. Interestingly, in non-secreting conditions we did visualize effector export when SycH, SycO and SycE were overexpressed (Figure 18.C). This phenotype has been previously observed upon overexpression

of SycH in non-secreting conditions (Cambronne *et al*, 2000; Wulff-Strobel *et al*, 2002), but increased export in SycO and SycE expressing cultures in non-secreting conditions has not been documented to the best of our knowledge. Since SycO and SycE have been shown to interact with YscM1 and YscM2, these chaperones may demonstrate behavior similar to SycH – although not to the same degree (Swietnicki *et al*, 2004; Dittmann *et al*, 2007).

Seeing that overexpression of chaperones did not have significant effects on secretion, we then explored the effects of chaperone deletion on secretion. Deletion of SycH and SycE resulted in either complete inhibition or significant impairment of secretion, respectively, and complementation of the chaperone did not restore secretion for either mutant (Supplementary Figure 10.A). Since some of the deletion strains exhibit the loss of the pYV or a large deletion of essential components, further study could not be continued (Supplementary Figure 10.B and C). Although we could not directly study the effects, effector chaperone deletion of SycH and SycE have been shown to effect secretion. Deletion of SycH has been shown to significantly reduce effector export where SycH interacts with YscM1 and YscM2, allowing them to be exported with YopH (Wulff-Strobel *et al*, 2002). However, when deleted, YscM1, and YopH cannot be exported (Cambronne *et al*, 2000), which represses *yop* expression and thus results in reduction of export. SycE is known to stabilize YopE and without the chaperone could result in reduction of YopE export (Frithz-Lindsten *et al*, 1995; Swietnicki *et al*, 2004). Although a direct link between SycE and YscM1 and YscM2 has not been found, it would be interesting to see if SycE is involved in Yop regulation – whether through interaction with YscM1 and YscM2 or other regulatory proteins.

To gain insight into the effector export signals, we fused two reporters to either a secretion ($YopE_{1-15}$), translocation ($YopE_{1-53}$), or translocation signal with chaperone binding domain ($YopE_{1-138}$) and studied their secretion. Both EGFP and NanoLuc are capable of being exported by the T3SS, however, there are differences in the secretion patterns when these cargos are exported. In both cases, increase in the length of the export signal resulted in decreased export of the translocators when the cargo was overexpressed (Figure 20 and Figure 22.C). At native cargo levels, EGFP does not inhibit translocator export like NanoLuc (Figure 21.C and Figure 22.B-C). Also, the addition of the cognate chaperone SycE resulted in different secretion patterns, where folded NanoLuc cargo secretion was abolished (Figure 22.A-B) whereas in EGFP translocator export is enhanced (Figure 21.C). The reason for the different secretion patterns between these two proteins is unclear, especially considering that EGFP is the more stably folded protein compared to NanoLuc. For more stably folded cargo, could coexpression of the chaperone promote more controlled export of the cargo, thus allowing enhanced export for other substrates? In the case of less stably folded proteins, is the cognate chaperone needed less allowing

more efficient export of cargo with the shorter translocation signal? Is the coexpression of the chaperone more essential for protein export and functionality in native conditions than laboratory conditions, thus preventing efficient export *in vitro*? Although we were unable to gain further insight into the role of export signals, especially concerning different folding stabilities of cargo, we can gather that the coexpression of the chaperone does play a role, especially comparing the effects between secretion and translocation, as demonstrated in Chapter 3.2. The addition of the chaperone may play a more vital role in translocation than secretion, potentially working with other regulatory mechanisms that may occur upon host contact, which cannot be simulated *in vitro*.

The export signals may be essential in substrate specificity for some T3SS-utilizing bacteria. In *Y. enterocolitica*, non-native cargo has been successfully secreted and translocated without the CBD (Sory *et al*, 1995; Cheng *et al*, 1997), however this is not the case for *Salmonella* where the CBD is essential for translocation and ensures specificity between injectisome and flagellar substrates (Lee & Galán, 2004). A potential reason why the CBD may not be essential is because *Yersinia* do not have flagella during infection. It is known that the injectisome and flagella are counter-regulated in *Yersinia* (Darland et al, 1974; Bottone & Mollaret, 1977; Minnich Scott A. and Rohde, 2007) and without having to ensure specificity between the injectisome and flagellar T3SS, this extra level of regulation may not be required.

It is has been shown that not all effectors require their cognate chaperone for export and that chaperone-independent pathways exist (Letzelter *et al*, 2006; Ernst *et al*, 2018). Instead, the chaperones may play more of a role in preventing mislocalization within the bacteria than directly interacting with the injectisome. In the case of SycO, the chaperone binds to the membrane localization domain (MLD) of YopO and may prevent the effector from localizing at the bacterial membrane rather than being exported (Letzelter *et al*, 2006). YopE has also been found to have an MLD within the CBD (Krall *et al*, 2004) and without SycE, YopE is prone to aggregation by decreasing the protein's solubility (Birtalan *et al*, 2002; Letzelter *et al*, 2006). Thus for MLD-utilizing effectors, the use of the cognate chaperone may be used to ensure solubility rather than be directly linked to secretion. However, even if the chaperones' role is to prevent aggregation of effectors, they are still involved in improving secretion efficiency by ensuring that produced effectors are exported.

In order for *Yersinia* to prepare for an interaction with an immune cell, it would be conceivable for them to utilize a pre-synthesized effector pool. This would allow the bacteria to quickly respond to attack and avoid any lag time that would be required to synthesize new effectors, as well as avoid phagocytosis. We found *Y. enterocolitica* utilizes a small pool of effectors that are exported within 15 minutes following activation (Figure 23). The activated bacteria treated with chloramphenicol had a

distinctly lower level of secretion than the untreated activated bacteria, demonstrating that this pool is very small. If the bacteria are employing a pre-synthesized pool of effectors, during this time they are utilizing a post-translational export where the small pool is awaiting export and being protected by their chaperones to prevent premature degradation or mislocalization. Following depletion of the pool, it would be potentially beneficial for the bacteria to utilize co-translational export to translocate effectors as quickly as possible to combat an attack from an immune cell. Ultimately, our results suggest that *Y. enterocolitica* utilizes a small pool of pre-synthesized effectors that allows rapid activation of translocation to counter immune cell attack and promote survival during infection.

4.4 Role and location the gatekeepers

Gatekeepers play an essential role in controlling activation and deactivation of the T3SS (Day & Plano, 1998; Day *et al*, 2003; Iriarte *et al*, 1998). The overall function of the gatekeepers is well known, but how and where the gatekeeper complex interacts with the injectisome components and selects specific cargo to be exported still remains unclear. In the case of *E. coli*, the gatekeeper complex has been found to directly bind to the cytosolic interface of the injectisome and even interact with different chaperone-substrate complexes, allowing specific export of either the translocators or effectors (Deng *et al*, 2005; Younis *et al*, 2010; Deng *et al*, 2015; Shaulov *et al*, 2017; Portaliou *et al*, 2017; Gaytán *et al*, 2018).

We found that the *Y. enterocolitica* gatekeepers exhibit cytosolic localization in both non-secreting and secreting conditions (Figure 25.A). Since foci were not visible at the membrane, this suggests that the gatekeepers do not physically block effector export, but rather utilize an affinity-based hierarchy (Cheng *et al*, 2001). Cheng and colleagues proposed a delocalized model where SctW is bound to TyeA in high calcium conditions, preventing SctW and subsequent effectors from being exported. However, when the calcium level drops, newly synthesized SctW is unable to bind to TyeA and is then guided by the chaperones to the injectisome where SctW can be exported (Cheng *et al*, 2001). In this model, SctW would have to be consistently expressed and TyeA would require post-translation modification (Cheng *et al*, 2001). Additionally, this model would require that SctW is the first protein to be exported, also suggesting a secretion hierarchy.

Our results appear to follow this model, where the gatekeeper complex (SycN/YscB/SctW/TyeA) is localized in the cytosol. Under non-secreting conditions, the chaperones (SycN and TyeA) and TyeA (the calcium regulator) are bound to SctW, preventing export (Iriarte et al, 1998; Cheng et al, 2001; Day et al, 2003), and are localized in the cytosol. When TyeA reacts to the low calcium levels, the protein undergoes a conformational change (Ferracci et al, 2004) and disengages from SctW, thus allowing the chaperones to guide SctW to the injectisome for export. After SctW is exported SycN, YscB, and TyeA remain localized in the cytosol. The gatekeepers would then remain prepared to reestablish the gatekeeper complex to inhibit secretion. We showed that the gatekeepers can reassemble and secretion is reversible, since the bacteria are able to deactivate secretion when introduced into non-secreting conditions (Chapter 3.1).

It has been established that SycN, YscB and TyeA are all essential for the complex functionality and without any of these components, secretion is uncontrollable regardless of secreting conditions (Day & Plano, 1998). Thus it is conceivable that SycN and YscB interact with SctW prior to and during

secretion. Prior to secretion, the chaperones keep SctW partially unfolded and during secretion they potentially guide and prime the protein for export by keeping the N-terminus partially unfolded. Without either chaperone, Day and Plano found that SctW was not exported as efficiently (Day & Plano, 1998), suggesting that these chaperones may improve export of SctW. If high calcium concentrations can be sensed, then TyeA can quickly bind to SctW and reestablish the gatekeeper complex. Also it has been suggested that TyeA is located intracellularly and not associated with the membrane (Cheng & Schneewind, 2000), which further emphasizes that *Y. enterocolitica* may utilize a delocalized and affinity-based model for the gatekeepers.

How the gatekeepers directly interact with the injectisome, its export substrates, or other T3SS components remains unknown. It would be interesting to determine potential interaction partners between the gatekeeper and other components to visualize an interaction network that allows efficient regulation of effector export. Specifically, establishing if the gatekeepers interact with chaperone-effector complexes or components of the injectisome would allow insight into how this mechanism works in *Yersinia*. By gaining more understanding of how these proteins interact we can elucidate the molecular mechanisms that govern secretion.

5. Conclusion and Outlook

The aim of my PhD thesis was to gain a better understanding of the molecular regulation and mechanisms governing effector secretion and pathogenesis of *Y. enterocolitica*. I explored the activation, deactivation, and reactivation of secretion, as well as the link between growth retardation and secretion. Additionally, I looked to elucidate the effects of the export signals and effector chaperones on secretion of different cargo, as well as determine the presence of a pre-synthesized pool of effectors.

My results show that *Y. enterocolitica* can rapidly sense environmental cues and adapt to changing environments, allowing the bacteria to quickly activate, deactivate, and reactivate secretion with the same injectisomes. Additionally, *Yersinia* is able to reestablish growth and division following secretion, demonstrating that the T3SS can be potentially used multiple times to improve survival and dissemination during infection. I was able to establish infection assays within the lab that allowed us to apply the LITESEC-T3SS system *in vivo*, as well as demonstrate that chaperones play a vital role in the translocation of functional proteins into host cells. I also demonstrated that although chaperones may not directly interact with the injectisome, they do promote efficient secretion and translocation. Furthermore, it appears that *Y. enterocolitica* stores a small pool of effectors that allows rapid effector export once translocation is activated. Lastly, unlike *E. coli*, *Yersinia* appears to utilize a different mechanism to control effector export where the gatekeepers are located in the cytosol rather than directly interacting with the injectisome to inhibit secretion. Insight into the secretion kinetics, bacterial growth and division behavior, and the signals that promote effector specificity and efficient export allow insight into the pathogenesis of *Y. enterocolitica*. All these aspects of the T3SS ensure that effectors are exported precisely and efficiently during infection and by understanding these mechanisms we can gain further understanding into how to combat T3SS-utilizing pathogens.

Regardless of the progress made during my PhD in understanding the regulation governing secretion, the link between growth retardation and the role of the chaperones still remains unclear. The results show that secreting bacteria are not energetically exhausted when compared to non-secreting bacteria, suggesting that metabolic burden is not the link between growth retardation and secretion. However, exploring the energy charge of different strains of *Y. enterocolitica* in secreting and non-secreting conditions could elucidate if the metabolic burden changes over time and if the expression of the effectors increases the metabolic burden. On the other hand, inhibition of growth could be governed by an entirely different mechanism such as the loss of amino acids during secretion or a completely new mechanism. Additionally, the role and interaction of the chaperones prior to and during secretion remains unclear. Even though many studies have demonstrated the vital role

chaperones hold, determining their functions during secretion and translocation remains vague. Further studies into the metabolic burden and the function of the chaperones would give further insight into secretion regulation and ultimately how *Y. enterocolitica* coordinates precise and efficient secretion and translocation.

6. Material and methods

6.1 Bacterial strains

Bacterial strains and constructs used in this study are listed in Chapter 7.3.

6.2 Genetic constructions

E. coli Top10 was used for plasmid purification and *E. coli* SM10 λpir was used for allelic exchange. *E. coli* was routinely grown on Luria-Bertani (LB) agar plates and LB medium at 37°C. Ampicillin was used at a concentration of 200 µg/ml, to select for expression plasmids. Chloramphenicol and streptomycin were used to select for expression and suicide vectors at concentrations of 10 µg/ml and 50 µg/ml, respectively. Plasmids were created using Phu polymerase (New England Biolabs) or Taq polymerase (New England Biolabs). Constructs were confirmed by sequencing (Eurofin Genetics or Microsynth Seqlab) and homology was compared via BLAST. Oligonucleotides were utilized for genetic construction as listed in Chapter 7.5.

Mutators for exchange of genes on the pYV virulence plasmid were created as previously described by Diepold and colleagues (2011). Mutators for modification or deletion of genes on the pYV plasmid were constructed by overlapping PCR using purified ADMA4098 (pYV with a SctC deletion), including 200-250 base pair (bp) flanking regions on both sides of the modification or deletion of the gene of interest. For mutators containing GFP, pre-mutator vectors were produced as described above. As a result, GFP was inserted in frame into pre-digested pre-mutator vectors. Mutator vectors were transformed in chemically competent or electro-competent *E. coli* SM10 λpir cells. *Y. enterocolitica* mutants were generated by allelic exchange, resulting in the exchange of wild-type gene sequences with the mutated gene (Kaniga *et al*, 1991).

Vectors utilized for protein expression in *Y. enterocolitica* were constructed using standard cloning protocols. Genes of interest were amplified by PCR. PCR fragments and vector were digested with specific restriction enzymes. The digested insert and vector were ligated (New England Biolabs) and transformed into chemically competent or electro-competent *E. coli* Top10 cells. Resulting clones were identified first with colony PCR, followed by sequencing and subsequently electroporated into electro-competent *Y. enterocolitica*.

6.3 Bacteria medium conditions

E. coli cultures were grown in LB medium containing respective antibiotics at 37°C.

Y. enterocolitica cultures were grown in brain heart infusion (BHI) medium containing nalidixic acid (NAL, 35 µg/ml), and diaminopimelic acid (DAP, 60 µg/ml) for ΔHOPEMTasd strains. Day cultures were grown in BHI supplemented with NAL, DAP where required, $MgCl_2$ (20 mM), and glycerol (0.4% (w/v)). For non-secreting conditions, 5 mM $CaCl_2$ was added to the medium, whereas for secreting conditions, Ca^{2+} was chelated by addition of 5 mM EGTA.

6.4 Competent cell preparation

Chemically competent *E. coli* were grown over night at 37°C in LB medium containing streptomycin (50 µg/ml) or kanamycin (50 µg/ml) for Top10 and SM10 λpir cultures, respectively. 50 ml of media containing LB and respective antibiotics were prepared and inoculated with 500 µl of overnight culture. Culture was then incubated at 37°C until the OD_{600} reached 0.4 to 0.65. Culture was then placed on ice until the centrifuge was cooled to 4°C. Culture was aliquoted into falcon tubes and centrifuged at 4,700 x g for 10 minutes at 4°C. Supernatant was remove and cell pellets were resuspended in 3 ml TSS (transformation and storage solution) buffer and aliquoted in sterile Eppendorf tubes. Aliquots were then snap-freezed in liquid nitrogen and stored in the -80°C freezer.

Electro-competent *E. coli* and *Y. enterocolitica* were grown overnight at 37°C or 28°C, respectively. 100 ml of media prepared with corresponding growth medium, antibiotics and additives (*E. coli* – LB and respective antibiotics; *Y. enterocolitica* – BHI media with NAL and DAP) and inoculated to an OD_{600} of 0.1. Cultures were incubated at 37°C or 28°C for *E. coli* and *Y. enterocolitica*, respectively, until the OD_{600} reaches 0.45 to 0.6. Culture is then placed on ice for 30 minutes. Cultures are aliquoted into falcon tubes and centrifuged at 2,000 x g for 15 minutes at 4°C. Supernatant is discarded and pellet is resuspended in 20 ml sterile ice-cold water. Bacteria are centrifuged again at 2,000 x g for 15 minutes at 4°C. Supernatant is removed and pellet is resuspended in 10 ml ice-cold 10% glycerol (w/v). Bacteria are centrifuged again at the same settings and supernatant is remove. Pellet is then resuspended in 400-600 µl/tube of ice-cold 10% glycerol (400 µl/tube for *Y. enterocolitica*). Bacteria are then aliquoted into Eppendorf tubes and snap-freezed in liquid nitrogen and stored in the -80°C freezer.

6.5 General secretion and microscopy culture preparation of *Y. enterocolitica*

Y. enterocolitica overnight cultures were used to inoculate day culture media and were incubated at 28°C for 1.5 hours. Cultures were either grown in secreting or non-secreting cultures, depending on the experiment. Secreting cultures were inoculated at an OD_{600} of 0.15 and non-secreting cultures were inoculated at an OD_{600} of 0.12. After incubation, cultures were shifted to 37°C. If bacteria contained an inducible plasmid, arabinose was added at varying concentrations (depending on the level of induction required) to induce plasmid expression. Induction generally occurs prior to shifting to 37°C. Cultures incubate at 37°C for 2-3 hours prior to collection, unless indicated otherwise. Samples were collected at established times depending on the needs of the experiment.

When indicated, non-secreting cultures (containing 5 mM $CaCl_2$) could be activated with the addition of 10 mM EGTA to chelate the calcium and induce secretion.

6.6 Secretion analysis

2 ml of culture were centrifuged (20,000 *g*, 2 min) and 1.8 ml of the SN was collected. SN proteins were precipitated using trichloroacetic acid 10% (w/v) final for 24-48 h at 4°C. Samples were resuspended in 1x SDS-loading buffer (v/v) and boiled at 99°C for 10 minutes. Proteins were separated on either commercial or homemade SDS-PAGE gels (4-20% for commercially prepared gels; 11% or 15% gels for gels produced in house). Samples were normalized to contain the proteins secreted by 0.4 OD units of bacteria (the equivalent of 0.4 ml culture at an OD_{600} of 1), unless indicated otherwise. Secreted proteins were stained with “Instant Blue”, Coomassie-based staining solution (Expedeon).

6.7 Total cell analysis

2 ml of culture were centrifuged (20,000 *g*, 2 min) and supernatant was removed. Samples were resuspended in 1x SDS-loading buffer (v/v) and boiled at 99°C for 10 minutes. Proteins were separated on either commercial or homemade SDS-PAGE gels (4-20% for commercially prepared gels; 11% or 15% gels for gels produced in house). Samples were normalized to contain the proteins secreted by 0.24 OD units of bacteria (the equivalent of 0.24 ml culture at an OD_{600} of 1), unless indicated otherwise. Total cell proteins were prepared for western blot analysis.

6.8 Immunoblot analysis

For detection of specific proteins by immunoblotting, unstained gels were transferred onto nitrocellulose membranes by Turbo Blot (Bio-Rad) and incubated in 5% milk (w/v) (AppliChem) with PBS (or for anti-flag samples, PBS-T), the primary antibody was incubated for either 1 hour at RT or overnight at 4°C. Blots were washed with PBS and PBS-T (PBS-T only for anti-flag samples) prior to incubation of the secondary antibody for either 1 hour at RT or overnight at 4°C. After incubation, blots were washed with PBS and PBS-T (PBS-T only for anti-flag samples) prior to the addition of the chemiluminescent substrate (Pierce) for imaging with a CCD camera (Fuji).

Immunoblotting was carried out using rabbit or mouse polyclonal antibodies in 5% milk and PBS (or 2% milk and PBS-T for anti-flag antibodies). Secondary antibodies were used against rabbit or mouse Ig and conjugated with horseradish peroxidase at 1:10,000 dilution in 5% milk and PBS (or 2% milk and PBS-T).

6.9 β-lactamase assay

ΔHOPEMTasd-based *Y. enterocolitica* cultures for β-lactamase (bla) assays were inoculated from overnight cultures to an optical density at 600 nm (OD_{600}) of 0.10 (0.12 in validation experiment) in non-secreting BHI medium. After shaking incubation at 28°C for 1.5 hours, the culture was shifted to 37°C to induce the *yop* regulon. After 2 hours (1.5 hours in the initial validation experiment) of incubation at 37°C, bacteria were collected (unless stated differently, bacteria were collected by centrifugation (2,400 *g*, 4 min, 37°C), and resuspended in an equal amount of fresh medium pre-warmed to 37°C throughout the protocol), and resuspended in secreting BHI medium. Over the next 15 minutes, the activation kinetics analysis was performed (see below). To determine the deactivation kinetics, cultures were incubated for 2 hours at 37°C in secreting medium and were then collected and resuspended in non-secreting medium. Over the next 30 minutes, the deactivation kinetics analysis was performed (see below). To determine the reactivation kinetics, cultures were incubated in the secreting medium for 2 hours at 37°C and were then collected and resuspended in non-secreting medium pre-warmed to 28°C. Cultures were incubated at 28°C for 15 minutes, collected and resuspended in secreting medium at 37°C, where the reactivation kinetics analysis was performed.

Samples for the kinetics analysis of activation, deactivation and reactivation of secretion were treated as follows: after resuspension, 400-800 µl samples were removed from the culture at the indicated time points (0, 5, 10 minutes for activation; 0, 10, 20 minutes for deactivation; 0 minutes for reactivation), collected, resuspended in fresh medium as indicated and incubated in a table top shaking incubator at 37°C, 800 rpm for 5 minutes (activation and reactivation) or 10 minutes

(deactivation). After this incubation, bacteria were removed by centrifugation (16,000 *g*, 2 min, 20°C), and the supernatant was stored at room temperature until all samples of one experiment were collected. For each sample, 100 µl supernatant were added to a Sarstedt TC-Platte 96 well plate in triplicates. 10 µl/well of β-lactamase substrate solution (10 µM Nitrocefin (Merck) in phosphate buffered saline) were added. β-lactamase activity was quantified by the increase in absorbance at 483 nm, caused by β-lactamase catalyzed hydrolysis of Nitrocefin, for 40 rounds of 30 seconds each at 30°C using a Tecan Infinite 200 Pro photometer. The results are averages of β-lactamase activity, determined by linear regression within the linear range of the absorbance, of three independent experiments that were run in technical triplicates for each experiment.

The initial validation assay was performed as described above with the following modifications: 200 µl supernatant was added to a Sarstedt TC-Platte 96 well plate in triplicates, and 20 µl/well of β-lactamase substrate solution (20 µM Fluorocillin Green 495/525 (Life Technologies in 0.1 M Tris-HCl pH 7.5) was added. β-lactamase activity was quantified by the increase in fluorescence caused by β-lactamase catalyzed hydrolysis of the substrate, measured at 495 +/- 5 nm excitation and 525 +/- 10 nm emission for 30 rounds every 30 seconds using a Tecan Infinite 200 Pro photometer. The result is the increase of fluorescence over time of one experiment that was run in a technical triplicate.

6.10 Growth curve experiment

MRS40-based *Y. enterocolitica* cultures for growth curve experiments were inoculated from overnight cultures to an OD_{600} of 0.12 in non-secreting BHI medium. After incubating at 28°C for 1.5 h, the culture was divided in three parts and collected (2400 *g*, 4 min, 37°C). The pellet was then resuspended in either non-secreting medium (one part) or secreting medium (two parts), both pre-warmed at 37°C, to induce the *yop* regulon. The cultures were incubated to 37°C for 2 h incubation, and collected again (2400 *g*, 4 min, 37°C). One previously secreting culture was resuspended in secreting medium and the second was resuspended in non-secreting medium; the previously non-secreting culture was resuspended in fresh non-secreting medium, all pre-warmed at 37°C. Cultures were incubated at 37°C for 3.5 hours. Throughout the experiment, the optical density at 600 nm wavelength (OD_{600}) of all cultures was measured every 30 min in a 1:3 dilution. The number of divisions per time for each culture was determined using the OD_{600} values for -1.5 hours and 0 hours (28°C), 0 hours and 2 hours (first incubation), and 2 hours and 4 hours (second incubation).

6.11 Fluorescence microscopy – visualization of growth under secreting and non-secreting conditions

ΔHOPEMTasd-based *Y. enterocolitica* AD4483 (EGFP-SctL ΔSctD) and ADTM4521 (mCherry-SctL) cultures for microscopy were inoculated from overnight cultures to an OD_{600} of 0.15 in secreting medium. Cultures were incubated at 28°C for 1.5 hours and then shifted to 37°C for 2 hours. Next, 750 µl of each culture were centrifuged (2,400 *g*, 3 min), and resuspended in 100 µl of either secreting or non-secreting medium for both strains. 2 µl of resuspended culture were spotted on preheated (37°C) agarose pads containing 1.5% (w/v) low melting agarose, LB, NAL (35 µg/ml), glycerol (0.4% (w/v)), $MgCl_2$ (20mM) and either oxalate (20 mM) for secreting conditions, or $CaCl_2$ (5 mM) for non-secreting conditions. Bright field images were taken every 5 minutes and fluorescence images were taken every 20 minutes for 2 hours at 37°C with a Deltavision Spectris optical sectioning microscope (Applied Precision) using a 100x oil immersion objective (Olympus) with a numerical aperture of 1.40. The exposure time was set to 0.2 seconds, with a light intensity of 32% for bright field, 587 nm and 485 nm excitation lights. Following image acquisition, images were deconvolved using softWoRx 5.5 (standard "conservative" settings). Images were further processed with ImageJ-Fiji (National Institute of Health) using a binary mask for measuring cell growth. Red and green fluorescence was manually adjusted to discriminate T3SS-positive and T3SS-negative bacteria, respectively.

6.12 Fluorescence microscopy – quantification of assembled T3SS under secreting and non-secreting conditions

ΔHOPEMTasd-based *Y. enterocolitica* AD4085 (EGFP-SctQ) and AD4306 (EGFP-SctD) cultures for microscopy were inoculated from an overnight culture to an OD_{600} of 0.12. Cultures were incubated at 28°C for 1.5 hours. After incubation, cultures were shifted to 37°C for 3 hours. Next, 400 µl of culture was centrifuged (2,400 *g*, 2 min) and concentrated in 200 µl microscopy imaging buffer (100 mM HEPES pH 7.2, 100 mM NaCl, 5 mM ammonium sulfate, 20 mM sodium glutamate, 10 mM $MgCl_2$, 5 mM K_2SO_4, 0.5% (w/v) casamino acids) containing DAP (60 µg/ml) and $CaCl_2$ (5mM) or EGTA (5 mM) according to the imaging conditions (non-secreting or secreting). To test for possible loss of T3SS during extended secretion, cultures were incubated under secreting or non-secreting conditions at 28°C for 1.5 hours, and then shifted to 37°C for 3 hours. For visualization, 2 µl of resuspended culture where mounted on a 1.5% (w/v) agar pad casted with the same buffer in a depression slide and visualized in a Deltavision Spectris Optical Sectioning Microscope (Applied Precision), equipped with a UApo N 100x/1.49 oil TIRF UIS2 objective (Olympus), using an Evolve EMCCD Camera (Photometrics). The sample was illuminated for 0.15 seconds with a 488 laser in a TIRF depth of 3440.0, except for the

extended secretion assay, where the exposure time was 0.3 seconds under non-TIRF conditions. The micrographs where then deconvolved using softWoRx 5.5 (standard “conservative” settings) and further processed for presentation with ImageJ-Fiji. Cells were manually counted in several fields of view.

6.13 Needle Staining

MRS40-based Y. enterocolitica CH4006 ($SctF_{S5C}$) and a MRS40 wild-type control were inoculated from overnight cultures to an OD_{600} of 0.15 in secreting medium. Cultures were incubated at 28°C for 1.5 hours and then shifted to 37°C for 2 hours. At this point, 500 µl were transferred to a 2 ml tube and washed with minimal medium adjusted for secreting conditions. The cells were concentrated in 100 µl microscopy imaging buffer containing EGTA (5 mM) and CF-633 maleimide dye (Sigma-Aldrich, USA) (5µM) for 5 minutes. The cells were then collected and washed with microscopy imaging buffer containing EGTA (5 mM) once or four times, as indicated. Images were acquired as z-stacks of 11 images with a stacking of 0.15 µm. The micrographs where then deconvolved using softWoRx 5.5 (standard “conservative” settings) and further processed for presentation with ImageJ-Fiji.

6.14 Measuring AXP levels in secreting and non-secreting samples

Intracellular metabolites were extracted from the total cellular biomass of wildtype1HOPEMTasd cultures, used in this experiment for biosafety reasons, based on a sequential quenching–extraction approach. 3 ml culture aliquots were pipetted into 9 ml of 60% (v/v) cold methanol (−60°C). Cells were immediately pelleted by centrifugation (10 min, −10°C, 20,000 x g), and the supernatant was removed. Pellets were stored at −80°C until extracted. Intracellular metabolites were extracted by adding a volume equivalent to 300µl per 3 ml of a sample at an OD_{600} of 1 of both extraction fluid {50% (v/v) methanol, 50% (v/v) TE buffer [10 mM TRIZMA (pH 7.0), 1 mM EDTA]; −20°C} and chloroform (−20°C) to each cell pellet. The resulting mixture was incubated at 4°C for 2 hours on a shaking device (Eppendorf shaker) and centrifuged (10 min, −10°C, 20,000 x g). The upper phase of the two-phase system was filtered (0.22µm, PTFE, 4 mm diameter, Phenomenex) and stored at −80°C until the polar metabolites were analyzed. Quantification of nucleotides was performed using a LC-MS/MS. The chromatographic separation was performed on an Agilent Infinity II 1290 HPLC system using a SeQuantZIC-HILIC column (150 × 2.1 mm; 3.5µm, 100 Å, Merck, Germany) equipped with a 20 × 2.1 mm guard column of similar specificity (Merck, Germany) at a constant flow rate of 0.4ml/min with mobile phase A being 20 mM ammonium acetate (Sigma-Aldrich, USA) adjusted to pH 9.2 with ammonium hydroxide (Honeywell, USA) and phase B being acetonitrile (Honeywell, USA). The injection volume was 3µl. The mobile phase profile consisted of the following steps and linear

gradients: 0–1 minutes from 20% B to 25% B; 1–4 minutes from 25 to 35% B; 4–5 minutes from 35 to 80% B; 5–6 minutes constant at 80% B; 6–7 minutes from 80 to 20% B; 7–8 minutes constant at 20% B. An Agilent 6495 ion funnel mass spectrometer was used in negative mode with an electrospray ionization source and the following conditions: ESI spray voltage 3,500 V, sheath gas 350°C at 11 l/min, nebulizer pressure 20 psig and drying gas 225°C at 14 l/min. Compounds were identified based on their exact mass and retention time compared to standards. Extracted ion chromatograms of the [M-H] - forms were integrated using MassHunter software (Agilent, Santa Clara, CA, USA). Absolute concentrations were calculated based on an external calibration curve.

6.15 Luciferase assay

ΔHOPEMTasd *Y. enterocolitica* overnight cultures were utilized to inoculate 5 ml of secreting or non-secreting medium and incubated for 1.5 hours at 27°C. Expression of NanoLuc-flag cargo was then induced with pBAD expression with 0.3% arabinose (w/v). The cultures incubated for 3 hours at 37°C. Following incubation 300 µ of sample was taken and centrifuged (16,000 x g, 2 min). The supernatant was extracted and put in a fresh Eppendorf tube. The total cell pellet was resuspended in minimal media containing (5 mM $CaCl_2$ or 5 mM EGTA, as well as the addition of DAP in both secreting conditions). 5 µl of supernatant and total cell were harvested for enzymatic assay. The NanoLuc detection assay was performed according to the manufacturers recommendations.

6.16 Infection assay

HEp-2 cells were maintained in Roswell Park Memorial Institute (RPMI) 1640 medium (Gibco) supplemented with 7.5% newborn calf serum(Sigma-Aldrich) in 5% CO_2 at 37°C. For the β-lactamase translocation assay, the infection assay was adapted from (Wolters *et al*, 2015). HEp-2 cells were seeded into Nuncion Delta Surface 96-well flat plates (Thermo Scientific) at a cell density of 2.0×10^4 cells per well. Prior to infection, 5 mM DAP was added to the medium of the seeded HEp-2 cells. Day cultures were inoculated from stationary overnight cultures (1:25 dilution) in BHI supplemented with DAP (60 µg ml−1), $MgCl_2$ (20 mM), and glycerol (0.4% w/v). Expression of the cargo protein from the pBAD plasmid was induced with 0.2% arabinose (w/v), unless stated differently. The cultures were incubated for 90 minutes at 37°C under activating conditions (dark for LITESEC-supp/light for LITESEC-act) to induce T3SS formation. After incubation, cultures were centrifuged for 4 minutes at 4500 × g and 4°C. The bacteria were resuspended in ice-cold PBS containing DAP to a density of approximately 2.5×10^8 cfu/ml, incubated on ice in “off” conditions (light for LITESEC-supp/dark for LITESEC-act) for 15 minutes, then added to a semi-confluent layer of HEp2-cells at a multiplicity of infection (MOI) of approximately 140, and incubated under blue light or dark conditions for 60 minutes at 37°C in 5%

CO_2. Following incubation, the cell culture medium was removed and 100 µl of working solution were added (1:3 dilution RPMI 1640 medium without phenol red (Gibco) in PBS (Gibco) with 25 mM probenecid acid (Alfa Aesar) dissolved in cell culture grade dimethyl sulfoxide (DMSO) (Santa Cruz)). For β-lactamase translocation assays, 20 µl of CCF2-AM were added (0.12 µl solution A,1.2 µl solution B and 18.68 µl solution C (solutions A, B and C provided from Invitrogen CCF2-AM loading kit)). After 5 minutes of incubation, the working solution and CCF2-AM were removed and 100 µl of fresh working solution was added. Plates were then incubated at 37°C in 5% CO_2 for 10 minutes. Next, cells were fixed by addition of 100 µl of ice-cold 1% paraformaldehyde (PFA) (w/v) and incubation on ice for 10 minutes. As a last step, the PFA solution was replaced by PBS. Fields of view were chosen in the differential interference contrast (DIC) channel, preventing any bias, and all fields of view were analyzed. Translocation of $YopE_{1-53}$-β-lactamase was detected by comparing the fluorescence emission at 525/48 nm (FRET-based emission of uncleaved CCF2) vs. 435/48 nm (emission of cleaved CCF2, equivalent to substrate translocation), both at an excitation at 390/18 nm. Both channels were background-corrected. For the apoptosis assay, the protocol outlined in (Ittig *et al*, 2015) was adapted as follows. HEp-2 cells were seeded to a density of 1.18×10^5 cells per well into Nuncion Delta Surface 24-well plate (Thermo Scientific). Prior to infection, DAP and 0.2% arabinose (w/v) were added to each well of HEp-2 cells. Bacteria were first grown at 28°C for 90 minutes and then shifted to 37°C for 120 minutes, collected by centrifugation, and resuspended in PBS (pre-warmed to 37°C) containing 5 mM DAP at a density of approximately 2.5×10^8 cfu/ml. The bacteria were added to a semi-confluent layer of HEp2-cells at an MOI of approximately 140, and incubated under blue light or dark conditions for 60 minutes at 37°C in 5% CO_2. Following incubation, the cell culture medium was removed and 300 µl of RPMI 1640 medium (Gibco) containing gentamycin (100 µg/ml) was added. Cells were incubated for further 60 minutes at 37°C in 5% CO_2 under the specified light conditions and were then imaged with a binocular microscope (x5 objective) or on an inverse fluorescence microscope (Deltavision Elite) (×20 objective). Fluorescence and cell shape of HEp-2 cells were manually classified by blinded observers.

6.17 Effector pool secretion

MRS40 wild-type *Y. enterocolitica* was grown overnight at 28°C. Non-secreting and secreting media was prepared and the overnight culture was used to inoculate the fresh media to an OD_{600} of 0.12 and 0.15. Cultures were incubated at 28°C for 1.5 hours. Cultures were then shifted to 37°C for 2.5 hours. Following incubation, secreting and non-secreting conditions were split into two equal cultures, where one culture from each condition was treated with chloramphenicol (15 µg/ml). Following 10 minutes of chloramphenicol incubation a baseline sample was taken from all conditions (-5 minutes). At 0

minutes, 10 mM EGTA was added to non-secreting conditions to activate secretion. Samples from all conditions were taken at 15-, 30-, 45-, and 60-minute time points and processed for SDS-PAGE analysis.

6.18 Fluorescence microscopy – Gatekeeper localization

ΔHOPEMTasd-based *Y. enterocolitica* AD4616 (SycN-sfGFP), AD4617 (TyeA-sfGFP), BMD4015 (EGFP-YscB), AD4085 (EGFP-YscQ) and wild-type strains were grown overnight. Secreting and non-secreting cultures were inoculated to an OD_{600} of 0.15 and 0.12, respectively. Cultures were incubated at 28°C for 1.5 hours. After incubation, cultures were then shifted to 37°C for 3 hours. 200 ul of samples were taken and centrifuged (4,800 x g for 2 minutes) and resuspended in 100 ul minimal media containing DAP containing 5 mM EGTA and 5 mM $CaCl_2$. 1.5 ul of culture is plated on 1.5% agarose patch in minimal medium corresponding culture conditions.

Bright field and fluorescence images were taken with a Deltavision Spectris optical sectioning microscope (Applied Precision) using a 100x oil immersion objective (Olympus) with a numerical aperture of 1.40. The exposure time was set to 0.2 seconds, with a light intensity of 32% for bright field, 485 nm excitation lights. Following image acquisition, images were deconvolved using softWoRx 5.5 (standard "conservative" settings). Images were further processed with ImageJ-Fiji (National Institute of Health) using a binary mask for measuring cell growth. Cells were manually counted in several fields of view.

6.19 Proteomics sample preparation

Total cell samples were collected from secretion assay, as described in Chapter 6.5. The total cell pellet was washed twice with ice-cold PBS. 300 µl of 2% SLS (sodium lauryl sarcosinate) solution (in 100 mM ammonium bicarbonate [ABC]) (v/v) was used to re-suspend the pellet and the mixture was boiled at 99°C for 10 minutes followed by sonication (Vial Tweeter). Cell lysates were then reduced by the addition of 5 mM Tris (2-caboxyethyl)phosphine and incubated at 95°C for 15 min, followed by alkylation (10 mM iodoacetamide for 30 min at 25°C). The cell lysates were cleared by centrifugation, and the total protein was estimated for each sample with a Pierce bicinchoninic acid (BCA) protein assay kit (Thermo Fisher Scientific). The cell lysate containing 50 µg total protein was then diluted with 100mM ammonium bicarbonate to a final detergent concentration of 0.5% and digested with 1 µg trypsin (Promega) overnight at 30°C. Next, SLS was removed by precipitation with 1.5% trifluoroacetic acid (TFA) and centrifugation. Peptides were purified using C_{18} microspin columns according to the manufacturer's instructions (Harvard Apparatus, USA).

Purified peptides were dried, resuspended in 0.1% TFA, and analyzed by liquid chromatography-mass spectrometry (MS) carried out on a Q-Exactive Plus instrument connected to an Ultimate 3000 rapid-separation liquid chromatography (RSLC) nano instrument and a nanospray flex ion source (all Thermo Scientific, Germany). Peptide separation was performed on a reverse-phase high-performance liquid chromatography (HPLC) column (75 µm by 42 cm) packed in-house with C_{18} resin (2.4 µm; Dr. Maisch GmbH, Germany). The peptides were first loaded onto a C_{18} precolumn (preconcentration set-up) and then eluted in backflush mode with a gradient from 98% solvent A (0.15% formic acid) and 2% solvent B (99.85% acetonitrile, 0.15% formic acid) to 25% solvent B over 66 min, continued from 25 to 40% of solvent B up to 90 min. The flow rate was set to 300 nL/min. The data acquisition mode for the initial label-free quantification study was set to obtain one high-resolution MS scan at a resolution of 70,000 (*m/z* 200) with scanning range from 375 to 1500 *m/z* followed by MS/MS scans of the 10 most intense ions at a resolution of 17,500. To increase the efficiency of MS/MS shots, the charged state screening modus was adjusted to exclude unassigned and singly charged ions. The dynamic exclusion duration was set to 10 s. The ion accumulation time was set to 50 ms (both MS and MS/MS). The automatic gain control (AGC) was set to 3×10^6 for MS survey scans and 1×10^5 for MS/MS scans.

Spectral counting-based analysis was performed using MASCOT (v2.5), executed from the Proteome Discoverer platform (v1.4, Thermo Scientific). The *Yersinia enterocolitica* protein database was downloaded from Uniprot. The following search parameters were used: full tryptic specificity required (cleavage after lysine or arginine residues); two missed cleavages allowed; carbamidomethylation (C) set as a fixed modification; oxidation (M) and deamidation (N,Q) set as a variable modification. The mass tolerance was set to 10 ppm for precursor ions and 0.02 Da for high energy-collision dissociation (HCD) fragment ions. The results were then imported into Scaffold (v4.6.2, Proteome Software). Within Scaffold, the data was adjusted to obtain a Protein FDR of 1%. The resulting data was used for further data extraction.

7. Appendix

7.1 Abbreviations

a.a.	Amino acid
ABC	Ammonium bicarbonate
ADP	Adenosine diphosphate
AGC	Automatic gain control
AMP	Adenosine monophosphate
ara.	Arabinose
ATP	Adenosine triphosphate
a.u.	Arbitrary unit
AXP	Adenosine X-phosphate
BCA	Bicinchoninic acid assay
BHI	Brain heart infusion medium
Bla	β-lactamase
Ca^{2+}	Calcium ion
CBD	Chaperone binding domain
CCF2-AM	Cephalosporin core linking a 7-hydroxycoumarin to fluoresein
Chlor.	Chloramphenicol
DAP	Diaminopimelic acid
DIC	Differential interference contrast
DMSO	Dimethylsulfoxide
DNA	Deoxyribonucleic acid
E. coli	*Escherichia coli*
EC	Energy charge
EGFP	Enhanced green fluorescent protein
EGTA	Egtazic acid
EHEC	Enterohemorrhagic *Escherichia coli*
EPEC	Enteropathogenic *Escherichia coli*
HCD	High energy-collision dissociation
HM	Host membrane
HPLC	High performance liquid chromatography
HSVTK	Herpes simplex virus – thymidine kinase
IM	Inner membrane
kb	Kilobases

kDa	KiloDalton
LITESEC-act	Light-induced translocation of effectors through the sequestration of endogenous components – activation by light
LITESEC-supp	Light-induced translocation of effectors through the sequestration of endogenous components – suppression by light
LITESEC-T3SS	Light-induced translocation of effectors through the sequestration of endogenous components of the type III secretion
FRET	Förster resonance energy transfer
fwd.	Forward primer
g	Gravitational acceleration constant
h/hrs	Hour(s)
LB	Luria-Bertani medium
MAPK	Mitogen-activating protein kinases
min	Minute(s)
MLD	Membrane localization domain
mRNA	Messenger ribonucleic acid
MS ring	Membrane/supramembrane ring
MOI	Multiplicity of infection
MW	Molecular weight
Na^+	Sodium ion
Nal	Nalidixic acid
NCS	Newborn calf serum
neg. ctrl.	Negative control
NF-κB	Nuclear factor-kappa light chain enhancer of activated B cells
n.s.	Not significant
NS/non-secr./n.secr.	Non-secreting medium
OD_{600}	Optical density at 600 nm
OM	Outer membrane
ovrl.	Overlapping
P. aeruginosa	*Pseudomonas aeruginosa*
PAGE	Polyacrylamide gel electrophoresis
PARP	poly (ADP-ribose) polymerase
PBS	Phosphate buffered saline
PBS-T	Phosphate buffered saline with Tween

PCR	Polymerase chain reaction
PEPC	Phosphoenolpyruvate carboxylase
pos. ctrl.	Positive control
PUMA	p53 upregulated modulator of apoptosis
pYV	Plasmid of *Yersinia* virulence
rev.	Reverse primer
RNA	Ribonucleic acid
RNAT	Ribonucleic acid thermometer
RPMI 1640 medium	Roswell Park Memorial Institute 1640 medium
RSLC	Rapid separation liquid chromatography
RT	Room temperature
S/sec./secret.	Secreting medium
sec	Seconds
S. enterica	*Salmonella enterica*
S. flexneri	*Shigella flexneri*
SDS	Sodium dodecyl sulfate
sfGFP	Super-folded green fluorescent protein
SLS	Sodium lauryl sulfate
SPI-1	*Salmonella* pathogenicity island 1
SPI-2	*Salmonella* pathogenicity island 2
spp.	Species
t	Time
T3SS	Type III secretion system
T3SS-neg.	Type III secretion system negative
T3SS-pos.	Type III secretion system positive
tBID	Truncated BID
TCA	Trichloro-acetic acid
TFA	Trifluoroacetic acid
TMH	Transmembrane-helix
Tris	Tris(hydroxymethylaminomethane)
TSS	Transformation and storage solution
Y. enterocolitica	*Yersinia enterocolitica*
Y. pestis	*Yersinia pestis*
Y. pseudotuberculosis	*Yersinia pseudotuberculosis*

Yop	*Yersinia* outer protein

7.2 Software

Genetic analysis

Primers were designed using Primer3 (Altschul *et al*, 1990).

Plasmids were designed using Serial Cloner 2.6.1 (SerialBasics).

Sequence homology searches were completed using BLAST (Rozen & Skaletsky, 2000).

Image processing

Stacks of fluorescence micrographs were deconvolved using SoftWoRx 5.5 with conservative settings (Applied Precision, Issaquah, WA, USA).

Image analysis and processing was completed using ImageJ (US National Institutes of Health, Bethesda, MS, USA).

Densitometric analysis

Western blot band quantification was completed using ImageJ (US National Institutes of Health, Bethesda, MS, USA).

Mass spectrometry

Proteomics mass spectrometry data was analyzed using MASCOT (v2.5, Matrix Science, London, UK), Uniport (Collaboration between European Bioinformatics Institute, Swiss Institute for Bioinformatics and Protein Information Resources), Proteome Discoverer platform (v1.4, Thermo Fisher Scientific) Scaffold (v4.6.2, Proteome Software, Inc., Portland, OR, USA).

Metabolomics mass spectrometry data was analyzed using QQQ Quantitative Analysis (Agilent Technologies, Inc., Santa Clara, CA, USA).

7.3 Bacterial strains

Table 1: Bacterial strains details

Strain	Relevant characteristics of virulence plasmid	References
MRS40	Wild-type pYV plasmid of *Y. enterocolitica* E40 (pYVe40) ΔblaA	(Sory *et al*, 1995)
IML421*asd* (ΔHOPEMTasd)	pYVmrs40 $yopO_{\Delta 2\text{-}427}$ $yopE_{21}$ $yopH_{\Delta 1\text{-}352}$ $yopM_{23}$ $yopP_{23}$ $yopT_{135}$ *Δasd*	(Kudryashev *et al*, 2013)
AD4051	pYVmrs40 *ΔsctD*	(Diepold *et al*, 2010)
AD4085	pYViml421asd *egfp-sctQ*	(Kudryashev *et al*, 2013)
AD4306	pYViml421asd *egfp-sctD*	(Diepold *et al*, 2015)
AD4419	pYViml421asd *ΔsctQ*	(Diepold *et al*, 2015)
AD4483	pYViml421asd *egfp-sctL ΔsctD*	(Diepold *et al*, 2017)
AD4616	pYViml421asd sycN-*sfgfp*	This study
AD4617	pYViml421asd tyeA-*sfgfp*	This study
FL4003	pYViml421asd z*dk1-SctQ, mCherry-sctL*	(Lindner *et al*, 2020)
FL4005	pYViml421asd *sspB_Nano-sctQ, mCherry-sctL*	(Lindner *et al*, 2020)
BMD4015	pYViml421asd *egfp-yscB*	This study
BMD4019	pYVmrs40 *ΔsycH*	This study
BMD4020	pYVmrs40 *ΔsycE*	This study
ADMA4098	pYVmrs40 *ΔsctC*	Diepold lab stock, unpublished
ADTM4521	pYViml421asd *mCherry-sctL*	(Milne-Davies *et al*, 2019)
BK021	pYViml421asd *ΔsctW*	Diepold lab stock, unpublished
CH4006	pYViml421asd $sctF_{S5C}$	(Milne-Davies *et al*, 2019)
IM41	pYVmrs40 $sctW_{45}$ (does not encode *sctW*=*yopN*)	(Boland *et al*, 1996)

7.4 Plasmids

Table 2: Plasmid details

Plasmid	Relevant characteristics	References
pACYC184	Expression vector	New England Biolabs
pBAD	Expression vector	Commercial
pKNG101	oriR6K sacBR$^+$ oriTRK2 strAB$^+$ *(suicide vector)*	(Kaniga *et al*, 1991)
pAD301	pUC19::*egfp*	Diepold lab stock, unpublished
pAD612	pKNG101::*Zdk1-sctQ*	(Lindner *et al*, 2020)
pAD626	pACYC184::*yopH$_{1-17}$-bla* (β-lactamase from pBAD::His-B cloned in-frame with first 17 amino acids of *Y. enterocolitica* yopH)	(Milne-Davies *et al*, 2019)
pAD627	pACYC184::*bla*	(Milne-Davies *et al*, 2019)
pAD681	pBAD::*yopH$_{1-17}$-NanoLuc-flag*	(Lindner *et al*, 2020)
pAD683	pBAD::*yopE$_{1-53}$-egfp*	This study
pAD686	pBAD::*yopE$_{1-138}$-egfp*	This study
pAD694	pKNG101:: *Δ*SycH	This study
pAD695	pKNG101:: *Δ*SycE	This study
pAD723	pKNG101::*sycN-sfgfp*	This study
pAD724	pKNG101::*tyeA::sfgfp*	This study
pFL118	pKNG101::*SspB_Nano-sctQ*	(Lindner *et al*, 2020)
pFL126	pACYC184::*TMH-flag-(L1)- LOV2$_{V416L}$*	(Lindner *et al*, 2020)
pFL127	pACYC184::*TMH-flag-(L1)- iLID*	(Lindner *et al*, 2020)
pFL133	pBAD::*yopE$_{1-53}$-NanoLuc-flag*	(Lindner *et al*, 2020)
pFL134	pBAD::*yopE$_{1-138}$-NanoLuc-flag*	This study
pFL137	pBAD::*yopE$_{1-53}$-PUMA-flag*	This study
pFL138	pBAD::*yopE$_{1-53}$-HVSTK-flag*	This study
pFL139	pBAD::*yopE$_{1-53}$-p53-flag*	This study
pFL140	pBAD::*yopE$_{1-138}$-PUMA-flag*	This study
pFL142	pBAD::*yopE$_{1-138}$-p53-flag*	This study
pFL144	pBAD::*yopE$_{1-138}$-HVSTK-flag*	This study
pFL157	pBAD::*sycE-yopE$_{1-138}$-egfp*	This study
pBMD005	pKNG101::*yscB-pre-fluorescent protein*	This study
pBMD011	pKNG101::*sycN-pre-fluorescent protein*	This study
pBMD012	pKNG101::*tyeA-pre-fluorescent protein*	This study
pBMD013	pKNG101::*yscB-egfp*	This study
pBMD028	pBAD::*yopE$_{1-53}$*	(Lindner *et al*, 2020)
pBMD029	pBAD::*yopE$_{1-138}$*	This study
pBMD040	pBAD::*yopE$_{1-53}$-bla*	(Lindner *et al*, 2020)
pBMD043	pBAD::*sycT*	This study
pBMD044	pBAD::*sycE*	This study
pBMD045	pBAD::*sycH*	This study
pBMD046	pBAD::*sycD*	This study
pBMD055	pBAD::*sycO*	This study
pBMD059	pBAD:: *yopE$_{1-15}$*	This study
pBMD061	pBAD::*yopE$_{1-15}$-egfp*	This study
pBMD062	pBAD::*yopE$_{1-15}$-NanoLuc*	This study
pBMD063	pBAD::*sycE-yopE$_{1-138}$-NanoLuc*	This study

pADTM521	pKNG101::*mCh-sctL* (*pamCherry* and flexible linker cloned in-frame at the N-terminus of *sctL*)	(Diepold *et al*, 2017)
pCH06	pKNG101 $sctF_{S5C}$ (serine to cysteine point mutation of amino acid 5 in *sctF*)	(Milne-Davies *et al*, 2019)
pNL1.1	NanoLuc luciferase template	Commercial
pSi_87	pBAD::*sycE-yopE*$_{1-138}$*-tBID*	(Ittig *et al*, 2015)
	pMA-T::*HSVTK*	GeneArt DNA
	pMA-RQ::*PUMA-BBC2*	GeneArt DNA
	pENTR-p53-WT	(Stiewe *et al*, 2002)

7.5 Oligonucleotides

Table 3: Oligonucleotides details

No.	Sequences	Features	Used for cloning of	Template
AD301	GACTGGATCCAGATCTGGTGCTGGCGTGAGCAAG GGCGAGGAG	BglII and BamHI sites	GFP – fwd.	pAD301
AD302	GACTGTCGACAATTGACCTGCCCCCTTGTACAGC TCGTCCATGC	MfeI and SalI sites	GFP – rev.	pAD301
AD339	ATGCCATAGCATTTTTATCC		pBAD sequencing – fwd.	pBAD
AD340	GCGTTCTGATTTAATCTGTATCAGG		pBAD sequencing – rev.	pBAD
AD341	TATTAATTGATCTGCATCAACTTAACG		pKNG101 sequencing – fwd.	pKNG101
AD342	GACTATACTAGTATACTCCGTCTACTGTACG		pKNG101 sequencing – rev.	pKNG101
AD742	GACTGGGCCCGCAACCACAGGCTAAAATTATCTG	ApaI site	pBMD005 – fwd.	pYV (MRS40)
AD743	GCCCGAACCACCGAATTCGAGACCAGATCTATTT TGCATTATTTCTCAGATGGTT	MfeI site	pBMD005 – ovrl. rev.	pYV (MRS40)
AD744	GGTCTCGAATTCGGTGGTTCGGGCGGGTCTGGTG GCCAAAATTTACTAAAAAACTTGGCTACC	BsaI site	pBMD005 – ovrl. fwd.	pYV (MRS40)
AD745	GACTTCTAGAGCGGAAAAGCCATATTACTTAATT CC	XbaI site	pBMD005 – rev.	pYV (MRS40)
AD746	GACTGGATCCTTGACTGATCATGAACTTATCATT AAGCGATCTTCATCGTCAGGTATCTCGATTGGTG CAGCACCCAGAAACGCTGGTG	BamHI site	pAD626 – fwd.	pBAD
AD747	GACTGGATCCTTGACTGATCATGCACCCAGAAAC GCTGGTG	BamHI site	pAD627 – fwd.	pBAD
AD748	GACTGTCGACTTACCAATGCTTAATCAGTGAGG	XhoI site	pAD626 and pAD627 – rev.	pBAD
AD749	GACTGGGCCCTGGCTATTGAGAGTGAAGAGGA	ApaI site	pBMD011 – fwd.	pYV (MRS40)
AD750	AGATCTGCCACCAGACCCGCCCGAACCACCCGGC GCAAGCACCTCTTG	BglII site	pBMD011 – ovrl. rev.	pYV (MRS40)
AD751	TCGGGCGGGTCTGGTGGCAGATCTCAGTCAATTG GAGGTGCTTGCGCCG*TGA*	MfeI site	pBMD011 – ovrl. fwd.	pYV (MRS40)
AD752	GACTTCTAGACCTGTTGTCGTTTGGTTAAAGT	XbaI site	pBMD011 – rev.	pYV (MRS40)
AD753	GACTGGGCCCTCAACAAAGCGGGTCTGAAC	ApaI site	pBMD012 – fwd.	pYV (MRS40)
AD754	AGATCTGCCACCAGACCCGCCCGAACCACTACTC AATTCTTCCTCTTCACTCTCA	BglII site	pBMD012 – ovrl. rev.	pYV (MRS40)
AD755	TCGGGCGGGTCTGGTGGCAGATCTCAGTCAATTG GAGGAAGAATTGAGTGAGTTGGA	MfeI site	pBMD012 – ovrl. fwd.	pYV (MRS40)

AD756	GACTTCTAGAATTATGCGACTCACGGCG	XbaI site	pBMD012 – rev.	pYV(MRS40)
AD876	GACTAGATCTGGAGAGGAGCCGCAGTCAGATC	BglII site	P53 – fwd.	pENTR-p53-WT
AD877	GACTGTCGACGAATTCTCACTTATCATCGTCGTCCTTGTAGTCTCCGCCACCGTCTGAGTCAGGCCCTTCTG	EcoRI and XhoI site	P53 – rev.	pENTR-p53-WT
AD894	GATCTCATGAAAATATCATCATTTATTTCTACATCACTGC	BspHI site	pBMD028 and pBMD059 – fwd.	pYV (MRS40)
AD895	GATCGAATTCGCGCAGATCTTCCGCCGGAACCCTGAGGGCTTTCAGTGC	EcoRI site	pBMD028 – rev.	pYV (MRS40)
AD896	GATCCCATGGGTAAAATATCATCATTTATTTCTACATCACTGC	NcoI site	pBMD029 – fwd.	pYV (MRS40)
AD897	GATCGAATTCGCGCAGATCTTCCGCCCGTGGCGAACTGGTCATGATTTT	EcoRI site	pBMD029 – rev.	pAD627/ pBMD028
AD903	GACTGTCGACGCAAGCTT*TTA*AAGTTCTTTTG	XhoI	pFL126 – rev.	pAD610
AD904	GACTGTCGACTCAGCTAATTAAGCTTTTAAAAGT	XhoI	pFL127 – rev.	pFL108
AD909	AGTCGGGCCCATGACACAATTAGAGGAGCAACTGCATAAC	ApaI site	pCH06 – fwd.	pYV (MRS40)
AD910	TGTAAACCCGCAGAAATTACTCATTTATTTTAGAC		pCH06 – ovrl. rev.	pYV (MRS40)
AD911	AGTAATTTCTGCGGGTTTACAAAAGGGAACGATATC		pCH06 – ovrl. fwd.	pYV (MRS40)
AD912	AGTCTCTAGATTTCATGCTACGAACTATGGTTGAGCTTATATTG	XbaI site	pCH06 – rev.	pYV (MRS40)
AD913	GCAGGAGGTCTAAAATAAATGAGTAATTTCTGC		pCH06 – test	pYV (MRS40)
AD921	GACTAGATCTTTGACTGAATGGGTGGTATCAGTATTTGGC	BglII site	pFL126 and pFL127 – fwd.	pAD610 /pFL108
AD933	GACTTCATGAACTTATCATTAAGCGATCTTCATCGTCAGGTATCTCGATTGGTGCAGGGAGGTAGATCTGGCGCAGGTGTCTTCACACTCGAAGATTTCGTT	BglII site	NanoLuc – fwd.	pNL1.1
AD934	GACTAAGCTTTTAGAATTCGCCTGCACCCTTATCATCGTCGTCCTTGTAGTCACCTCCCGCCAGAATGCGTTCGCA	Flag and BspHI site	NanoLuc – rev.	pNL1.1
AD968	GATCCCATGGGGCAGACAACCTTCACAGAACT	NcoI site	pBMD043 – fwd.	pYV (MRS40)
AD969	GATCGAATTCTCAGATGAATAATATAGGTGATGTCGAGTT	EcoRI site	pBMD043 – rev.	pYV (MRS40)
AD971	GATCCCATGGGGTATTCATTTGAACAAGCTATCACTCAA	NcoI site	pBMD044 – fwd.	pYV (MRS40)
AD972	GATCAGATCTTCAACTAAATGACCGTGGTG	BglII site	pBMD044 – rev.	pYV (MRS40)
AD974	GATCCCATGGGGCGCACTTACAGTTCATTACTTGA	NcoI site	pBMD045 – fwd.	pYV (MRS40)
AD975	GATCGAATTCTTAAACCAGTAAATGAGATGATGAAGG	EcoRI site	pBMD045 – rev.	pYV (MRS40)
AD977	GATCTCATGAGTCAACAAGAGACGACAGACACTCAAGA	BspHI site	pBMD046 – fwd.	pYV (MRS40)
AD978	GATCGAATTCTCATGGGTTATCAACGCACTC	EcoRI site	pBMD046 – rev.	pYV (MRS40)

AD1009	GACTGGTCTCGGGCCCGCCAGCTCAGACCTCATCAA	BsaI and ApaI sites	pAD694 – fwd.	pYV (MRS40)
AD1010	GATACCGTACGTCTCCTTCCCAGATGCTACCC		pAD694 – ovrl. rev.	pYV (MRS40)
AD1011	TCTGGGAAGGAGACGTACGGTATCCATTAATGGGT		pAD694 – ovrl. fwd.	pYV (MRS40)
AD1012	GACTGGTCTCTCTAGATCTGATTAAGTTGGCTGAAGGACA	BsaI and XbaI sites	pAD694 – rev.	pYV (MRS40)
AD1013	GACTGGTCTCGGGCCCGCGCCCAGACATTTCTCCTA	BsaI and ApaI sites	pAD695 – fwd.	pYV (MRS40)
AD1014	AAGGCAACAAGCATAACCAAAGCACTCTCGGCA		pAD695 – ovrl. rev.	pYV (MRS40)
AD1015	GAGTGCTTTGGTTATGCTTGTTGCCTTATTATACGGA		pAD695 – ovrl. fwd.	pYV (MRS40)
AD1016	GACTGGTCTCTCTAGACGTCGGTTACGTCCGGTTAT	BsaI and XbaI sites	pAD695 – rev.	pYV (MRS40)
AD1070	TATACTCGAG*TTA*GAATTCGACTAGATCTTATTTTCATGACTATTTATTCCCTTGGC	BglII site with spacer and EcoRI site	pBMD059 – rev.	pYV (MRS40)
AD1152	GATCTCATGATTAACACCACCTTTACTGAGCT	BspHI site	pBMD055 – fwd.	pYV (MRS40)
AD1153	GATCGAAT*TCA*TCCCCATTTAACCGATTGAGT	EcoRI site	pBMD055 – rev.	pYV (MRS40)

7.6 Antibodies

Table 4: Antibody details

No.	Specificity	Donor organism	Dilution	Source
57	anti-SctP	rabbit	1:3,000	(1)
73	anti-YopE	rabbit	1:1,000	(1)
220	anti-SctA/LcrV	rabbit	1:2,000	(1)
223	anti-SctF	rabbit	1:1,000	(1)
235	anti-SctQ	Rabbit	1:1,000	(1)
	anti-Flag	rabbit	1:4,000	(2)
	anti-GFP	mouse	1:1,000	(3)
	HRP anti-rabbit secondary antibody	goat	1:5,000	(4)
	HRP anti-rabbit secondary antibody	goat	1:10,000	(5)
	HRP anti-mouse secondary antibody	sheep	1:5,000 -10,000	(6)
	anti-cleaved PARP	rabbit	1:500	(7)
	anti-β-actin	mouse	1:200	(8)

(1) Centre d'économie rurale, Laboratoire d'hormonologie, Marloie, Belgium

(2) Rockland, Limerick, Pennsylvania, USA

(3) Proteintech, St. Leon-Rot, Germany

(4) DAKO, Glostrup, Denmark

(5) Sigma-Aldrich, Munich, Germany

(6) Amersham, Freiburg, Germany

(7) Cell Signaling Technology, Danvers, Massachusetts, USA

(8) Santa Cruz, Dallas, Texas, USA

8. References

Adkins I, Köberle M, Gröbner S, Bohn E, Autenrieth IB & Borgmann S (2007) Yersinia outer proteins E, H, P, and T differentially target the cytoskeleton and inhibit phagocytic capacity of dendritic cells. *Int. J. Med. Microbiol.* **297:** 235–44

Aepfelbacher M, Trasak C, Wilharm G, Wiedemann A, Trülzsch K, Krauss K, Gierschik P & Heesemann J (2003) Characterization of YopT effects on Rho GTPases in Yersinia enterocolitica-infected cells. *J. Biol. Chem.* **278:** 33217–33223

Agrain C, Sorg I, Paroz C & Cornelis GR (2005) Secretion of YscP from Yersinia enterocolitica is essential to control the length of the injectisome needle but not to change the type III secretion substrate specificity. *Mol. Microbiol.* **57:** 1415–1427

Aili M, Isaksson EL, Carlsson SE, Wolf-Watz H, Rosqvist R & Francis MS (2008) Regulation of Yersinia Yop-effector delivery by translocated YopE. *Int. J. Med. Microbiol.* **298:** 183–192

Akeda Y & Galán JE (2005) Chaperone release and unfolding of substrates in type III secretion. *Nature* **437:** 911–5

Allaoui A, Woestyn S, Sluiters C & Cornelis GR (1994) YscU, a Yersinia enterocolitica Inner Membrane Protein Involved in Yop Secretion. *J. Bacteriol.* **176:** 4534–4542

Altegoer F, Schuhmacher J, Pausch P & Bange G (2014) From molecular evolution to biobricks and synthetic modules: A lesson by the bacterial flagellum. *Biotechnol. Genet. Eng. Rev.* **30:** 49–64

Altschul SF, Gish W, Miller W, Myers EW & Lipman DJ (1990) Basic Local Alignment Search Tool. *J. Mol. Biol* **215:** 403–410

Andor A, Trülzsch K, Essler M, Roggenkamp A, Wiedemann A, Heesemann J & Aepfelbacher M (2001) YopE of Yersinia, a GAP for Rho GTPases, selectively modulates Rac-dependent actin structures in endothelial cells. *Cell. Microbiol.* **3:** 301–310

Archuleta TL & Spiller BW (2014) A Gatekeeper Chaperone Complex Directs Translocator Secretion during Type Three Secretion. *PLoS Pathog.* **10:** e1004498

Armentrout EI & Rietsch A (2016) The Type III Secretion Translocation Pore Senses Host Cell Contact. *PLoS Pathog.* **12:** e1005530

Ashida H, Mimuro H & Sasakawa C (2015) Shigella manipulates host immune responses by delivering effector proteins with specific roles. *Front. Immunol.* **6:** 219

Autenrieth SE, Linzer T-R, Hiller C, Keller B, Warnke P, Köberle M, Bohn E, Biedermann T, Bühring H-J, Hämmerling GJ, Rammensee H-G & Autenrieth IB (2010) Immune Evasion by Yersinia enterocolitica: Differential Targeting of Dendritic Cell Subpopulations In Vivo. *PLoS Pathog.* **6:** e1001212

Avican K, Fahlgren A, Huss M, Heroven AK, Beckstette M, Dersch P & Fällman M (2015)

Reprogramming of Yersinia from Virulent to Persistent Mode Revealed by Complex In Vivo RNA-seq Analysis. *PLoS Pathog.* **11:** e1004600

Bahrani FK, Sansonetti PJ & Parsot C (1997) Secretion of Ipa Proteins by Shigella flexneri: Inducer Molecules and Kinetics of Activation. *Infect. Immun.* **65:** 4005–4010

Bai F, Li Z, Umezawa A, Terada N & Jin S (2018) Bacterial type III secretion system as a protein delivery tool for a broad range of biomedical applications Elsevier Inc.

Bamyaci S, Ekestubbe S, Nordfelth R, Erttmann SF, Edgren T & Forsberg Å (2018) YopN Is Required for Efficient Effector Translocation and Virulence in Yersinia pseudotuberculosis. *Infect. Immun.* **86:** e00957-17

Bamyaci S, Nordfelth R & Forsberg Å (2019) Identification of specific sequence motif of YopN of Yersinia pseudotuberculosis required for systemic infection. *Virulence* **10:** 10–25

Barber NC & Stark LA (2014) Engaging with Molecular Form to Understand Function. *CBE—Life Sci. Educ.* **13:** 21–24

Behnsen J, Jellbauer S, Wong CP, Edwards RA, George MD, Ouyang W & Raffatellu M (2014) The Cytokine IL-22 Promotes Pathogen Colonization by Suppressing Related Commensal Bacteria. *Immunity* **40:** 262–273

Ben-Gurion R & Shafferman A (1981) Essential virulence determinants of different Yersinia species are carried on a common plasmid. *Plasmid* **5:** 183–187

Berger CN, Crepin VF, Baruch K, Mousnier A, Rosenshine I & Frankel G (2012) EspZ of enteropathogenic and enterohemorrhagic escherichia coli regulates type III secretion system protein translocation. *MBio* **3:** e00317-12

Bernardini ML, Mounier J, Ne Dwhauteville H, Coquis-Rondont M & Sansonetti PJ (1989) Identification of jcsA, a plasmid locus of Shigella flexneri that governs bacterial intra-and intercellular spread through interaction with F-actin (pathogenicity/intracellular movement). *Proc. Natil. Acad. Sci. USA* **86:** 3867–3871

Beuzón CR, Banks G, Deiwick J, Hensel M & Holden DW (1999) pH-dependent secretion of SseB, a product of the SPI-2 type III secretion system of Salmonella typhimurium. *Mol. Microbiol.* **33:** 806–16

Birtalan SC, Phillips RM & Ghosh P (2002) Three-Dimensional Secretion Signals in Chaperone-Effector Complexes of Bacterial Pathogens et al forms a complex in the bacterial cytosol with YopE but is not translocated into host cells. *Mol. Cell* **9:** 971–980

Bleves S, Marenne MN, Detry G & Cornelis GR (2002) Up-regulation of the Yersinia enterocolitica yop regulon by deletion of the flagellum master operon flhDC. *J. Bacteriol.* **184:** 3214–3223

Bliska JB, Guant K, Dixont JE & Falkow S (1991) Tyrosine phosphate hydrolysis of host proteins by an

essential Yersinia virulence determinant. *Microbiology* **88:** 1187–1191

Blocker A, Gounon P, Larquet E, Niebuhr K, Cabiaux V, Parsot C & Sansonetti P (1999) The Tripartite Type III Secreton of Shigella flexneri Inserts IpaB and IpaC into Host Membranes. *J. Cell Biol.* **147:** 683–693

Bodey GP, Bolivar R, Fainstein V & Jadeja L (1983) Infections Caused by Pseudomonas aeruginosa. *Rev. Infect. Dis.* **5:** 279–313

Böhme K, Steinmann R, Kortmann J, Seekircher S, Heroven AK, Berger E, Pisano F, Thiermann T, Wolf-Watz H, Narberhaus F & Dersch P (2012) Concerted actions of a thermo-labile regulator and a unique intergenic RNA thermosensor control Yersinia virulence. *PLoS Pathog.* **8:** e1002518

Boland A, Sory MP, Iriarte M, Kerbourch C, Wattiau P & Cornelis GR (1996) Status of YopM and YopN in the Yersinia Yop virulon: YopM of Y.enterocolitica is internalized inside the cytosol of PU5-1.8 macrophages by the YopB, D, N delivery apparatus. *EMBO J.* **15:** 5191–5201

Botteaux A, Sani M, Kayath CA, Boekema EJ & Allaoui A (2008) Spa32 interaction with the inner-membrane Spa40 component of the type III secretion system of Shigella flexneri is required for the control of the needle length by a molecular tape measure mechanism. *Mol. Microbiol.* **70:** 1515–1528

Bottone EJ (1997) Yersinia enterocolitica: The Charisma Continues. *Clin. Microbiol. Rev.* **10:** 257–276

Bottone EJ (1999) Yersinia enterocolitica: overview and epidemiologic correlates. *Microbes Infect.* **1:** 323–33

Bottone EJ & Mollaret HH (1977) Yersinia enterocolitica: A panoramic view of a charismatic microorganism. *Crit. Rev. Microbiol.* **5:** 211–241

Boyd AP, Lambermont I & Cornelis GR (2000) Competition between the Yops of Yersinia enterocolitica for delivery into eukaryotic cells: Role of the SycE chaperone binding domain of YopE. *J. Bacteriol.* **182:** 4811–4821

Broz P, Mueller CA, Müller SA, Philippsen A, Sorg I, Engel A & Cornelis GR (2007) Function and molecular architecture of the Yersinia injectisome tip complex. *Mol. Microbiol.* **65:** 1311–1320

Brubaker RR (1967) Growth of Pasteurella Pseudotuberculosis in Simulated Intracellular and Extracellular Environments. *J. Infect. Dis.* **117:** 403–417

Brubaker RR (1983) The Vwa+ Virulence Factor of Yersiniae: The Molecular Basis of the Attendant Nutritional Requirement for Ca++. *Rev. Infect. Dis.* **5:** S748–S758

Brubaker RR (2005) Influence of Na(+), dicarboxylic amino acids, and pH in modulating the low-calcium response of Yersinia pestis. *Infect. Immun.* **73:** 4743–52

Büttner D (2012) Protein export according to schedule: architecture, assembly, and regulation of type III secretion systems from plant- and animal-pathogenic bacteria. *Microbiol. Mol. Biol. Rev.* **76:**

262–310

Button JE & Galán JE (2011) Regulation of chaperone/effector complex synthesis in a bacterial type III secretion system. *Mol. Microbiol.* **81:** 1474–1483

Bykov VJN, Eriksson SE, Bianchi J & Wiman KG (2018) Targeting mutant p53 for efficient cancer therapy. *Nat. Rev. Cancer* **18:** 89–102

Cambronne ED, Cheng LW & Schneewind O (2000) LcrQ/YscM1, regulators of the Yersinia yop virulon, are injected into host cells by a chaperone-dependent mechanism. *Mol. Microbiol.* **37:** 263–273

Cambronne ED, Sorg JA & Schneewind O (2004) Binding of SycH Chaperone to YscM1 and YscM2 Activates Effector yop Expression in Yersinia enterocolitica. *J. Bacteriol.* **186:** 829–841

Carafoli E (1987) High-affinity cytosolic calcium-binding proteins. *Ann. Rev. Biochem* **56:** 395–433

Charpentier X & Oswald E (2004) Identification of the secretion and translocation domain of the enteropathogenic and enterohemorrhagic Escherichia coli effector Cif, using TEM-1 beta-lactamase as a new fluorescence-based reporter. *J. Bacteriol.* **186:** 5486–5495

Cheng LW, Anderson DM & Schneewind O (1997) Two independent type III secretion mechanisms for YopE in Yersinia enterocolitica. *Mol. Microbiol.* **24:** 757–765

Cheng LW, Kay O & Schneewind O (2001) Regulated secretion of YopN by the type III machinery of Yersinia enterocolitica. *J. Bacteriol.* **183:** 5293–301

Cheng LW & Schneewind O (1999) Yersinia enterocolitica Type III Secretion on the role of SycE in targeting YopE into HeLa cells*. *J. Biol. Chem.* **274:** 222102–22108

Cheng LW & Schneewind O (2000) Yersinia enterocolitica TyeA, an Intracellular Regulator of the Type III Machinery, Is Required for Specific Targeting of YopE, YopH, YopM, and YopN into the Cytosol of Eukaryotic Cells. *J. Bacteriol.* **182:** 3183–3190

Cherradi Y, Schiavolin L, Moussa S, Meghraoui A, Meksem A, Biskri L, Azarkan M, Allaoui A & Botteaux A (2013) Interplay between predicted inner-rod and gatekeeper in controlling substrate specificity of the type III secretion system. *Mol. Microbiol.* **87:** 1183–1199

Chung L, Philip N, Schmidt V, Koller A, Strowig T, Flavell RA, Brodsky IE & Bliska JB (2014) IQGAP1 is important for activation of caspase-1 in macrophages and is targeted by Yersinia pestis type III effector YopM. *MBio* **5:** e01402-14

Cisz M, Lee P-C & Rietsch A (2008) ExoS controls the cell contact-mediated switch to effector secretion in Pseudomonas aeruginosa. *J. Bacteriol.* **190:** 2726–2738

Coburn B, Sekirov I & Finlay BB (2007) Type III secretion systems and disease. *Clin. Microbiol. Rev.* **20:** 535–49

Cornelis GR (2006) The type III secretion injectisome. *Nat. Rev. Microbiol.* **4:** 811–825

Cornelis GR & Gijsegem F Van (2000) Assembly and function of the type III secretory systems. *Annu.*

Rev. Microbiol **54:** 735–74

Cornelis GR, Vanooteghem J, Sluiters C, Vanootegem JC & Sluiters C (1987) Transcription of the yop regulon from Y. enterocolitica requires trans acting pYV and chromosomal genes. *Microb. Pathog.* **2:** 367–379

Cowell BA, Evans DJ & Fleiszig SMJ (2005) Actin cytoskeleton disruption by ExoY and its effects on Pseudomonas aeruginosa invasion. *FEMS Microbiol. Lett.* **250:** 71–76

Czechowska K, McKeithen-Mead S, Moussawi K Al & Kazmierczak BI (2014) Cheating by type 3 secretion system-negative Pseudomonas aeruginosa during pulmonary infection. *Proc. Natl. Acad. Sci. U. S. A.* **111:** 7801–7806

D'haeze W, De Rycke R, Mathis R, Goormachtig S, Pagnotta S, Verplancke C, Capoen W & Holsters M (2003) Reactive oxygen species and ethylene play a positive role in lateral root base nodulation of a semiaquatic legume. *Proc. Natl. Acad. Sci. U. S. A.* **100:** 11789–11794

Darland G, Ewing WH & Üavis BR (1974) The Biochemical Characteristics o f Yersinia enterocolitica and Yersinia pseudotuberculosis U.S. DHEW Publication No. (CDC) 75-8294

Davis AJ & Mecsas J (2006) Mutations in the Yersinia pseudotuberculosis type III secretion system needle protein, YscF, that specifically abrogate effector translocation into host cells. *J. Bacteriol.* **189:** 83–97

Davis KM & Isberg RR (2019) One for All, but Not All for One: Social Behavior during Bacterial Diseases. *Trends Microbiol.* **27:** 64–74

Day JB, Ferracci F & Plano G V (2003) Translocation of YopE and YopN into eukaryotic cells by Yersinia pestis yopN, tyeA, sycN, yscB and lcrG deletion mutants measured using a phosphorylatable peptide tag and phosphospecific antibodies. *Mol. Microbiol.* **47:** 807–23

Day JB & Plano G V (1998) A complex composed of SycN and YscB functions as a specific chaperone for YopN in Yersinia pestis. *Mol. Microbiol.* **30:** 777–88

Deane JE, Roversi P, Cordes FS, Johnson S, Kenjale R, Daniell S, Booy F, Picking WD, Picking WL, Blocker AJ & Lea SM (2006) Molecular model of a type III secretion system needle: Implications for host-cell sensing. *Proc. Natl. Acad. Sci.* **103:** 12529–12533

Deiwick J, Nikolaus T, Erdogan S & Hensel M (1999) Environmental regulation of Salmonella pathogenicity island 2 gene expression. *Mol. Microbiol.* **31:** 1759–1773

Deng W, Li Y, Hardwidge PR, Frey EA, Pfuetzner RA, Lee S, Gruenheid S, Strynakda NCJ, Puente JL & Finlay BB (2005) Regulation of type III secretion hierarchy of translocators and effectors in attaching and effacing bacterial pathogens. *Infect. Immun.* **73:** 2135–2146

Deng W, Marshall NC, Rowland JL, McCoy JM, Worrall LJ, Santos AS, Strynadka NCJ & Finlay BB (2017) Assembly, structure, function and regulation of type III secretion systems. *Nat. Rev. Microbiol.*

15: 323–337

Deng W, Puente JL, Gruenheid S, Li Y, Vallance BA, Vá Zquez † A, Barba J, Ibarra JA, O'donnell P, Metalnikov P, Ashman K, Lee S, Goode D, Pawson T & Finlay BB (2004) Dissecting virulence: Systematic and functional analyses of a pathogenicity island. *Proc. Natl. Acad. Sci.* **101:** 3597–3602

Deng W, Yu HB, Li Y & Finlay BB (2015) SepD/SepL-dependent secretion signals of the type III secretion system translocator proteins in enteropathogenic Escherichia coli. *J. Bacteriol.* **197:** 1263–1275

Dewoody R, Merritt PM, Houppert AS & Marketon MM (2011) YopK regulates the Yersinia pestis type III secretion system from within host cells. *Mol. Microbiol.* **79:** 1445–1461

Dewoody RS, Merritt PM & Marketon MM (2013) Regulation of the Yersinia type III secretion system: traffic control. *Front. Cell. Infect. Microbiol.* **3:** 1–13

Diard M, Garcia V, Maier L, Remus-Emsermann MNP, Regoes RR, Ackermann M & Hardt WD (2013) Stabilization of cooperative virulence by the expression of an avirulent phenotype. *Nature* **494:** 353–356

Diepold A, Amstutz M, Abel S, Sorg I, Jenal U & Cornelis GR (2010) Deciphering the assembly of the Yersinia type III secretion injectisome. *EMBO J.* **29:** 1928–1940

Diepold A & Armitage JP (2015) Type III secretion systems: the bacterial flagellum and the injectisome. *Philos. Trans. R. Soc. B Biol. Sci.* **370:** 20150020

Diepold A, Kudryashev M, Delalez NJ, Berry RM & Armitage JP (2015) Composition, Formation, and Regulation of the Cytosolic C-ring, a Dynamic Component of the Type III Secretion Injectisome. *PLoS Biol.* **13:** e1002039

Diepold A, Sezgin E, Huseyin M, Mortimer T, Eggeling C & Armitage JP (2017) A dynamic and adaptive network of cytosolic interactions governs protein export by the T3SS injectisome. *Nat. Commun.* **8:** 15940

Diepold A & Wagner S (2014) Assembly of the bacterial type III secretion machinery. *FEMS Microbiol. Rev.* **38:** 802–22

Diepold A, Wiesand U & Cornelis GR (2011) The assembly of the export apparatus (YscR,S,T,U,V) of the Yersinia type III secretion apparatus occurs independently of other structural components and involves the formation of an YscV oligomer. *Mol. Microbiol.* **82:** 502–514

Dittmann S, Schmid A, Richter S, Trülzsch K, Heesemann J & Wilharm G (2007) The Yersinia enterocolitica type three secretion chaperone SycO is integrated into the Yop regulatory network and binds to the Yop secretion protein YscM1. *BMC Microbiol.* **7:** 67

Du J, Reeves AZ, Klein JA, Twedt DJ, Knodler LA & Lesser CF (2016) The type III secretion system apparatus determines the intracellular niche of bacterial pathogens. *Proc. Natl. Acad. Sci. U. S.*

A. **113:** 4794–4799

Enninga J, Mounier JJ, Sansonetti P, Tran G, Nhieu V, Tran Van Nhieu G, Nhieu GT Van, Tran G & Nhieu V (2005) Secretion of type III effectors into host cells in real time. *Nat. Methods* **2:** 959–65

Erfurth SE, Gröbner S, Kramer U, Gunst DSJ, Soldanova I, Schaller M, Autenrieth IB & Borgmann S (2004) Yersinia enterocolitica induces apoptosis and inhibits surface molecule expression and cytokine production in murine dendritic cells. *Infect. Immun.* **72:** 7045–54

Ernst NH, Reeves AZ, Ramseyer JE & Lesser CF (2018) High-throughput screening of type III secretion determinants reveals a major chaperone-independent pathway. *MBio* **9:** e01050-18

Esseling JJ, Lhuissier FGP & Emons AMC (2003) Nod factor-induced root hair curling: Continuous polar growth towards the point of nod factor application. *Plant Physiol.* **132:** 1982–1988

Fàbrega A & Vila J (2012) Yersinia enterocolitica: Pathogenesis, virulence and antimicrobial resistance. *Enferm. Infecc. Microbiol. Clin.* **30:** 24–32

Felgner S, Pawar V, Kocijancic D, Erhardt M & Weiss S (2017) Tumour-targeting bacteria-based cancer therapies for increased specificity and improved outcome. *Microb. Biotechnol.* **10:** 1074–1078

Ferber D & Brubaker R (1981) Plasmids in Yersinia pestist. *Infect. Immun.* **31:** 839–841

Feria JM, García-Gómez E, Espinosa N, Minamino T, Namba K & González-Pedrajo B (2012) Role of escp (Orf16) in Injectisome Biogenesis and Regulation of Type III Protein Secretion in Enteropathogenic Escherichia coli. *J. Bacteriol.* **194:** 6029–6045

Ferracci F, Day JB, Ezelle HJ & Plano G V (2004) Expression of a Functional Secreted YopN-TyeA Hybrid Protein in Yersinia pestis Is the Result of a 1 Translational Frameshift Event. *J. Bacteriol.* **186:** 5160–5166

Ferracci F, Schubot FD, Waugh DS & Plano G V. (2005) Selection and characterization of Yersinia pestis YopN mutants that constitutively block Yop secretion. *Mol. Microbiol.* **57:** 970–987

Figueira R & Holden DW (2012) Functions of the Salmonella pathogenicity island 2 (SPI-2) type III secretion system effectors. *Microbiology* **158:** 1147–1161

Finck-Barbanç V, Goranson J, Zhu L, Sawa T, Wiener-Kronish JP, Fleiszig SMJ, Wu C, Mende-Mueller L & Frank DW (1997) ExoU expression by Pseudomonas aeruginosa correlates with acute cytotoxicity and epithelial injury. *Mol. Microbiol.* **25:** 547–557

Finn CE, Chong A, Cooper KG, Starr T & Steele-Mortimer O (2017) A second wave of Salmonella T3SS1 activity prolongs the lifespan of infected epithelial cells. *PLoS Pathog.* **13:** e1006354

Forsberg A, Virtanen A-M, Skurnik M & Wolf-Watz H (1991) The surface-located YopN protein is involved in calcium signal transduction in Yersinia pseudotuberculosis. *Mol. Microbiol.* **5:** 977–986

Fowler JM & Brubaker RR (1994) Physiological Basis of the Low Calcium Response in Yersinia pestis.

Infect. Immun. **62:** 5234–5241

Fowler JM, Wulff CR, Straley SC & Brubaker RR (2009) Growth of calcium-blind mutants of Yersinia pestis at 37 C in permissive Ca2+-deficient environments. *Microbiology* **155:** 2509–2521

Fredriksson-Ahomaa M, Stolle A & Korkeala H (2006) Molecular epidemiology of Yersinia enterocolitica infections. *FEMS Immunol. Med. Microbiol.* **47:** 315–329

Friedlander RS, Vlamakis H, Kim P, Khan M, Kolter R & Aizenberg J (2013) Bacterial flagella explore microscale hummocks and hollows to increase adhesion. *Proc. Natl. Acad. Sci.* **110:** 5624–5629

Friedlander RS, Vogel N & Aizenberg J (2015) Role of Flagella in Adhesion of Escherichia coli to Abiotic Surfaces. *Langmuir* **31:** 6137–6144

Frithz-Lindsten E, Du Y, Rosqvist R & Ke Forsberg A˚ (1997) Intracellular targeting of exoenzyme S of Pseudomonas aeruginosa via type III-dependent translocation induces phagocytosis resistance, cytotoxicity and disruption of actin microfilaments. *Mol. Microbiol.* **25:** 1125–1139

Frithz-Lindsten E, Rosqvist R, Johansson L & Forsberg A (1995) The chaperone-like protein YerA of Yersinia pseudotuberculosis stabilizes YopE in the cytoplasm but is dispensible for targeting to the secretion loci. *Mol. Microbiol.* **16:** 635–647

Galán J & Wolf-Watz H (2006) Protein delivery into eukaryotic cells by type III secretion machines. *Nature* **444:** 567–573

Galán JE (2009) Common Themes in the Design and Function of Bacterial Effectors. *Cell Host Microbe* **5:** 571–579

Garcia JT, Ferracci F, Jackson MW, Joseph SS, Pattis I, Plano LRW, Fischer W & Plano G V. (2006) Measurement of effector protein injection by type III and type IV secretion systems by using a 13-residue phosphorylatable glycogen synthase kinase tag. *Infect. Immun.* **74:** 5645–5657

Gayraud M, Scavizzi MR, Mollaret HH, Guillevin L & Hornstein MJ (1993) Antibiotic Treatment of Yersinia enterocolitica Septicemia: A Retrospective Review of 43 Cases. *Clin. Infect. Dis.* **17:** 405–410

Gaytán MO, Monjarás Feria J, Soto E, Espinosa N, Benítez JM, Georgellis D & González-Pedrajo B (2018) Novel insights into the mechanism of SepL-mediated control of effector secretion in enteropathogenic Escherichia coli. *Microbiol. Open* **7:** e00571

Gemski P, Lazere J & Casey T (1980a) Plasmid Associated with Pathogenicity and Calcium Dependency of Yersinia enterocolitica. *Infect. Immun.* **27:** 682–685

Gemski P, Lazere J, Casey T & Wohlhieter J (1980b) Presence of a Virulence-Associated Plasmid in Yersinia pseudotuberculosis. *Infect. Immun.* **28:** 1044–1047

Ghosh P (2004) Process of Protein Transport by the Type III Secretion System. *Microbiol. Mol. Biol. Rev.* **68:** 771–795

Giannella R (1996) Salmonella. In *Medical Microbiology* Galveston (TX): University of Texas Medical Branch at Galveston

Goure J, Pastor A, Faudry E, Chabert J, Dessen A & Attree I (2004) The V antigen of Pseudomonas aeruginosa is required for assembly of the functional PopB/PopD translocation pore in host cell membranes. *Infect. Immun.* **72:** 4741–4750

Grosdent N, Maridonneau-Parini I, Sory M-P & Cornelis GR (2002) Role of Yops and adhesins in resistance of Yersinia enterocolitica to phagocytosis. *Infect. Immun.* **70:** 4165–76

Grutzkau A, Hanski C, Hahn H & Riecken EO (1990) Involvement of M cells in the bacterial invasion of Peyer's patches: A common mechanism shared by Yersinia enterocolitica and other enteroinvasive bacteria. *Gut* **31:** 1011–1015

Håkansson S, Bergman T, Vanooteghem J, Cornelis G, Wolf-watz H, Hakansson S, Forsberg A, Norlander L, Maceliaro A, Backman A, Bolin I, Wolf-Watz H, Price SB, Leung KY, Barve SS, Straley SC & Bacteriol J (1993) YopB and YopD Constitute a Novel Class of Yersinia Yop Proteins. *Infect. Immun.* **61:** 1607–1616

Håkansson S, Schesser K, Persson C, Galyov EE, Rosqvist R, Homblé F, Wolf-Watz H, Haikansson S, Schesser K, Persson C, Galyov1 EE, Rosqvist R, Homble2 F & Wolf-Watz3 H (1996) The YopB protein of Yersinia pseudotuberculosis is essential for the translocation of Yop effector proteins across the target cell plasma membrane and displays a contact-dependent membrane disrupting activity. *EMBO J.* **15:** 5812–5823

Hauser AR (2009) The type III secretion system of Pseudomonas aeruginosa: Infection by injection. *Nat. Rev. Microbiol.* **7:** 654–665

Van Der Heijden J & Finlay BB (2012) Type III effector-mediated processes in Salmonella infection. *Future Microbiol.* **7:** 685–703

Heroven AK & Dersch P (2014) Coregulation of host-adapted metabolism and virulence by pathogenic yersiniae. *Front. Cell. Infect. Microbiol.* **4:** 146

High N, Mounier J, Prevost MC & Sansonetti PJ (1992) IpaB of Shigella flexneri causes entry into epithelial cells and escape from the phagocytic vacuole. *EMBO J.* **11:** 1991–1999

Ho O, Rogne P, Edgren T, Wolf-Watz H, Login FH & Wolf-Watz M (2017) Characterization of the ruler protein interaction interface on the substrate specificity switch protein in the Yersinia type III secretion system. *J. Biol. Chem.* **292:** 3299–3311

Hoe NP & Goguen JD (1993) Temperature Sensing in Yersinia pestis: Translation of the LcrF Activator Protein Is Thermally Regulated. *J. Bacteriol.* **175:** 7901–7909

Hoiczyk E & Blobel G (2001) Polymerization of a single protein of the pathogen Yersinia enterocolitica into needles punctures eukaryotic cells. *Proc. Natl. Acad. Sci. U. S. A.* **98:** 4669–4674

Holmström A, Pettersson J, Rosqvist R, Hå S, Tafazoli F, Fä M, Magnusson K-E, Wolf-Watz H & Ke Forsberg A˚ (1997) YopK of Yersinia pseudotuberculosis controls translocation of Yop effectors across the eukaryotic cell membrane. *Mol. Microbiol.* **24:** 73–91

Horne SM, Prüss BM., Horne SM, Prüß BM, Horne SM & Prüss BM. (2006) Global gene regulation in Yersinia enterocolitica: effect of FliA on the expression levels of flagellar and plasmid-encoded virulence genes. *Arch. Microbiol.* **185:** 115–126

Hu B, Lara-Tejero M, Kong Q, Galán JE & Liu J (2017) In Situ Molecular Architecture of the Salmonella Type III Secretion Machine. *Cell* **168:** 1065-1074.e10

Hu B, Morado DR, Margolin W, Rohde JR, Arizmendi O, Picking WL, Picking WD & Liu J (2015) Visualization of the type III secretion sorting platform of Shigella flexneri. *Proc. Natl. Acad. Sci. U. S. A.* **112:** 1047–1052

Hu P, Elliott J, Mccready P, Skowronski E, Garnes J, Kobayashi A, Brubaker RR & Garcia E (1998) Structural Organization of Virulence-Associated Plasmids of Yersinia pestis. *J. Bacteriol.* **180:** 5192–5202

Hueck CJ (1998) Type III protein secretion systems in bacterial pathogens of animals and plants. *Microbiol. Mol. Biol. Rev.* **62:** 379–433

Iriarte M & Cornelis GR (1999) Pathogenicity Islands and Other Mobile Virulence Elements Kaper JB & Hacker J (eds) American Society for Microbiology

Iriarte M, Sory MP, Boland A, Boyd AP, Mills SD, Lambermont I & Cornelis GR (1998) TyeA, a protein involved in control of Yop release and in translocation of Yersinia Yop effectors. *EMBO J.* **17:** 1907–18

Ittig SJ, Schmutz C, Kasper CA, Amstutz M, Schmidt A, Sauteur L, Vigano MA, Low SH, Affolter M, Cornelis GR, Nigg EA & Arrieumerlou C (2015) A bacterial type III secretion-based protein delivery tool for broad applications in cell biology. *J. Cell Biol.* **211:** 913–931

Jackson MW, Silva-Herzog E & Plano G V. (2004) The ATP-dependent ClpXP and Lon proteases regulate expression of the Yersinia pestis type III secretion system via regulated proteolysis of YmoA, a small histone-like protein. *Mol. Microbiol.* **54:** 1364–1378

Jiménez-Valera M, Gonzalez-Torres C, Moreno E & Ruiz-Bravo A (1998) Comparison of Ceftriaxone, Amikacin, and Ciprofloxacin in Treatment of Experimental Yersinia enterocolitica O9 Infection in Mice. *Antimicrob. Agents Chemother.* **42:** 3009–3011

Johnson S, Roversi P, Espina M, Olive A, Deane JE, Birket S, Field T, Picking WD, Blocker AJ, Galyov EE, Picking WL & Lea SM (2007) Self-chaperoning of the type III secretion system needle tip proteins IpaD and BipD. *J. Biol. Chem.* **282:** 4035–4044

Journet L, Agrain C, Broz P & Cornelis GR (2003) The Needle Length of Bacterial Injectisomes Is

Determined by a Molecular Ruler. *Science (80-.).* **302:** 1757–1760

Kaniga K, Delor I & Cornelis GR (1991) A wide-host-range suicide vector for improving reverse genetics in Gram-negative bacteria: inactivation of the blaA gene of Yersinia enterocolitica. *Gene* **109:** 137–141

Kearns DB (2010) A field guide to bacterial swarming motility. *Nat. Rev. Microbiol.* **8:** 634–644

Kenjale R, Wilson J, Zenk S, Saurya S, Picking WL & Blocker AJ (2005) The needle component of the type III secreton of Shigella regulates the activity of the secretion apparatus. *J. Biol. Chem.* **280:** 42929–42937

Kimbrough TG & Miller SI (2000) Contribution of Salmonella typhimurium type III secretion components to needle complex formation. *Proc. Natl. Acad. Sci. U. S. A.* **97:** 11008–11013

Knodler LA, Vallance BA, Celli J, Winfree S, Hansen B, Montero M & Steele-Mortimer O (2010) Dissemination of invasive Salmonella via bacterial-induced extrusion of mucosal epithelia . *Proc. Natl. Acad. Sci.* **107:** 17733–17738

Köberle M, Klein-Günther A, Schütz M, Fritz M, Berchtold S, Tolosa E, Autenrieth IB, Bohn E, Fritz M, Klein-Günther A, Tolosa E, Berchtold S, Schütz M & Köberle M (2009) Yersinia enterocolitica Targets Cells of the Innate and Adaptive Immune System by Injection of Yops in a Mouse Infection Model. *PLoS Pathog.* **5:** e1000551

Krall R, Zhang Y & Barbieri JT (2004) Intracellular Membrane Localization of Pseudomonas ExoS and Yersinia YopE in Mammalian Cells. *J. Biol. Chem.* **279:** 2747–2753

Kubori T, Sukhan A, Aizawa S-I & Galá JE (2000) Molecular characterization and assembly of the needle complex of the Salmonella typhimurium type III protein secretion system Materials and Methods Bacterial Strains, Culture Conditions, Quantitation of Bacterial Entry and Gene Expression, and Preparation of Culture Supernatant Proteins. *Proc. Natl. Acad. Sci.* **97:** 10225–10230

Kudryashev M, Diepold A, Amstutz M, Armitage JP, Stahlberg H & Cornelis GR (2015) Yersinia enterocolitica type III secretion injectisomes form regularly spaced clusters, which incorporate new machines upon activation. *Mol. Microbiol.* **95:** 875–884

Kudryashev M, Stenta M, Schmelz S, Amstutz M, Wiesand U, Castaño-Díez D, Degiacomi MTM, Münnich S, Bleck CCKC, Kowal J, Diepold A, Heinz DWD, Dal Peraro M, Cornelis GGRG & Stahlberg H (2013) In situ structural analysis of the Yersinia enterocolitica injectisome. *Elife* **2:** e00792

Kugelmass IN (1959) Biochemistry of Blood in Health and Disease Springfield: Charles C. Thomas, Inc.

Kupferberg LL & Higuchi K (1958) Role of calcium ions in the stimulation of growth of virulent strains of Pasteurella pestis. *J. Bacteriol.* **76:** 120–121

Lara-Tejero M, Kato J, Wagner S, Liu X & Galán JE (2011) A Sorting Platform Determines the Order of Protein Secretion in Bacterial Type III Systems. *Science (80-.).* **331:** 1188–91

Larock CN & Cookson BT (2012) The Yersinia Virulence Effector YopM Binds Caspase-1 to Arrest Inflammasome Assembly and Processing. *Cell Host Microbe* **12:** 799–805

Lee SH & Galán JE (2004) Salmonella type III secretion-associated chaperones confer secretion-pathway specificity. *Mol. Microbiol.* **51:** 483–495

Lee WL, Grimes JM & Robinson RC (2015) Yersinia effector YopO uses actin as bait to phosphorylate proteins that regulate actin polymerization. *Nat. Struct. Mol. Biol.* **22:** 248–55

Letzelter M, Sorg I, Mota LJ, Meyer S, Stalder J, Feldman M, Kuhn M, Callebaut I & Cornelis GR (2006) The discovery of SycO highlights a new function for type III secretion effector chaperones. *EMBO J.* **25:** 3223–3233

Lindner F, Milne-Davies B, Langenfeld K, Diepold A, Stiewe T & Diepold A (2020) LITESEC-T3SS - Light-controlled protein delivery into eukaryotic cells with high spatial and temporal resolution. *Nat. Commun.* **11:** 2381

Lou L, Zhang P, Piao R & Wang Y (2019) Salmonella Pathogenicity Island 1 (SPI-1) and Its Complex Regulatory Network. *Front. Cell. Infect. Microbiol.* **9:** 270

MacDonald J, Miletic S, Gaildry T, Chin-Fatt A & Menassa R (2017) Co-expression with the type 3 secretion chaperone CesT from enterohemorrhagic E. coli increases accumulation of recombinant Tir in plant chloroplasts. *Front. Plant Sci.* **8:** 283

Macho A & Zipfel C (2015) Targeting of plant pattern recognition receptor-triggered immunity by bacterial type-III secretion system effectors. *Curr. Opin. Microbiol.* **23:** 14–22

Marketon MM, DePaolo RW, DeBord KL, Jabri B & Schneewind O (2005) Plague Bacteria Target Immune Cells During Infection. *Science (80-.).* **309:** 1739–1741

Marlovits TC, Kubori T, Sukhan A, Thomas DR, Galán JE & Unger VM (2004) Structural Insights into the Assembly of the Type III Secretion Needle Complex. *Science (80-.).* **306:** 1040–1042

Martinez-Argudo I & Blocker AJ (2010) The Shigella T3SS needle transmits a signal for MxiC release, which controls secretion of effectors. *Mol. Microbiol.* **78:** 1365–1378

McCarter LL, Hilmen M & Silverman M (1988) Flagellar dynamometer controls swarmer cell differentiation of V. parahaemolyticus. *Cell* **54:** 345–351

Mehigh RJ, Sample AK & Brubaker RR (1989) Expression of the low calcium response in Yersinia pestis. *Microb. Pathog.* **6:** 203–217

Mejía E, Bliska JB & Viboud GI (2008) Yersinia Controls Type III Effector Delivery into Host Cells by Modulating Rho Activity. *PLoS Pathog.* **4:** e3

Mesnil M & Yamasaki H (2000) Bystander effect in herpes simplex virus-thymidine kinase/ganciclovir cancer gene therapy: role of gap-junctional intercellular communication. *Cancer Res.* **60:** 3989–99

Michiels T, Vanooteghem J-C, De Rouvroit CL, China B, Gustin A, Boudry P & Cornelis GR (1991) Analysis of virC, an Operon Involved in the Secretion of Yop Proteins by Yersinia enterocolitica. *J. Bacteriol.* **173:** 4994–5009

Mills E, Baruch K, Aviv G, Nitzan M & Rosenshine I (2013) Dynamics of the type III secretion system activity of enteropathogenic Escherichia coli. *MBio* **4:** e00303-13

Mills E, Baruch K, Charpentier X, Kobi S & Rosenshine I (2008) Real-Time Analysis of Effector Translocation by the Type III Secretion System of Enteropathogenic Escherichia coli. *Cell Host Microbe* **3:** 104–113

Mills SD, Boland A, Sory MP, van der Smissen P, Kerbourch C, Finlay BB & Cornelis GR (1997) Yersinia enterocolitica induces apoptosis in macrophages by a process requiring functional type III secretion and translocation mechanisms and involving YopP, presumably acting as an effector protein. *Proc. Natl. Acad. Sci. U. S. A.* **94:** 12638–43

Milne-Davies B, Helbig C, Wimmi S, Cheng DWC, Paczia N & Diepold A (2019) Life After Secretion—Yersinia enterocolitica Rapidly Toggles Effector Secretion and Can Resume Cell Division in Response to Changing External Conditions. *Front. Microbiol.* **10:** 2128

Minnich Scott A.and Rohde HN (2007) A Rationale for Repression and/or Loss of Motility by Pathogenic Yersinia in the Mammalian Host. In *The Genus Yersinia: From Genomics to Function*, Perry Robert D.and Fetherston JD (ed) pp 298–311. New York, NY: Springer New York

Monack DM, Mecsas J, Ghori N & Falkow S (1997) Yersinia signals macrophages to undergo apoptosis and YopJ is necessary for this cell death. *Proc. Natl. Acad. Sci. U. S. A.* **94:** 10385–90

Mueller CA, Broz P, Müller SA, Ringler P, Erne-Brand F, Sorg I, Kuhn M, Engel A & Cornelis GR (2005) The V-antigen of Yersinia forms a distinct structure at the tip of injectisome needles. *Science (80-.).* **310:** 474–476

Müller AJ, Hoffmann C, Galle M, Van Den Broeke A, Heikenwalder M, Falter L, Misselwitz B, Kremer M, Beyaert R & Hardt WD (2009) The S. Typhimurium Effector SopE Induces Caspase-1 Activation in Stromal Cells to Initiate Gut Inflammation. *Cell Host Microbe* **6:** 125–136

Nakano K & Vousden KH (2001) PUMA, a novel proapoptotic gene, is induced by p53. *Mol. Cell* **7:** 683–94

Nauth T, Huschka F, Schweizer M, Bosse JB, Diepold A, Failla AV, Steffen A, Stradal TEB, Wolters M & Aepfelbacher M (2018) Visualization of translocons in Yersinia type III protein secretion machines during host cell infection. *PLoS Pathog.* **14:** e1007527

Navarro L, Alto NM & Dixon JE (2005) Functions of the Yersinia effector proteins in inhibiting host immune responses. *Curr. Opin. Microbiol.* **8:** 21–27

Neeld D, Jin Y, Bichsel C, Jia J, Guo J, Bai F, Wu W, Ha UH, Terada N & Jin S (2014) Pseudomonas

aeruginosa injects NDK into host cells through a type III secretion system. *Microbiol. (United Kingdom)* **160:** 1417–1426

Nelson MS & Sadowsky MJ (2015) Secretion systems and signal exchange between nitrogen-fixing rhizobia and legumes. *Front. Plant Sci.* **6:** 491

Neyt C & Cornelis GR (1999) Insertion of a Yop translocation pore into the macrophage plasma membrane by Yersinia enterocolitica: requirement for translocators YopB and YopD, but not LcrG. *Mol. Microbiol.* **33:** 971–981

Nieto JM, Madrid C, Miquelay E, Parra JL, Rodríguez S & Juárez A (2002) Evidence for direct protein-protein interaction between members of the enterobacterial Hha/YmoA and H-NS families of proteins. *J. Bacteriol.* **184:** 629–635

De Nisco NJ, Rivera-Cancel G & Orth K (2018) The Biochemistry of Sensing: Enteric Pathogens Regulate Type III Secretion in Response to Environmental and Host Cues. *MBio* **9:** e02122-17

Orth K, Palmer LE, Bao ZQ, Stewart S, Rudolph AE, Bliska JB & Dixon JE (1999) Inhibition of the mitogen-activated protein kinase kinase superfamily by a Yersinia effector. *Science* **285:** 1920–3

Orth K, Xu Z, Mudgett MB, Bao ZQ, Palmer LE, Bliska JB, Mangel WF, Staskawicz B & Dixon JE (2000) Disruption of signaling by Yersinia effector YopJ, a ubiquitin-like protein protease. *Science* **290:** 1594–7

Page AL & Parsot C (2002) Chaperones of the type III secretion pathway: Jacks of all trades. *Mol. Microbiol.* **46:** 1–11

Park D, Lara-Tejero M, Waxham MN, Li W, Hu B, Galán JE & Liu J (2018) Visualization of the type III secretion mediated salmonella–host cell interface using cryo-electron tomography. *Elife* **7:**

Parsot C, Ménard R, Gounon P, Sansonetti P, Menard R, Gounon P & Sansonetti PJ (1995) Enhanced secretion through the Shigella flexneri Mxi-Spa translocon leads to assembly of extracellular proteins into macromolecular structures. *Mol. Microbiol.* **16:** 291–300

Pederson KJ & Barbieri JT (1998) Intracellular expression of the ADP-ribosyltransferase domain of Pseudomonas exoenzyme S is cytotoxic to eukaryotic cells. *Mol. Microbiol.* **30:** 751–759

Perdomo JJ, Gounon P & Sansonetti PJ (1994a) Polymorphonuclear Leukocyte Transmigration Promotes Invasion of Colonic Epithelial Monolayer by Shigella flexneri. *J. Clinial Investig.* **93:** 633–643

Perdomo O, Cavaillon J, Huerre M, Ohayon H, Gounon P & Sansonettill P (1994b) Acute Inflammation Causes Epithelial Invasion and Mucosal Destruction in Experimental Shigellosis. *J. Exp. Med.* **180:** 1307–1319

Pettersson J, Nordfelth R, Dubinina E, Bergman T, Gustafsson M, Magnusson KE & Wolf-Watz H (1996) Modulation of virulence factor expression by pathogen target cell contact. *Science (80-.).* **273:**

1231–1233

Pha K & Navarro L (2016) Yersinia type III effectors perturb host innate immune responses. *World J. Biol. Chem.* **7:** 1–13

Philip NH, Zwack EE & Brodsky IE (2016) Activation and Evasion of Inflammasomes by Yersinia. In *Current topics in microbiology and immunology* pp 69–90.

Picking WL, Nishioka H, Hearn PD, Baxter MA, Harrington AT, Blocker A & Picking WD (2005) IpaD of Shigella flexneri is independently required for regulation of Ipa protein secretion and efficient insertion of IpaB and IpaC into host membranes. *Infect. Immun.* **73:** 1432–1440

Portaliou AG, Tsolis KC, Loos MS, Balabanidou V, Rayo J, Tsirigotaki A, Crepin VF, Frankel G, Kalodimos CG, Karamanou S & Economou A (2017) Hierarchical protein targeting and secretion is controlled by an affinity switch in the type III secretion system of enteropathogenic Escherichia coli . *EMBO J.* **36:** 3517–3531

Portnoy DA, Wolf-Watz H, Bolin I, Beeder AB & Falkow S (1984) Characterization of Common Virulence Plasmids in Yersinia Species and Their Role in the Expression of Outer Membrane Proteins Downloaded from. *Infect. Immun.* **43:** 108–114

Poyraz Ö, Schmidt H, Seidel K, Delissen F, Ader C, Tenenboim H, Goosmann C, Laube B, Thünemann AF, Zychlinsky A, Baldus M, Lange A, Griesinger C & Kolbe M (2010) Protein refolding is required for assembly of the type three secretion needle. *Nat. Struct. Mol. Biol.* **17:** 788–792

Radics J, Königsmaier L & Marlovits TC (2013) Structure of a pathogenic type 3 secretion system in action. *Nat. Struct. Mol. Biol.* **21:** 82–87

La Ragione RMR, Cooley WWA, Velge P, Jepson MA & Woodward MMJ (2003) Membrane ruffling and invasion of human and avian cell lines is reduced for aflagellate mutants of Salmonella enterica serotype Enteritidis. *Int. J. Med. Microbiol.* **293:** 261–272

Ramos-Morales F (2012) Impact of Salmonella enterica Type III Secretion System Effectors on the Eukaryotic Host Cell. *ISRN Cell Biol.* **2012:** 1–36

Rappl C, Deiwick J & Hensel M (2003) Acidic pH is required for the functional assembly of the type III secretion system encoded by Salmonella pathogenicity island 2. *FEMS Microbiol. Lett.* **226:** 363–372

Råsbäck T, Rosendal T, Stampe M, Sannö A, Aspán A, Järnevi K & Lahti ET (2018) Prevalence of human pathogenic Yersinia enterocolitica in Swedish pig farms. *Acta Vet. Scand.* **60:** 39

Rathinavelan T, Zhang L, Picking WL, Weis DD, De Guzman RN & Im W (2010) A repulsive electrostatic mechanism for protein export through the type III secretion apparatus. *Biophys. J.* **98:** 452–61

Rietsch A & Mekalanos JJ (2006) Metabolic regulation of type III secretion gene expression in Pseudomonas aeruginosa. *Mol. Microbiol.* **59:** 807–820

Rimpilainen M, Forsberg A & Wolf-Watz H (1992) A Novel Protein, LcrQ, Involved in the Low-Calcium Response of Yersinia pseudotuberculosis Shows Extensive Homology to YopH. **174:** 3355–3363

Robertson JMC, McKenzie NH, Duncan M, Allen-Vercoe E, Woodward MJ, Flint HJ & Grant G (2003) Lack of flagella disadvantages Salmonella enterica serovar Enteritidis during the early stages of infection in the rat. *J. Med. Microbiol.* **52:** 91–99

Rocha CL, Coburn J, Rucks EA & Olson JC (2003) Characterization of Pseudomonas aeruginosa exoenzyme S as a bifunctional enzyme in J774a.1 macrophages. *Infect. Immun.* **71:** 5296–5305

Roehrich AD, Guillossou E, Blocker AJ & Martinez-Argudo I (2013) Shigella IpaD has a dual role: signal transduction from the type III secretion system needle tip and intracellular secretion regulation. *Mol. Microbiol.* **87:** 690–706

Rosner BM, Stark K & Werber D (2010) Epidemiology of reported Yersinia enterocolitica infections in Germany, 2001-2008. *BMC Public Health* **10:** 337

Rosqvist R, Forsberg A, Rimpilainen M, Bergman T & Wolf-Watz H (1990) The cytotoxic protein YopE of Yersinia obstructs the primary host defence. *Mol. Microbiol.* **4:** 657–667

de Rouvroit CL, Sluiters C & Cornelis GR (1992) Role of the transcriptional activator, VirF, and temperature in the expression of the pYV plasmid genes of Yersinia enterocolitica. *Mol. Microbiol.* **6:** 395–409

Rozen S & Skaletsky H (2000) Primer3 on the WWW for General Users and for Biologist Programmers. *Methods Mol. Biol.* **132:** 365–386

Ruckdeschel K, Harb S, Roggenkamp A, Hornef M, Zumbihl R, Köhler S, Heesemann J & Rouot B (1998) Yersinia enterocolitica impairs activation of transcription factor NF-kappaB: involvement in the induction of programmed cell death and in the suppression of the macrophage tumor necrosis factor alpha production. *J. Exp. Med.* **187:** 1069–79

Ruckdeschel K, Machold J, Roggenkamp A, Schubert S, Pierre J, Zumbihl R, Liautard JP, Heesemann J & Rouot B (1997a) Yersinia enterocolitica promotes deactivation of macrophage mitogen-activated protein kinases extracellular signal-regulated kinase-1/2, p38, and c-Jun NH2-terminal kinase. Correlation with its inhibitory effect on tumor necrosis factor-alpha production. *J. Biol. Chem.* **272:** 15920–7

Ruckdeschel K, Roggenkamp A, Lafont V, Mangeat P, Heesemann JR & Rouot B (1997b) Interaction of Yersinia enterocolitica with Macrophages Leads to Macrophage Cell Death through Apoptosis. *Infect. Immun.* **65:** 4813–4821

Rundell EA, McKeithen-Mead SA & Kazmierczak BI (2016) Rampant Cheating by Pathogens? *PLOS Pathog.* **12:** e1005792

Sánchez-Romero MA & Casadesús J (2018) Contribution of SPI-1 bistability to Salmonella enterica

cooperative virulence: insights from single cell analysis. *Sci. Rep.* **8:** 14875

Sansonetti PJ, Ryter A, Clerc P, Maurelli AT & Mounier1 J (1986) Multiplication of Shigella flexneri within HeLa Cells: Lysis of the Phagocytic Vacuole and Plasmid-Mediated Contact Hemolysis. *Infect. Immun.* **51:** 461–469

Schesser K, Frithz-Lindsten E & Wolf-Watz H (1996) Delineation and Mutational Analysis of the Yersinia pseudotuberculosis YopE Domains Which Mediate Translocation across Bacterial and Eukaryotic Cellular Membranes. *J. Bacteriol.* **178:** 7227–7233

Schlumberger MC, Müller A, Ehrbar K, Winnen B, Duss I, Stecher B, Hardt W-D & Mu AJ (2005) Real-time imaging of type III secretion: Salmonella SipA injection into host cells. *Proc. Natl. Acad. Sci. U. S. A.* **102:** 12548–12553

Schmid A, Neumayer W, Trülzsch K, Israel L, Imhof A, Roessle M, Sauer G, Richter S, Lauw S, Eylert E, Eisenreich W, Heesemann J & Wilharm G (2009) Cross-talk between type three secretion system and metabolism in Yersinia. *J. Biol. Chem.* **284:** 12165–12177

Schneewind O (2016) Classic Spotlight: Studies on the Low-Calcium Response of Yersinia pestis Reveal the Secrets of Plague Pathogenesis. *J. Bacteriol.* **198:** 2018

Schroeder GN, Jann NJ & Hilbi H (2007) Intracellular type III secretion by cytoplasmic Shigella flexneri promotes caspase-1-dependent macrophage cell death. *Microbiology* **153:** 2862–2876

Schulte M, Sterzenbach T, Miskiewicz K, Elpers L, Hensel M & Hansmeier N (2019) A versatile remote control system for functional expression of bacterial virulence genes based on the tetA promoter. *Int. J. Med. Microbiol.* **309:** 54–65

Shao F, Merritt PM, Bao Z, Innes RW & Dixon JE (2002) A Yersinia Effector and a Pseudomonas Avirulence Protein Define a Family of Cysteine Proteases Functioning in Bacterial Pathogenesis. *Cell* **109:** 575–588

Shao F, Vacratsis PO, Bao Z, Bowerst KE, Fierke CA & Dixon JE (2003) Biochemical characterization of the Yersinia YopT protease: Cleavage site and recognition elements in Rho GTPases. *Proc. Natl. Acad. Sci. U. S. A.* **100:** 904–909

Shaulov L, Gershberg J, Deng W, Finlay BB & Sal-Man N (2017) The Ruler Protein EscP of the Enteropathogenic Escherichia coli Type III Secretion System Is Involved in Calcium Sensing and Secretion Hierarchy Regulation by Interacting with the Gatekeeper Protein SepL. *MBio* **8:** e01733-16

Shen DK, Moriya N, Martinez-Argudo I & Blocker AJ (2012) Needle length control and the secretion substrate specificity switch are only loosely coupled in the type III secretion apparatus of Shigella. *Microbiol. (United Kingdom)* **158:** 1884–1896

Skurnik M, Bölin I, Heikkinen H, Piha S, Wolf-Watz H, Bolin I, Heikkinen H, Piha S, Wolf-Watz2 H, Bölin

I, Heikkinen H, Piha S, Wolf-Watz H, Bolin I & Heikkinen H (1984) Virulence plasmid-associated autoagglutination in Yersinia spp. *J. Bacteriol.* **158:** 1033–1036

Skurnik M & Toivanen P (1992) LcrF Is the Temperature-Regulated Activator of the yadA Gene of Yersinia enterocolitica and Yersinia pseudotuberculosis. *J. Bacteriol.* **174:** 2047–2051

Song M, Sukovich DJ, Ciccarelli L, Mayr J, Fernandez-Rodriguez J, Mirsky EA, Tucker AC, Gordon DB, Marlovits TC & Voigt CA (2017) Control of type III protein secretion using a minimal genetic system. *Nat. Commun.* **8:** 14737

Sory MP, Boland A, Lambermont I & Cornelis GR (1995) Identification of the YopE and YopH domains required for secretion and internalization into the cytosol of macrophages, using the cyaA gene fusion approach. *Proc. Natl. Acad. Sci. U. S. A.* **92:** 11998–2002

Soscia C, Hachani A, Bernadac A, Filloux A & Bleves S (2007) Cross talk between type III secretion and flagellar assembly systems in Pseudomonas aeruginosa. *J. Bacteriol.* **189:** 3124–3132

Spaeth K, Chen Y-S & Valdivia R (2009) The Chlamydia type III secretion system C-ring engages a chaperone-effector protein complex. *PLoS Pathog.* **5:** e1000579

Spaink HP, H Okker RJ, Wijffelman -carel A, Tak T, Goosen-de Roo L, Pees E, N Van Brussel AA & J Lugtenberg BJ (1989) Symbiotic Properties of Rhizobia Containing a Flavonoid-Independent Hybrid nodD Product. *J. Bacteriol. JUIY***:** 4045–4053

Stainier I & Cornelis GR (1997) YscM1 and YscM2, two Yersinia enterocolitica proteins causing downregulation of yop transcription. *Mol. Microbiol.* **26:** 833–834

Stebbins C & Galan J (2001) Maintenance of an unfolded polypeptide by a cognate chaperone in bacterial type III secretion. *Nature* **414:** 77–81

Stecher B, Robbiani R, Walker AW, Westendorf AM, Barthel M, Kremer M, Chaffron S, Macpherson AJ, Buer J, Parkhill J, Dougan G, Von Mering C & Hardt WD (2007) Salmonella enterica serovar typhimurium exploits inflammation to compete with the intestinal microbiota. *PLoS Biol.* **5:** 2177–2189

Stiewe T & Haran TE (2018) How mutations shape p53 interactions with the genome to promote tumorigenesis and drug resistance. *Drug Resist. Updat.* **38:** 27–43

Stiewe T, Theseling CC & Pützer BM (2002) Transactivation-deficient ΔTA-p73 inhibits p53 by direct competition for DNA binding. Implications for tumorigenesis. *J. Biol. Chem.* **277:** 14177–14185

Sturm A, Heinemann M, Arnoldini M, Benecke A, Ackermann M, Benz M, Dormann J & Hardt W-D (2011) The cost of virulence: retarded growth of Salmonella Typhimurium cells expressing type III secretion system 1. *PLoS Pathog.* **7:** e1002143

Sukhan A, Kubori T, Wilson J & Galán JE (2001) Genetic analysis of assembly of the Salmonella enterica serovar Typhimurium type III secretion-associated needle complex. *J. Bacteriol.* **183:** 1159–1167

Swietnicki W, O'Brien S, Holman K, Cherry S, Brueggemann E, Tropea JE, Hines HB, Waugh DS & Ulrich RG (2004) Novel protein-protein interactions of the Yersinia pestis type III secretion system elucidated with a matrix analysis by surface plasmon resonance and mass spectrometry. *J. Biol. Chem.* **279:** 38693–38700

Thorslund SE, Edgren T, Pettersson J, Nordfelth R, Sellin ME, Ivanova E, Francis MS, Isaksson EL, Wolf-Watz H & Fällman M (2011) The RACK1 signaling scaffold protein selectively interacts with Yersinia pseudotuberculosis virulence function. *PLoS One* **6:** e16784

Torres-Vargas CE, Kronenberger T, Roos N, Dietsche T, Poso A & Wagner S (2019) The inner rod of virulence-associated type III secretion systems constitutes a needle adapter of one helical turn that is deeply integrated into the system's export apparatus. *Mol. Microbiol.* **112:** 918–931

Torruellas J, Jackson MW, Pennock JW & Plano G V. (2005) The Yersinia pestis type III secretion needle plays a role in the regulation of Yop secretion. *Mol. Microbiol.* **57:** 1719–1733

Vasselon T, Mounier J, Prevost MC, Hellio R & Sansonettil PJ (1991) Stress Fiber-Based Movement of Shigella flexneri within Cells

Veenendaal AKJ, Hodgkinson J, Schwarzer L, Stabat D, Zenk S & Blocker AJ (2007) The type III secretion system needle tip complex mediates host cell sensing and translocon insertion. *Mol. Microbiol.* **63:** 1719–1730

Viboud GI & Bliska JB (2001) A bacterial type III secretion system inhibits actin polymerization to prevent pore formation in host cell membranes. *EMBO J.* **20:** 5373–82

Viprey V, Greco A Del, Golinowski W, Broughton WJ & Perret X (1998) Symbiotic implications of type III protein secretion machinery in Rhizobium. *Mol. Microbiol.* **28:** 1381–1389

Wagner S & Diepold A (2020) A Unified Nomenclature for Injectisome-Type Type III Secretion Systems. *Curr. Top. Microbiol. Immunol.* **427:** 1–10

Wagner S, Königsmaier L, Lara-Tejero M, Lefebre M, Marlovits TC & Galán JE (2010) Organization and coordinated assembly of the type III secretion export apparatus. *Proc. Natl. Acad. Sci. U. S. A.* **107:** 17745–17750

Walker BJ, Stan G-B V & Polizzi KM (2017) Intracellular delivery of biologic therapeutics by bacterial secretion systems. *Expert Rev. Mol. Med.* **19:** e6

Wang H, Avican K, Fahlgren A, Erttmann SF, Nuss AM, Dersch P, Fällman M, Edgren T & Wolf-Watz H (2016) Increased plasmid copy number is essential for Yersinia T3SS function and virulence. *Science (80-.).* **353:** 492–495

Wassef JS, Keren DF & Mailloux JL (1989) Role of M Cells in Initial Antigen Uptake and in Ulcer Formation in the Rabbit Intestinal Loop Model of Shigellosis. *Infect. Immun.* **57:** 858–863

Wattiau P, Bernier B, Deslae P, Michiels T & Cornelis GR (1994) Individual chaperones required for Yop

secretion by Yersinia. *Proc. Natl. Acad. Sci.* **91:** 10493–10497

Wattiau P & Cornelis GR (1994) Identification of DNA Sequences Recognized by VirF, the Transcriptional Activator of the Yersinia yop Regulon. *J. Bacteriol.* **176:** 3878–3884

Weigel WA & Dersch P (2018) Phenotypic heterogeneity: a bacterial virulence strategy. *Microbes Infect.* **20:** 570–577

Westerhausen S, Nowak M, Torres-Vargas CE, Bilitewski U, Bohn E, Grin I & Wagner S (2020) A NanoLuc Luciferase-Based Assay Enabling the Real-Time Analysis of Protein Secretion and Injection by Bacterial Type III Secretion Systems. *Mol. Microbiol.* **113:** 745471

Wiley DJ, Rosqvist R & Schesser K (2007) Induction of the Yersinia Type 3 Secretion System as an All-or-None Phenomenon. *J. Mol. Biol.* **373:** 27–37

Wilharm G, Dittmann S, Schmid A & Heesemann J (2007) On the role of specific chaperones, the specific ATPase, and the proton motive force in type III secretion. *Int. J. Med. Microbiol.*

Wilharm G & Heider C (2014) Interrelationship between type three secretion system and metabolism in pathogenic bacteria. *Front. Cell. Infect. Microbiol.* **4:** 150

Wilharm G, Lehmann V, Neumayer W, Trček J & Heesemann J (2004) Yersinia enterocolitica type III secretion: Evidence for the ability to transport proteins that are folded prior to secretion. *BMC Microbiol.* **4:** 27

Wimmi S, Balinovic A, Jeckel H, Selinger L, Lampaki D, Eisemann E, Meuskens I, Linke D, Drescher K, Endesfelder U & Diepold A (2019) Dynamic relocalization of the cytosolic type III secretion system components ensures specific protein secretion. *bioRxiv*

Wölke S, Ackermann N & Heesemann J (2011) The Yersinia enterocolitica type 3 secretion system (T3SS) as toolbox for studying the cell biological effects of bacterial Rho GTPase modulating T3SS effector proteins. *Cell. Microbiol.* **13:** 1339–1357

Wolters M, Zobiak B, Nauth T & Aepfelbacher M (2015) Analysis of Yersinia enterocolitica Effector Translocation into Host Cells Using Beta-lactamase Effector Fusions. *J. Vis. Exp.* **104:** 53115

Wulff-Strobel C, Williams A & Straley S (2002) LcrQ and SycH function together at the Ysc type III secretion system in Yersinia pestis to impose a hierarchy of secretion. *Mol. Microbiol.* **43:** 411–123

Younis R, Bingle LEH, Rollauer S, Munera D, Busby SJ, Johnson S, Deane JE, Lea SM, Frankel G & Pallen MJ (2010) SepL resembles an aberrant effector in binding to a class 1 type III secretion chaperone and carrying an N-terminal secretion signal. *J. Bacteriol.* **192:** 6093–6098

Yu XJ, McGourty K, Liu M, Unsworth KE & Holden DW (2010) pH sensing by intracellular salmonella induces effector translocation. *Science (80-.).* **328:** 1040–1043

Zahorchak RJ, Charnetzky WT, Little R V. & Brubaker RR (1979) Consequences of Ca2+deficiency on

macromolecular synthesis and adenylate energy charge in Yersinia pestis. *J. Bacteriol.* **139:** 792–799

Zumbihl R, Aepfelbacher M, Andor A, Jacobi CA, Ruckdeschel K, Rouot B & Heesemann J (1999) The cytotoxin YopT of Yersinia enterocolitica induces modification and cellular redistribution of the small GTP-binding protein RhoA. *J. Biol. Chem.* **274:** 29289–93

Zychlinsky A, Kenny B, Ménard R, Prévost M, Holland I & Sansonetti P (1994) IpaB mediates macrophage apoptosis induced by Shigella flexneri. *Mol. Microbiol.* **11:** 619–627

9. Curriculum Vitae

10. Acknowledgments

This thesis would not have been possible without the unwavering support and help of so many people.

I would like to especially recognize my PhD supervisor, **Andreas Diepold**. Thank you so much for this opportunity to learn and work in in your lab. You have allowed me to grow and learn as a scientist and I am immensely grateful you took this chance with me. You have offered great support, guidance and conversation throughout my thesis and I have sincerely enjoyed your enthusiasm for science. I am so appreciative for everything.

Thank you to my thesis advisory committee, **Anke Becker** and **Simon Ringgaard**, for the guidance and feedback in my project over the years, you both have really allowed my project and I to grow and I am so grateful for all you have helped me accomplish.

I would like to acknowledge and thank **Dušica**, for all your support and endless conversation during my PhD. I am immensely appreciative in all the work you have done to make this program the best it can be.

To the past and present members of the **Diepold Lab**, I am so grateful to have had such an amazing lab family here. You all have been so supportive during my time in the lab, allowing for lab shenanigans and invaluable scientific conversations. Thank you so much **Katja** for always being there for me and offering help and company. You have really been a great friend and lab mate, I have really enjoyed working together. **Stephan**, thank you for your friendship, support, company and endless conversation throughout the years. I am so appreciative for you being there and pushing me throughout my PhD. To **Lisa** and **Carlos**, thank you so much for brightening up the lab and being great friends. A special thanks to **Florian Lindner**, **Dimi Lampaki**, **Kirsten Stahl, Moritz Fleck**, **Hend Selim**, **Anna-Lena Koida**, **Saskia Schott**, and **Vera Jensen** for the good conversation and making the lab a great work place.

I am also especially appreciative to the **Ringgaard Lab** for offering great company, coffee corner conversation and support throughout the years, you all made A2 so very special and are immensely missed.

Thank you so much to **Timo Glatter**, **Witold Szymanski**, **Jörg Kahnt**, and **Nicole Paczia** for your help doing mass spectrometry.

I would like to give a big thank you to **Ale** for being such an amazing friend and my thesis fairy godmother! You have been such a help and blessing throughout this journey and I am so grateful for

you. Thank you **Sofya** and **Dobro** for being such great friends and for the much needed company exploring nature.

I wouldn't be here without the priceless guidance and support of **Monika**, thank you for opening my eyes to endless opportunities and convincing me to join you on your study abroad. You helped make this possible.

A very special appreciation to my family for all that you have done for me. Thank you so much to my **parents** for their endless and devoted support and love during my education and throughout life. You both have pushed and molded me into the person I am and I am forever grateful. To my husband, **Calvin**, thank you for all that you have done for me during this crazy time. I cannot thank you enough for your love and unyielding support. Thank you for being such an amazing partner.

11. Erklärung

Hermit versichere ich, dass ich die vorliegende Dissertation mit dem Titel

„**Characterization of type III secretion system-dependent protein secretion in *Y. enterocolitica*** "

selbstständing verfasst, keine anderen als die Text angegebenen Hilfsmittel verwendet und sämttliche Stellen, die im Wortlaut oder dem Sinn nach anderen Werken entnommen sind, mit Quellenangaben kenntlich gemacth habe.

Die Dissertation wurde in der jetzigen oder einer ähnlichen From noch bei keoner anderen Hochschule eingereicht und hat noch keinen sonstigen Prüfungswecjen gedient.

_____ _____

Ort, Datum Bailey Abigail Milne-Davies

12. Einverständniserklärung

Ich erkläre mich dam einverstanden, dass die vorliegende Dissertation

„**Characterization of type III secretion system-dependent protein secretion in *Y. enterocolitica*** "

in Bibliotheken allgemein zugänglich gemacht wird. Dazu gehört, dass sie

- von der Bibliothek der Einrichtung, in der ich meine Arbeit anfertig habe, zus Benutzung in ihren Räumen bereitgehalten wird;
- in konventionellen und maschinenlesbaren Katalogen, Verzeichnissen und Datenbanken verzeichnet wird;
- im Rahmen der urheberrechtichen Bestimmungen für Kopierzwecke genutzt werden kann.

Marburg, den ____.____._____ _____

Bailey Abigail Milne-Davies

_____

Dr. Andreas Diepold